The University of Southern Mississippi

The Aquila Digital Community

Dissertations

Fall 12-2009

Random and Block Copolymers of Poly(dodecamethyleneterephthalamide)

Theodore Frank Novitsky Jr.
University of Southern Mississippi

Follow this and additional works at: https://aquila.usm.edu/dissertations

Part of the Materials Chemistry Commons, and the Polymer Chemistry Commons

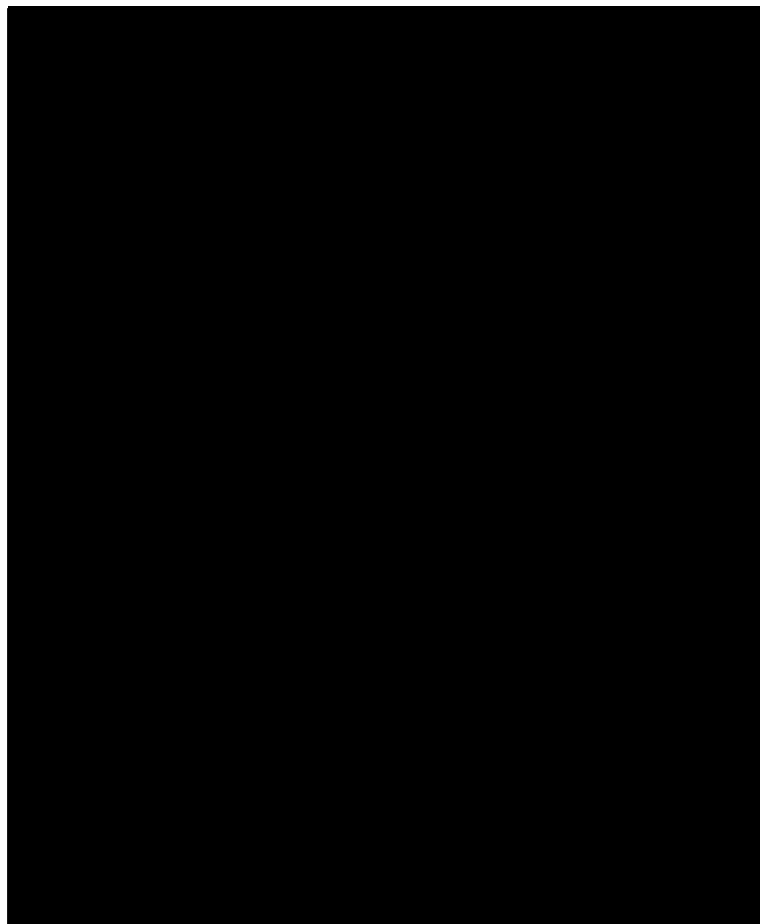The University of Southern Mississippi

RANDOM AND BLOCK COPOLYMERS OF

POLY(DODECAMETHYLENE TEREPHTHALAMIDE)

by

Theodore Frank Novitsky, Jr.

A Dissertation
Submitted to the Graduate School
of The University of Southern Mississippi
in Partial Fulfillment of the Requirements
for the Degree of Doctor of Philosophy

Approved:

December 2009

The University of Southern Mississippi

RANDOM AND BLOCK COPOLYMERS OF

POLY(DODECAMETHYLENE TEREPHTHALAMIDE)

by

Theodore Frank Novitsky, Jr.

Abstract of a Dissertation
Submitted to the Graduate School
of The University of Southern Mississippi
in Partial Fulfillment of the Requirements
for the Degree of Doctor of Philosophy

December 2009

ABSTRACT

RANDOM AND BLOCK COPOLYMERS OF

POLY(DODECAMETHYLENE TEREPHTHALAMIDE)

by Theodore Frank Novitsky, Jr.

December 2009

The following dissertation focuses on the synthesis and characterization of

poly(dodecamethylene terephthalamide) (PA-12,T) and novel copolymers.

Chapter I details the synthesis of PA-12,T homopolymer by melt condensation

polymerization. A series of homopolymers with different molecular weights were

obtained by adjusting the stoichiometry of the polymerization using

1,12-diaminododecane, terephthalic acid and benzoic acid. End group ^{13}C NMR

spectroscopy resonances were obtained by correlating peak intensities with intrinsic

viscosity values. From the NMR data, total end group concentrations and molecular

weights were determined for each sample. The data exhibited a linear trend when plotting

log (IV) versus log (M_n), and previously unknown PA-12,T Mark-Houwink solution

constants were found.

Chapter II examines the synthesis and characterization of PA-12,T, 6,T and 10,T,

6,T copolymers. Melt condensation procedures and solution constants from Chapter I

were used to synthesize and confirm that high molecular weight copolymers were

obtained. The substituted aromatic carbon resonance of ^{13}C NMR spectra was found to be

sensitive to copolymer sequence, and was used to determine that the copolymers are

random. Differential scanning calorimetry data shows that the copolymers exhibit

eutectic melting behavior, displaying a decrease in copolymer melting temperature and

enthalpy up to the eutectic point of 30 wt-% PA-6,T, and a corresponding increase in both up to 60 wt-% PA-6T. Optically clear materials were obtained at 30 wt-% PA-6,T. Data collection was stopped at 60 wt-% due to phase separation of PA-6,T rich phases. Wide angle x-ray diffraction data displayed three distinct regions: 1) sharp PA-10,T crystal diffractions from 0-20% PA-6,T, 2) broad amorphous scattering between 25-45% PA-6,T, 3) sharp diffraction peaks from 50-60 wt% PA-6,T. All copolymers had relatively high glass transition temperatures from 137-149 °C determined from dynamic mechanical analysis. This study provides a method in which crystallinity and optical clarity of semi-aromatic polyamides can be tuned while maintaining high glass transition temperatures.

In Chapter III, a novel, one pot polyamide-polyamide block copolymer synthetic strategy is explained. The synthesis of PA-12,T - PA-6 block copolymers occurs in two sequential steps, in which it was found that $CaCl_2$ is needed to avoid crosslinking of the material. First, reaction variables of the solution, step growth polymerization of 1,12-diaminododecane and biscaprolactam terephthalamide (BCT) in caprolactam were investigated. PA-12,T with an average degree of polymerization of 15 and n-terephthaloyl end groups was obtained using 5 mol-% excess BCT. The second stage of synthesis uses anionic polymerization of the caprolactam using the n-terephthaloyl caprolactam end groups. While $CaCl_2$ concentration had little effect on this step growth reaction, it was found that the $CaCl_2$ greatly effected the conversion and transamidation of the anionic polymerization. This effect yielded a variety of materials with different molecular weights and blockiness that display unique thermal and solubility properties not obtained with polymer blends. Furthermore, this technique can be applied to wide

variety of monomers to create novel polyamide-polyamide block copolymers currently

undiscovered.

Dedicated to my parents,

Ted and Pattie Novitsky

collective, everyday discussions in the lab where we really learned and figured out each individual's projects. This is a great group of people, and I am truly thankful for all of our times together.

My undergraduate advisor, Dr. Paul Koch was influential in getting me interested in organic and polymer chemistry. Because of him, I decided to pursue a PhD and further solidify his teachings at Penn State. Looking back on all I have learned in the past four years, it was one of the best decisions I have made, thank you Dr. Koch.

Thanks to my friends Chris Lange and Sam Tucker, these guys have always been there for me in good times and bad. The jam sessions with you guys were amazing and very much needed.

To my sweetheart, Tammy Nolan, for always knowing best how to bring me to reality when immersed in the complications of graduate school.

To my family, Ted and Pattie Novitsky and Jay and Angie Welch for their continuous support.

Finally, I would like to pay special recognition to my parents. Realizing the sacrifices that they have taken to advance the education of my sister and me, I owe everything to them. Being first generation college students, they have given us a priceless gift. Thank you Mom and Dad, I love you.

TABLE OF CONTENTS

LIST OF TABLES

INTRODUCTION

Poly (dodecamethylene terephthalamide) is a semi-crystalline polyamide synthesized by melt condensation polymerization of 1,12-diaminododecane and terephthalic acid. PA-12,T belongs to a family of semi-aromatic polyamides having unique properties that result from the aliphatic and aromatic nature of the polymer structure.

When introducing aromaticity into the backbone of aliphatic polyamides both performance properties and processability of the material are changed. With increasing aromaticity, performance properties such as strength and glass transition (T_g) are increased, while properties that define the processability of the material, such as the crystalline melting temperature and melt viscosity, are also increased. For example, the wholly aromatic polyamide, poly(p-phenylene terephthalamide) (Kevlar), is known for its superior strength, but cannot be melt processed due to its high melting temperature. Therefore, Kevlar is limited to high-end niche applications and is expensive because it is not easily processed. Semi-aromatic polyamides are an important class of polyamides because they display strength and glass transition enhancement while having melting temperatures suitable for melt processing.

Within the branch of semi-aromatic polyamides, there are practical limitations of processability on monomer selection. For example, PA-6,T has a crystalline melting temperature of 370 °C, which, similar to Kevlar, cannot be melt processed without degradation. However, increasing the length of the diamine monomer lowers the melting temperature of the polymer. For instance, the melting points of PA-9,T, PA-10,T, PA-

12,T and PA-18,T are approximately 309, 315, 295 and 245 °C, respectively. These semi-aromatic polyamides are well known in patent literature to be melt processable.

Additionally, PA-12,T has a T_g of 120 °C compared to 60 °C of nylon 6,6. Therefore, PA-12,T is suitable for under-the-hood automobile applications where wholly aliphatic polyamides cannot be utilized. The combination of high T_g and low melting point justifies our and our collaborators, Ascend Performance Materials (formerly Solutia), interest in PA-12,T.

My studies of PA-12,T are presented in the following three chapters. A more detailed background and introduction can be found in each section. In Chapter I, we developed Mark-Houwink solution constants by correlating intrinsic viscosities with ^{13}C NMR end group concentrations of PA-12,T synthesized with a variety of molecular weights. Since no solution constants are available for these types of polymers, this data provides a manner of determining molecular weights of copolymers synthesized in the following sections, and allows proper evaluation of the multitude of process patents available for PA-12,T and similar polyamides.

In Chapter II, the synthesis of PA-12,T with PA-6,T comonomer is detailed. Using a melt polycondensation of the salt mixture, random copolymers were obtained. While isomorphism of PA-12,T, 12,6 copolymers have been shown in literature, our work represents the first study to examine the eutectic melting behavior of PA-12,T and 10,T.

In Chapter III, the synthesis of PA-12,T - PA-6 block copolymers is discussed. Copolymers were synthesized by a novel one-pot process utilizing both step-growth and anionic polymerization methods in the presence of $CaCl_2$. Fundamental principles of melt

condensation of PA-12,T examined in Chapter I were applied to the solution

polymerization of biscaprolactam terephthalamide and 1,12-diaminododecane in

caprolactam. By adjusting the stoichiometry of the step growth reaction, PA-12,T with

anionic coinitiator end groups were obtained, followed by the addition of initiator to form

block copolymers. Due to the observed crosslinking of the material without $CaCl_2$, the

effect of the $CaCl_2$ concentration was studied for both reactions.

In the final conclusions section, extensions of the findings of these studies are

briefly discussed.

CHAPTER I

EFFECT OF STOICHIOMETRIC IMBALANCES ON THE MELT CONDENSATION

POLYMERIZATION OF POLY(DODECAMETHYLENE TEREPHTHALAMIDE)

STUDIED BY INTRINSIC VISCOSITY AND ^{13}C NMR.

Abstract

Poly(dodecamethylene terephthalamide) (PA-12,T) was synthesized by melt

condensation polymerization of 12,T salt with 0, 1, 3, 5, or 10 % molar excess of 1,12-

diaminododecane (DA), terephthalic acid (TA), or benzoic acid (BA). Intrinsic

viscosities (0.5 g/dL in 96% H_2SO_4 at 25 °C) were measured to determine relative

molecular weight differences. IV was highest for reactions containing 1 and 3 mol-%

excess DA (1.36 and 1.31 dL/g, respectively), followed by the product of pure 1:1 salt

(1.25 dL/g). For all concentrations of excess TA and BA, IV decreased progressively. ^{13}C

NMR chemical shifts for DA, TA, and BA end groups were identified and their

concentrations determined by comparison with the intensity of main chain polymer

peaks. A log-log plot of IV and M_n calculated from ^{13}C NMR data shows a linear trend

with Mark-Houwink constants of K=55.8*10^{-5} dL/g and a = 0.81.

Introduction

Semi-aromatic polyterephthalamides (SAPT) are reaction products of aliphatic

diamines and terephthalic diacids. SAPT's possess improved thermal and mechanical

properties relative to purely aliphatic polymers, while being easier to process than

aromatic polyamides.[1] Symmetrical aromaticty in the polymer backbone results in higher

melting and glass transition temperatures, rendering them useful for high temperature

automotive applications. For example, poly(hexamethylene terephthalamide) (PA-6,T)

has a melting temperature of 370 °C and a glass transition temperature of 125 °C

compared to 265 °C and 60 °C for PA-6,6. However, high melt viscosities and melting

temperatures that approach the degradation temperature makes conventional melt

processing of SAPT's difficult. Overcoming these obstacles has been the focus of much

patent literature.[2-13] Melting temperatures of SAPT's can be tuned to suitable ranges by

changing the chemical composition of monomers. For example, increasing the length of

diamine from 6 to 12 carbons decreases the polymer melting temperature from 370 °C to

295 °C.

Controlling molecular weight during melt condensation polymerizations of

SAPT's is crucial for obtaining desired mechanical properties and processability. For

instance, materials having a molecular weight less than a critical value have poor

mechanical properties and are brittle. Increasing molecular weight above the critical

value results in high melt viscosities and complicates processing. Control of molecular

weight in A-A B-B systems is attained by adjusting the stoichiometry of reactants.

Although perfect stoichiometric balance is theoretically most favorable for obtaining high

molecular weight condensation polymers, a practical discrepancy between relative

concentrations of starting materials and finished products exits. Industrial practices and

patents indicate that excess diamine [4] or terephthalic acid [6] have to be added to the

diacid/diamine salt to generate suitable products with the desired molecular weight.

Additionally, end capping is also used to limit the molecular weight during melt

condensation polymerizations.[14] In SAPT literature, end cappers are referred to as

terminal blocking agents[9], viscosity stabilizers[2], or molecular weight stabilizers[6].

Commonly used end capping agents for SAPT's are benzoic acid and acetic acid.

Although adjusting stoichiometry is common practice in SAPT patent literature, there is a need for a fundamental study that uses to quantify its effects on molecular weight and end group functionality. Typically, single-point intrinsic viscosity measurements are used to determine relative molecular weight changes. However, no Mark-Houwink constants are available for SAPT's. Therefore, the magnitude of the impact on molecular weight of the products is unknown.

Our group has developed ^{13}C NMR spectroscopic tools for examining end groups, *cis* amide content, and number average molecular weights of various aliphatic polyamides.[15,16] This study uses ^{13}C NMR spectroscopy to determine end group concentrations and number average molecular weights of poly(dodecamethylene terephthalamide) (PA-12,T) synthesized at varying molecular weights by adjusting the reaction stoichiometry of the melt condensation polymerization.

Experimental

Materials

Terephthalic acid, 1,12-diaminododecane, benzoic acid, hexafluoroisopropanol, concentrated sulfuric acid (96%) and chloroform-*d* were purchased from Aldrich Chemical Company. Benzoic acid and 1,12-diaminododecane were sublimed at 70 °C and dried at room temperature under vacuum before use. Hexafluoroisopropanol and chloroform-*d* were dried before use with molecular sieves.

Synthesis

PA-12,T Salt. Into a 2 L beaker, 1200 mL of deionized water, 40.1 grams (0.20 mol) of 1,12-diaminodecane and 32.9 grams (0.198 mol) of terephthalic acid were added, and the slurry was heated to a boil. Additional water was added and brought to boil to give a supersaturated clear salt solution (approximately 6.3 wt-%). The hot salt solution was then added to a 2 L beaker containing 800 mL of reagent alcohol and cooled to room temperature, followed by overnight cooling in a freezer at 0.5 °C. The precipitate was then filtered and washed with reagent alcohol, producing 68 g of PA-12,T salt with a 95% yield. The salt was then recrystallized using a water/ethanol mixture and dried overnight at 80 °C under vacuum (mp - 271.9 °C, $\Delta H_{melting}$ 428 J/g).

Melt Condensation Polymerization of Polyamide (12,T). PA-12,T salt, added excess reactant, and antioxidant (0.5 wt-%) were weighed and mixed with a mortar and pestle. The solid mixture was then added to a test tube and approximately 50 wt-% water was added and mixed to create a slurry. Twelve test tubes were then loaded into a Parr reactor, which was then sealed and purged with nitrogen. Heating steps were programmed into the reactor controller unit and monitored with a thermocouple placed in one of the test tubes. The reactor was surrounded by insulation for precise heating control. Pressure was controlled manually with nitrogen and measured by a gauge on the reactor head. Predetermined temperatures provided signals for pressure changes. With approximately 125 kPa nitrogen pressure and a 200 °C set point, the sample temperature remained at 125 °C until all water was evaporated. At 150 °C the pressure was elevated to 1724 kPa. At 280 °C the pressure was released and the temperature was allowed to rise and hold at 310-315 °C for 15 minutes with purging nitrogen.

Sample Preparation

Material plugs were immersed in liquid nitrogen for approximately 10 minutes, then ground using a Waring blender with stainless steel mixing jar. Resulting pellets were dried at 80 °C under vacuum for 24 hours, and placed in a desiccator before characterization.

Characterization

Nuclear Magnetic Resonance (NMR). NMR samples containing 10 wt-% polymer in a 3:1 volume ratio of hexafluoroisopropanol (HFIP) to $CDCl_3$ were prepared by dissolving pellets in HFIP, followed by addition of $CDCl_3$. Solution ^{13}C spectra were collected on a Varian ^{UNITY}INOVA NMR spectrometer operating at a frequency of 125.7 MHz. Routine acquisitions were obtained using a 1.3 second acquisition time, a 45° pulse width of 2.9 µs, and a 1 second recycle delay. The number of accumulate transients ranged from 15,000 to 30,000, involving 12-24 hour collection times. Spectra were recorded at 25 °C. Data was zero-filled up to 256k points and filtered with 1 Hz of line broadening prior to application of Fourier transformation. Baselines were corrected using a 10th order polynomial.

Viscometry. Solutions containing 0.5 g/dL of polymer in concentrated sulfuric acid were made to obtain a single point intrinsic viscosity (IV). The solutions were prepared by adding 0.25 grams of polymer and 25 mL of concentrated sulfuric acid into a 50 mL flask. After 12 hours of mixing using magnetic stirring, the solutions were diluted with an additional 25 mL of sulfuric acid, and stirring was continued for another 12 hours. If gelled material was visibly present, the samples were passed through a funnel packed with glass wool. Measurements were obtained using a Cannon viscometer in a 25

°C controlled water bath. The viscometer was washed with sulfuric acid and a portion of the next sample to be tested before measurements were recorded. Flow times were an average of three measurements that agree within +/- 0.2 seconds. Flow times of concentrated sulfuric acid and polymer solution were used to calculate the specific and relative viscosities. Single point IV's were then calculated using the Solomon and Ciuta relationship;

$$[\eta] = [(2*(\eta_{sp} - \ln(\eta_{rel}))]^{1/2})]/C$$

where η_{sp} is specific viscosity, η_{rel} is relative viscosity, and C is sample concentration.[17]

Results and Discussion

Synthesis and Intrinsic Viscosity

The synthesis scheme of PA-12,T is depicted in Figure 1.1. PA-12,T salt was first synthesized by creating a saturated solution in boiling water followed by addition of ethanol. After cooling, the precipitated salt was then recrystallized using a water/ethanol mixture. The salt had a sharp melting point of 271.9 °C and enthalpy of 428 J/g as observed by differential scanning calorimetry.

Melt condensation polymerizations were performed using a three stage method shown in Figure 1.2. After purging with nitrogen, the reactor is sealed for the first two stages, and vented during the third. During the first stage, the temperature remains at approximately 120 °C at 125 kPa while the water boils from the reaction. Following boiling, the temperature begins to rise, and the pressure is increased 1724 kPa in order to mitigate loss of 1,12-diaminododecane due to volatilization during the early stages of the reaction. The release of the high pressure marks the final stage of the reaction at 275 °C. In the hold stage, reaction temperature is increased to approximately 315 °C, and held for

15 minutes. The DSC first heating melting temperature of PA-12,T is 295 °C, ensuring

that the polymer is in the molten state during the hold stage of the polymerization.
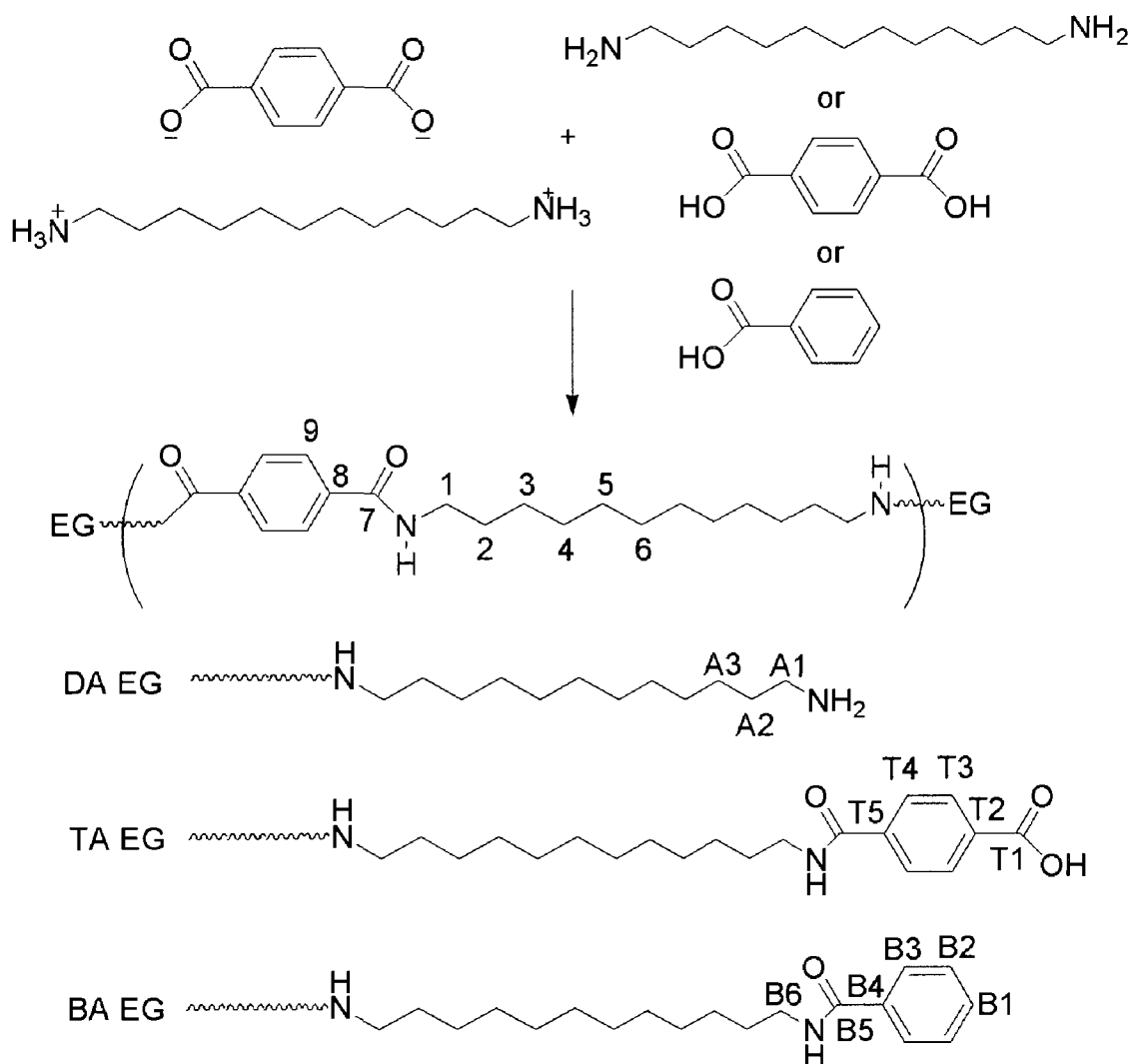
Figure 1.1. Synthesis of PA-12,T showing ^{13}C NMR end group (EG) spectral

assignments.
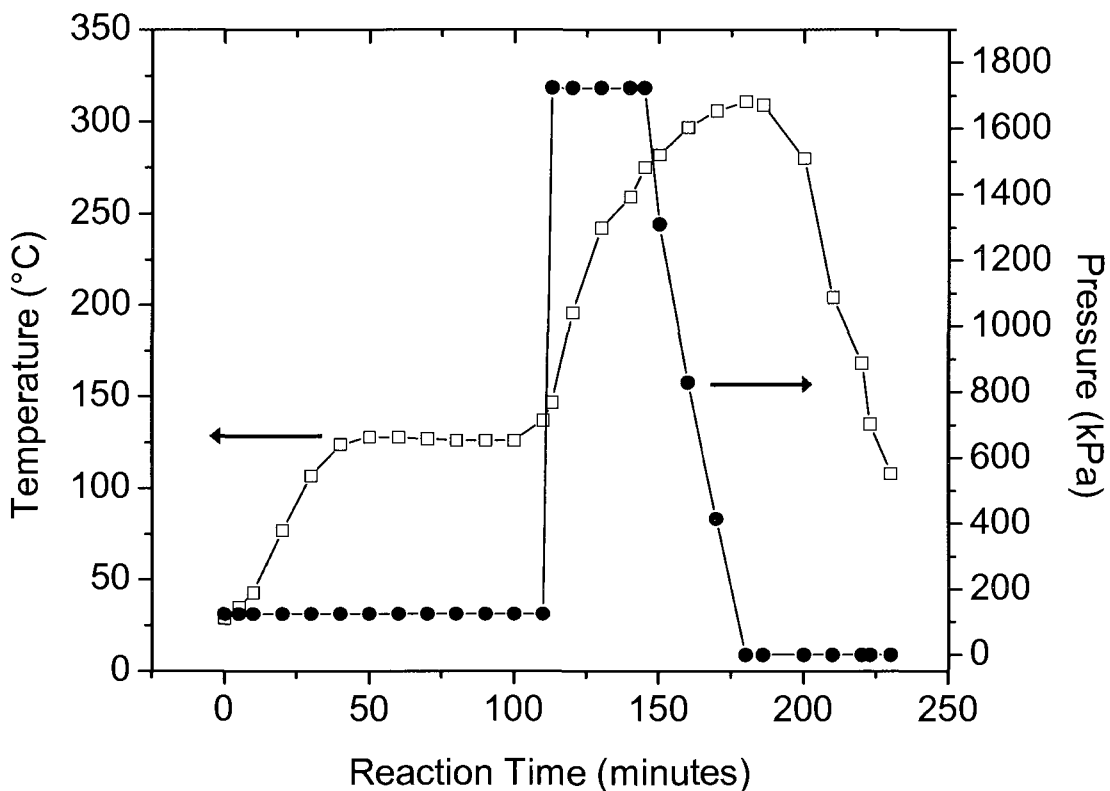
Figure 1.2. Temperature (□) and pressure (●) profiles of PA-12,T melt condensation

polymerization.

PA-12,T was synthesized using 0, 1, 3, 5, and 10 mol-% excess of 1,12-

diaminododecane (DA), terephthalic acid (TA), or benzoic acid (BA). Single-point IV

measurements of the resulting polymers are shown in Figure 1.3. The melt condensation

polymerization of pure 12,T salt using the standard process yields PA-12,T with an IV of

1.25 dL/g. Adding 1 and 3 mol-% excess DA to the reaction increases IV to 1.36 and

1.31 dL/g, respectively. However, DA in excess of 3 mol-% results in products with

lower IVs of 1.08 and 0.70 dL/g for 5 and 10 mol-% excess DA, respectively. The PA-

12,T salt is stoichiometrically balanced prior to the polymerization, and should yield the

highest molecular weight, but IV results indicate that PA-12,T synthesized using 1 and

3% excess DA have higher IV's and inherently higher molecular weights. Since 1,12-

diaminododecane boils at a lower temperature than terephthalic acid, an imbalance occurs during the polymerization. The addition of 1 and 3% DA compensates for this imbalance resulting in higher molecular weight. Adding 1 and 3 excess mol-% TA, however, decreases IV to 0.94 and 0.67 dL/g, respectively. Here, any excess TA contributes to the imbalance imposed by volatilization of DA and thus further decreases the molecular weight. Despite their differences in functionality, BA and TA appear to reduce IV to a similar extent at all concentrations.
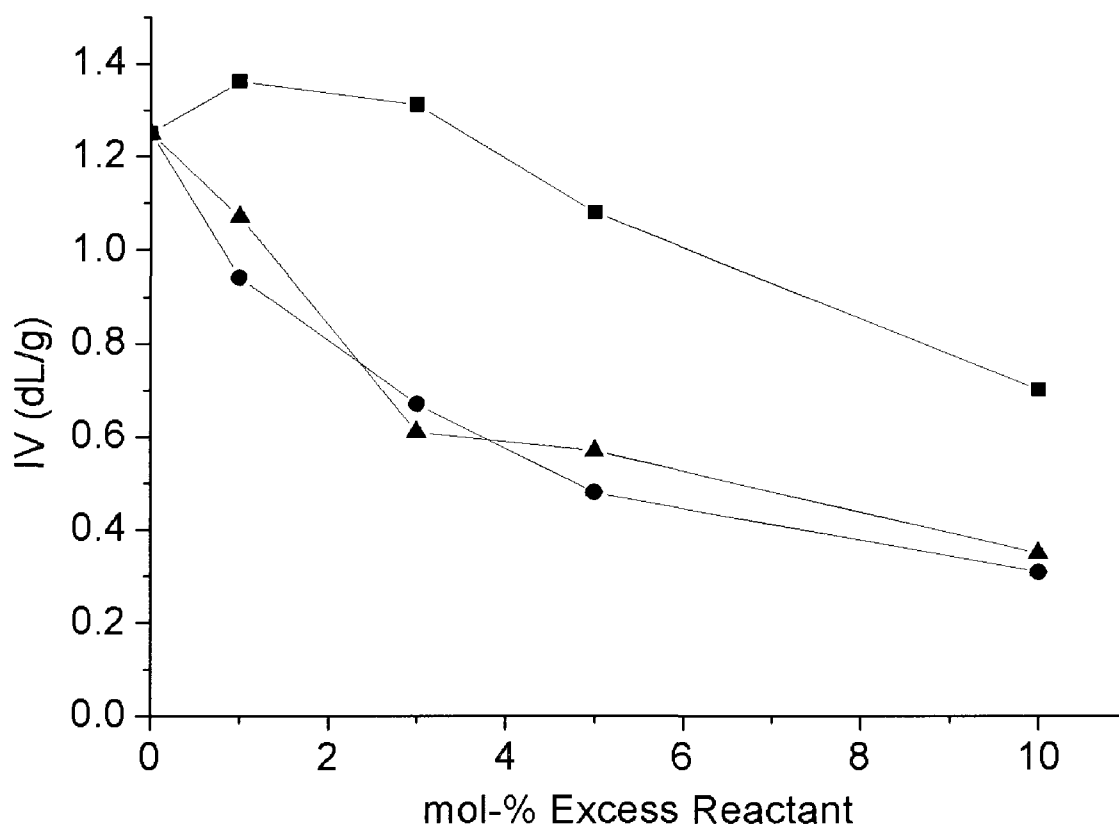
Figure 1.3. Single point intrinsic viscosities of PA-12,T salt polymerized with 1,12-diaminododecane (●), terephthalic acid (■), and benzoic acid (▲).

High Resolution Solution ^{13}C NMR Spectroscopy

Figures 1.4-1.6 show 0-200 ppm solution NMR spectra for each family of polymers. Backbone carbon atoms appear as intense peaks at expected chemical shifts.

Assignments for repeat units and anticipated end groups are shown in Figure 1.1. Additionally, three sets of solvent peaks are present in each spectrum and labeled accordingly. Vertical scales for each spectrum have been adjusted to maximize the intensity of the tallest polymer peak without truncation. These data confirm the identity of each polymer main chain as poly(dodecamethylene terephthalamide).

Horizontal and vertical scales have been expanded in Figures 1.7-1.15 to show end groups and other less populous peaks. Here the vertical scales in the aliphatic, aromatic and carbonyl regions have been normalized with respect to backbone carbon atoms **1**, **9**, and **7** respectively, in order to determine trends in the lesser peaks. Main chain carbon atoms appear as relatively broad, truncated peaks in these figures.

Figure 1.7 contains 3 peaks at 42.3 (**A1**), 27.8 (**A2**), and 26.2 (**A3**) ppm with intensities directly proportional to the concentration of excess DA present in starting materials. As excess DA increases from 0 to 10 mol-%, the relative intensity of these peaks (measured as peak heights) as compared to main chain peak **1** increases from 0 to 5.3%. For all concentrations of excess TA, these resonances are not observed (Figure 1.10). This behavior confirms their identities as amine end groups **A1**, **A2**, and **A3**. With specific assignments based on previous work on PA-6,6 and PA-12 materials.[17]

Figure 1.11 shows 4 peaks at 127.6 (**T4**), 131.5 (**T3**), 132.6 (**T5**), and 139.3 (**T2**) ppm with intensities directly proportional to the concentration of excess TA present in starting materials. As excess TA increases from 0 to 10 mol-%, the intensity of these peaks relative to main chain peak **9** increases from 1.5 to 10.7%, while the same resonances in Figure 1.8 are shown to be inversely proportional to molar excess DA. Additional peaks in the carbonyl region (Figure 1.9 and Figure 1.12) follow similar

trends with intensities directly proportional to excess acid concentration and inversely proportional to excess diamine concentration. This behavior confirms their assignments as acid end groups. Chemical shifts for peaks **T2** and **T4** are within 1 ppm of those reported by Hall and others[18] using HFIP as an NMR solvent to observe end groups of other terephthalic acid containing polyamides. However, **T3** and **T5** are different from those reported by Hall by 1-3 ppm. Two possible reasons are: 1) spectra in this study were acquired using a mixed solvent system, and 2) end group chemical shifts are sensitive to pH altered by changes in concentration of acid and amine end groups themselves.[18,20]

In Figure 1.14, the intensity of terephthalic end group peak **T3** increases from 1.47 to 5.16% relative to terephthalic main chain peak **9** as excess BA is increased from 0 to 10 mol-%. This increase in end group intensity is due to a corresponding decrease in number average molecular weight as the concentration of monofunctional BA increases. In addition to terephthalic end group peaks, 4 new peaks appear in the aromatic region at 133.6 (**B1**), 132.8 (**B4**), 129.9 (**B3**), and 127.4 (**B2**) ppm, a single new peak appears in the aliphatic region at 42.0 (**B6**) ppm (Figure 1.13), and a single new peak in the carbonyl region appears at 173.2 ppm (Figure 1.15). The peak at 129.9 ppm increases from 0 to 5.61% as the concentration of BA increases from 0 to 10 mol-%. Based on these trend resonances, these are assigned to benzamide end groups. This is further supported by previous work of Hall and others[20]; their assignments agree with our results within +/- 1 ppm. Chemical shifts of BA peaks in these systems are within 1 ppm of assignments
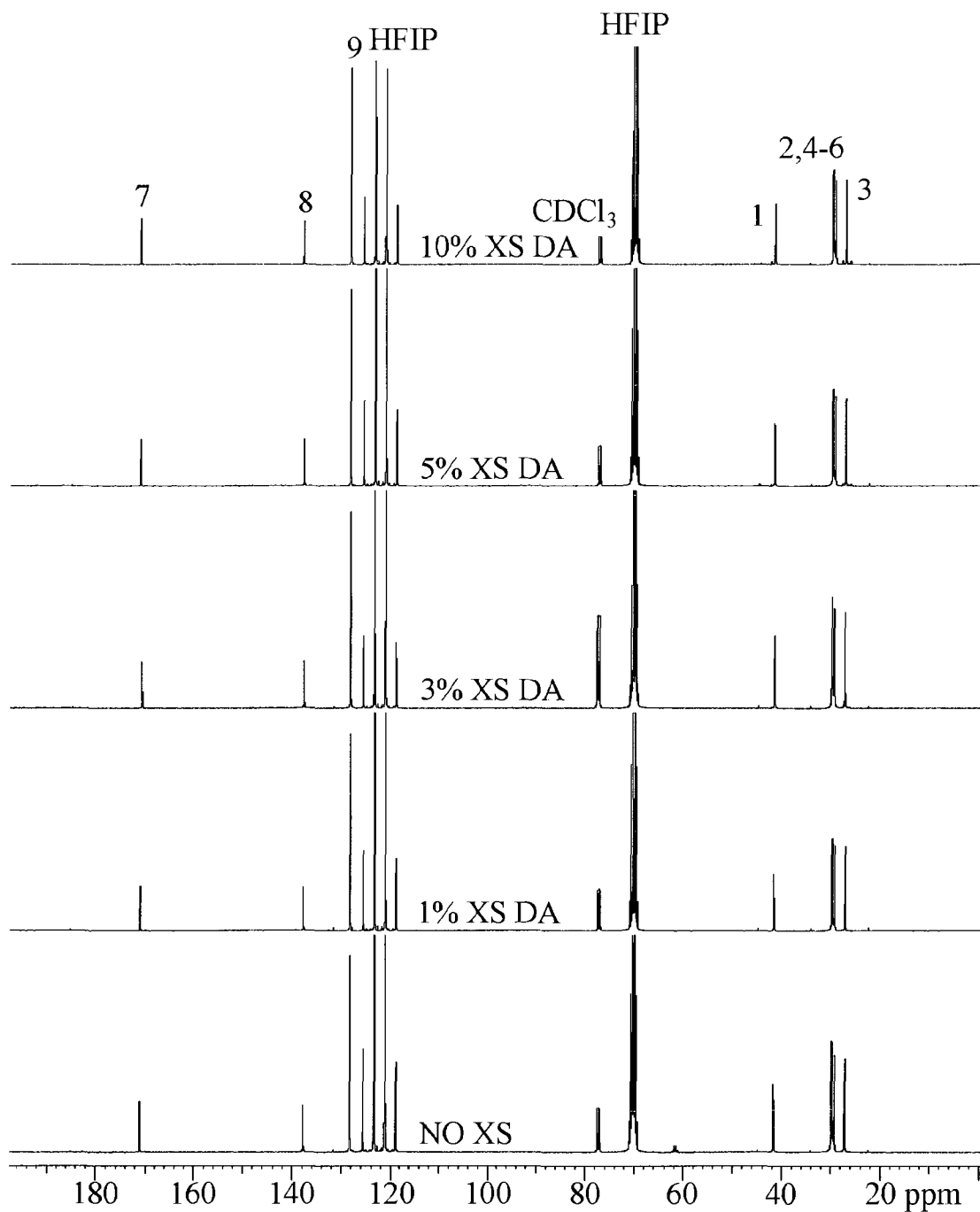
Figure 1.4. Solution ^{13}C NMR spectra of polymers synthesized from starting materials containing 0, 1, 3, 5, and 10 mol-% excess 1,12-diaminododecane (XS DA). Vertical scales for each spectrum have been adjusted to maximize polymer peak intensities without truncation.
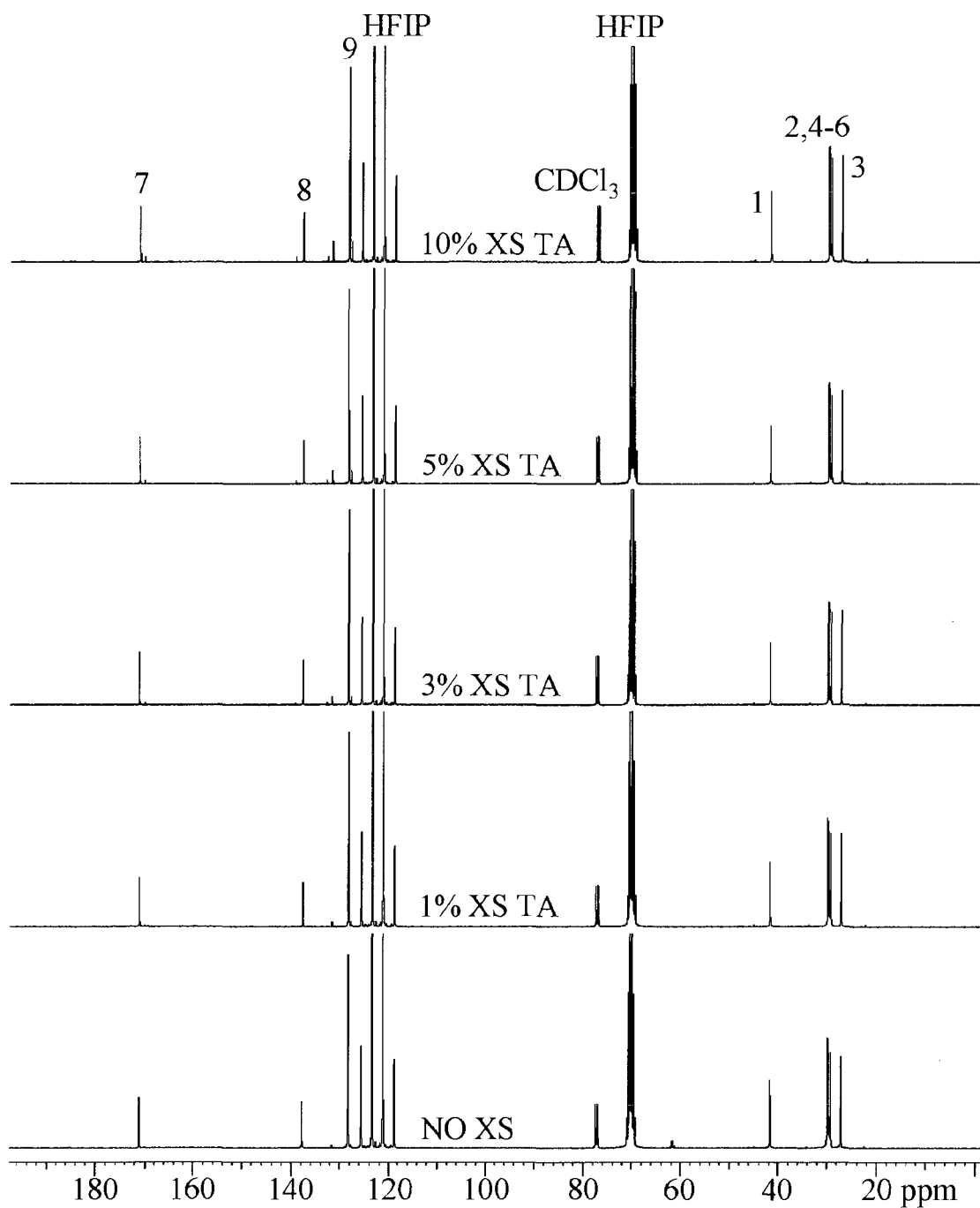
Figure 1.5. Solution ^{13}C NMR spectra of polymers synthesized from starting materials

containing 0, 1, 3, 5, and 10 mol-% excess terephthalic acid (XS TA). Vertical scales for

each spectrum have been adjusted to maximize polymer peak intensities without

truncation.
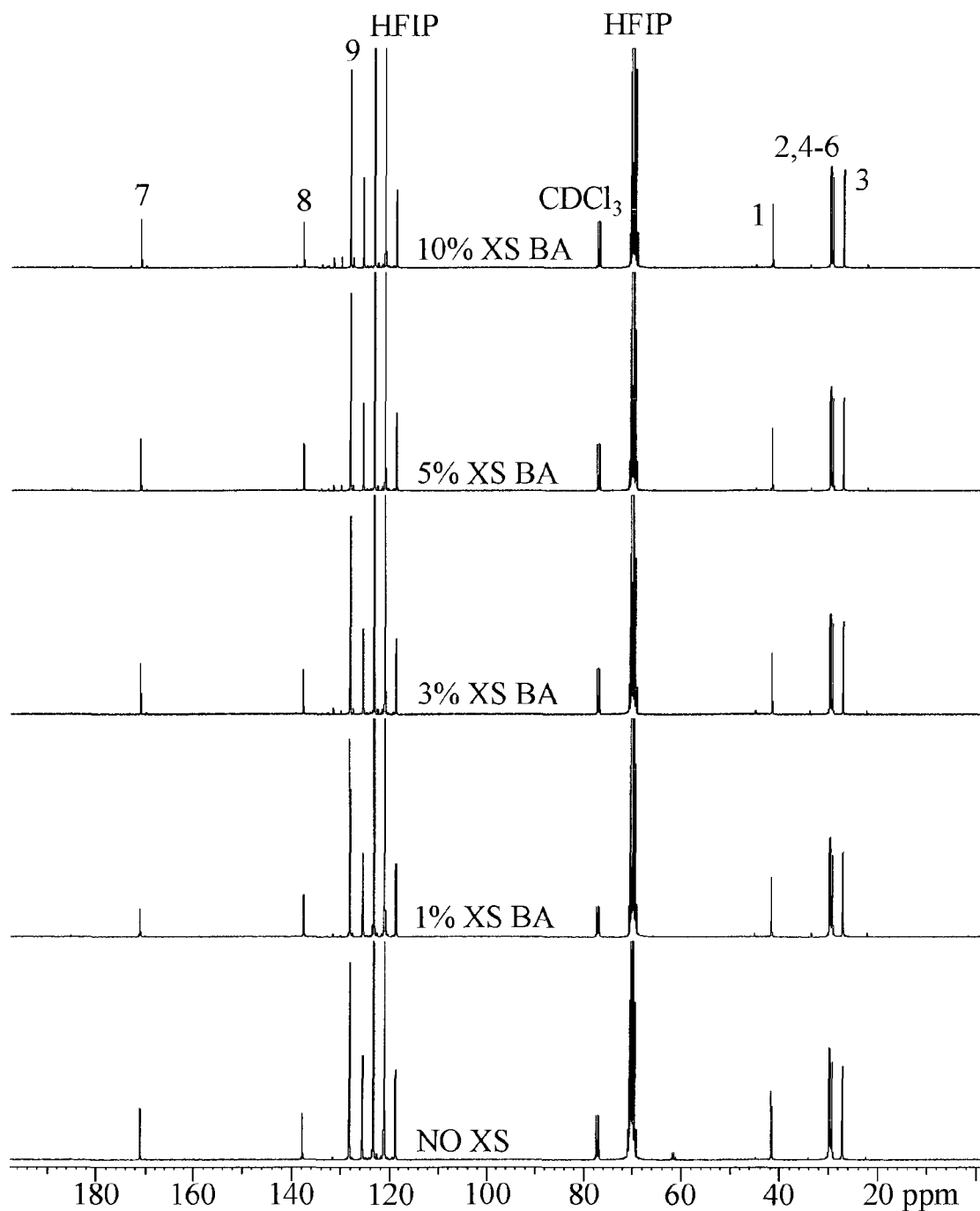
Figure 1.6. Solution ^{13}C NMR spectra of polymers synthesized from starting materials containing 0, 1, 3, 5, and 10 mol-% excess benzoic acid (XS BA). Vertical scales for each spectrum have been adjusted to maximize polymer peak intensities without truncation.
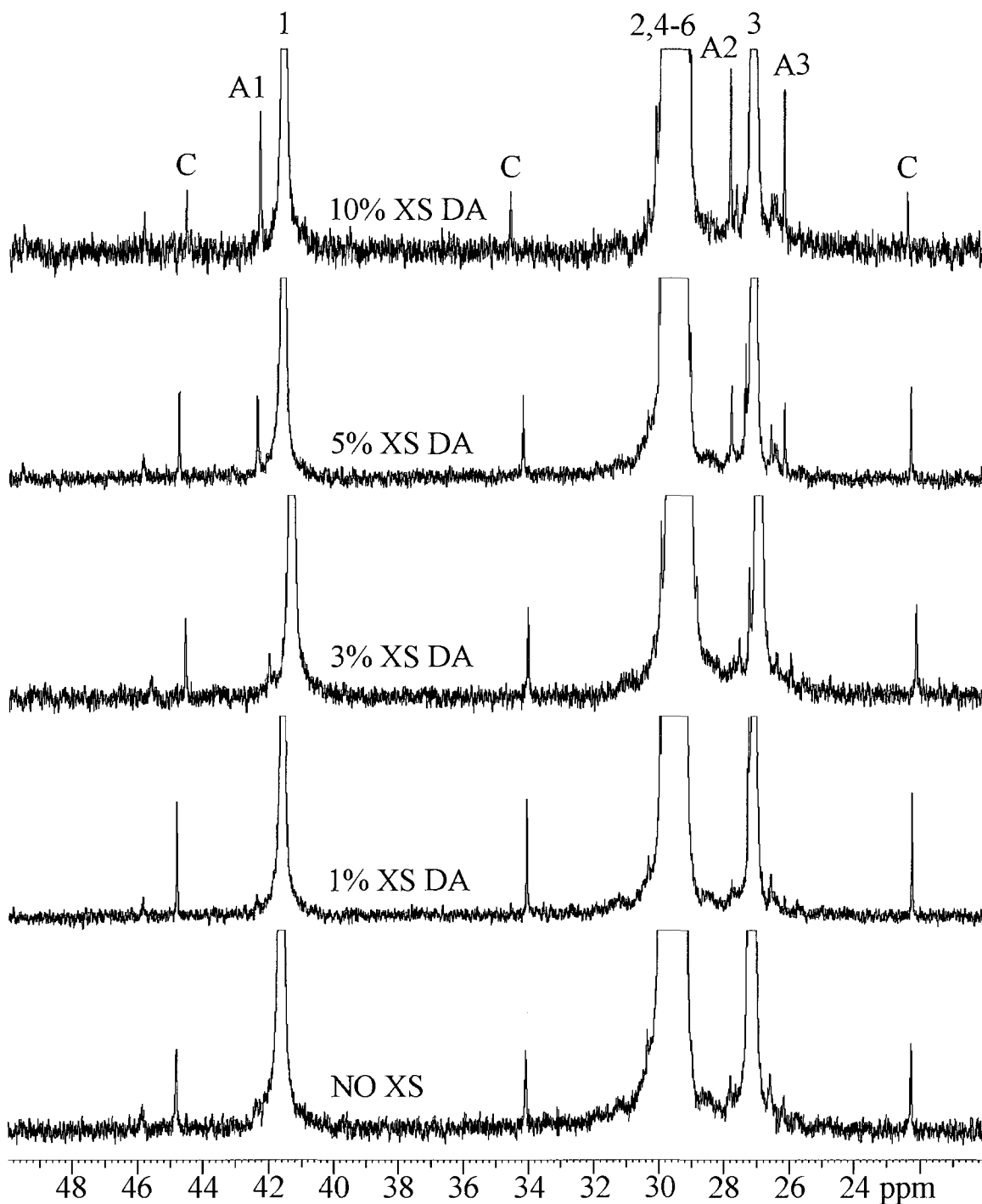
Figure 1.7. Aliphatic region of solution ^{13}C NMR spectra for polymers synthesized from starting materials containing 0, 1, 3, 5, and 10 mol-% excess diaminododecane (XS DA). Peak intensities are normalized with respect to backbone carbon **1**.
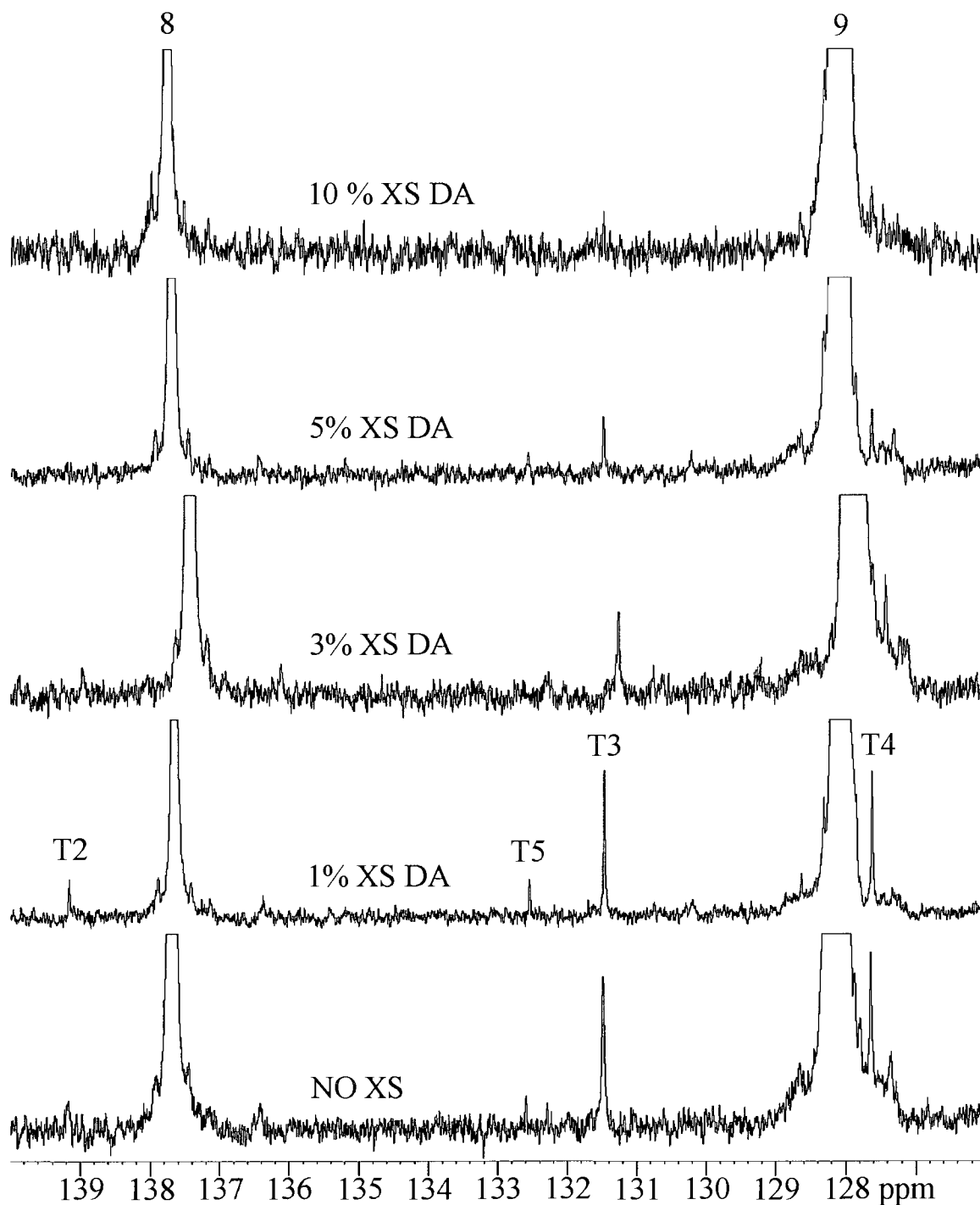
Figure 1.8. Aromatic region of solution ^{13}C NMR spectra for polymers synthesized from

starting materials containing 0, 1, 3, 5, and 10 mol-% excess diaminododecane (XS DA).

Peak intensities are normalized with respect to backbone carbon **9**.

7

10% XS DA

5% XS DA

3% XS DA

1% XS DA

NO XS

T1

188 186 184 182 180 178 176 174 172 170 168 166 164 ppm
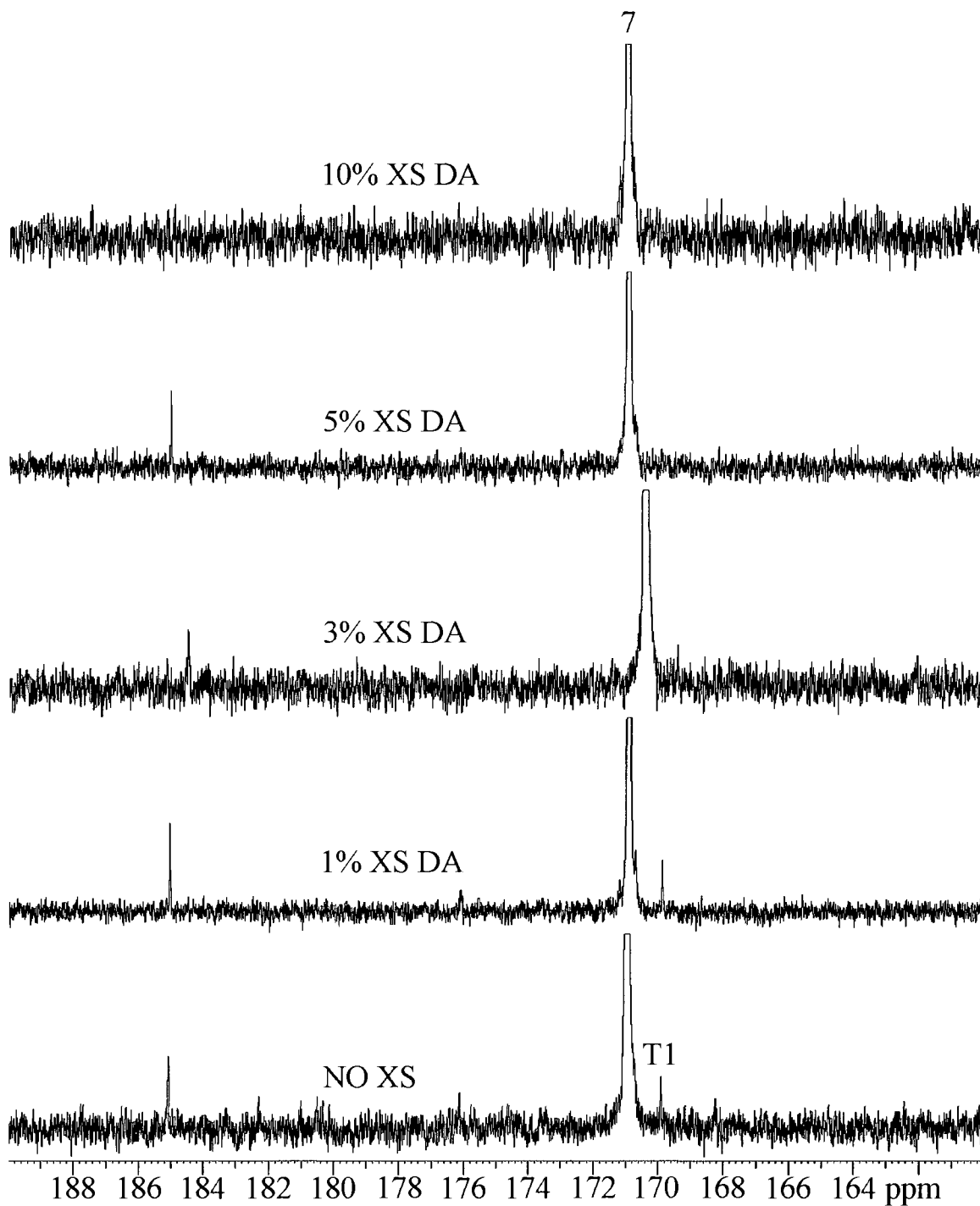
Figure 1.9. Carbonyl region of solution ^{13}C NMR spectra for polymers synthesized from

starting materials containing 0, 1, 3, 5, and 10 mol-% excess diaminododecane (XS DA).

Peak intensities are normalized with respect to backbone carbon **7**.
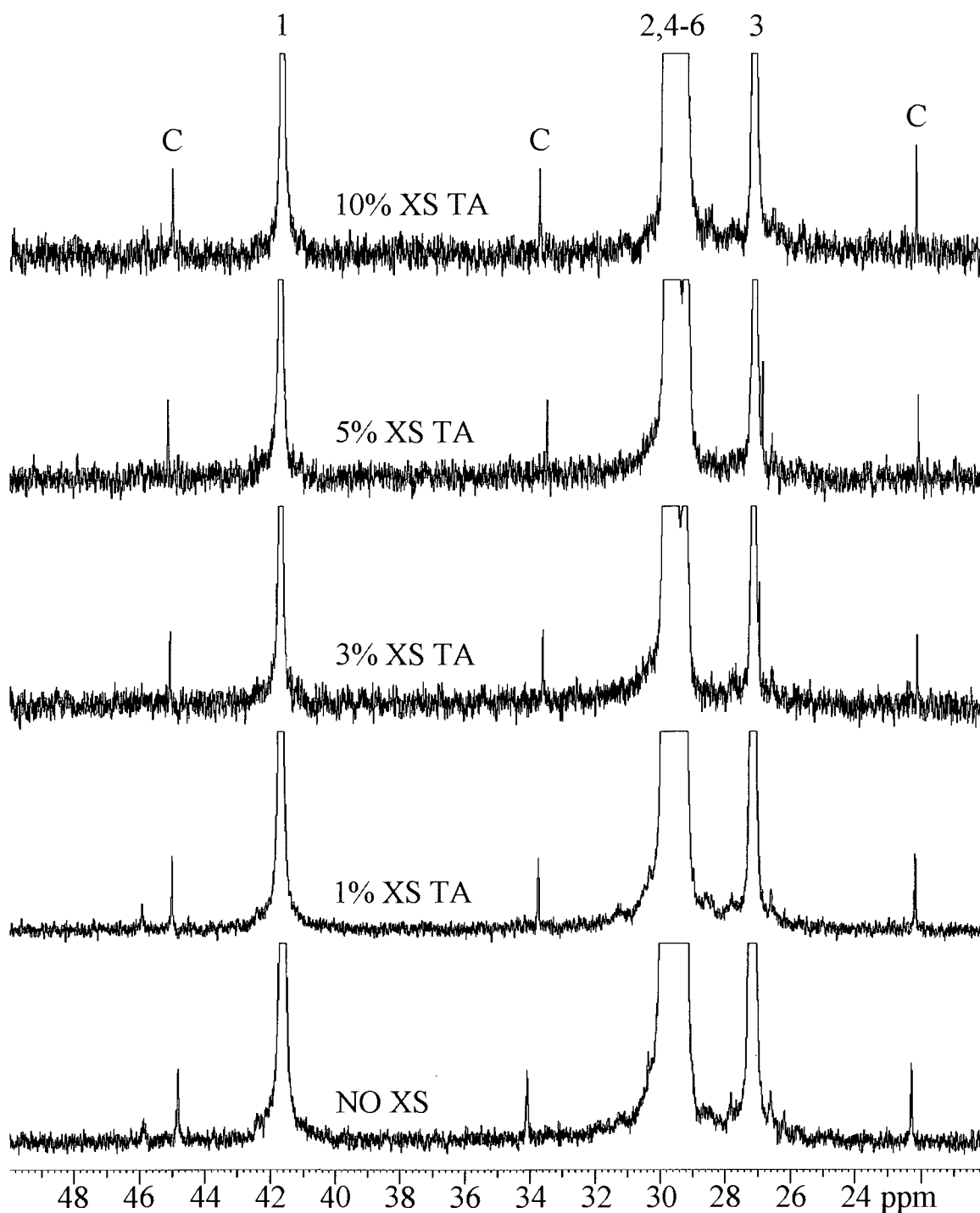
Figure 1.10. Aliphatic region of solution ^{13}C NMR spectra for polymers synthesized

from starting materials containing 0, 1, 3, 5, and 10 mol-% excess terephthalic acid (XS

TA). Peak intensities are normalized with respect to backbone carbon **1**.
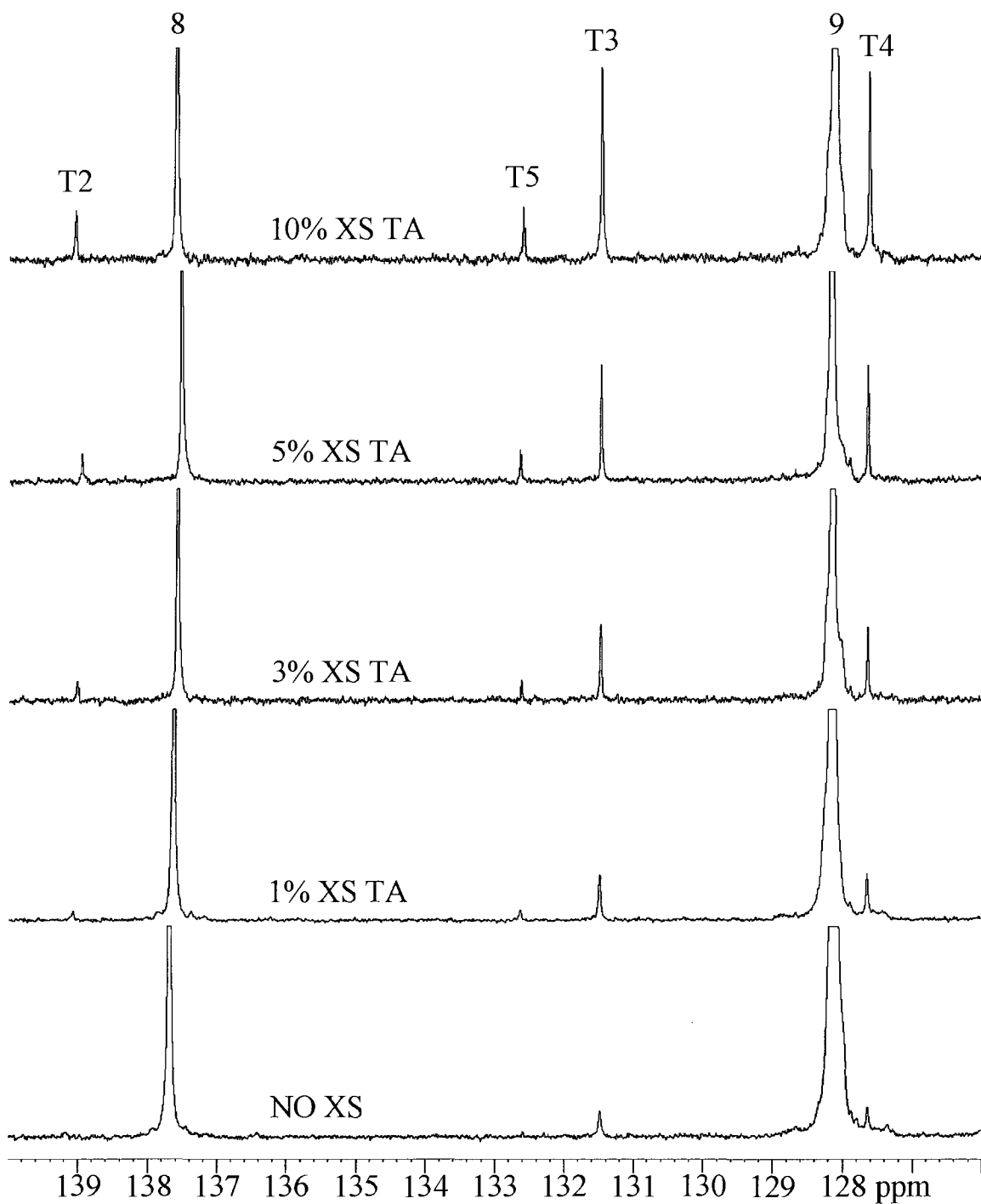
Figure 1.11. Aromatic region of solution ^{13}C NMR spectra for polymers synthesized

from starting materials containing 0, 1, 3, 5, and 10 mol-% excess terephthalic acid (XS

TA). Peak intensities are normalized with respect to backbone carbon **9**.
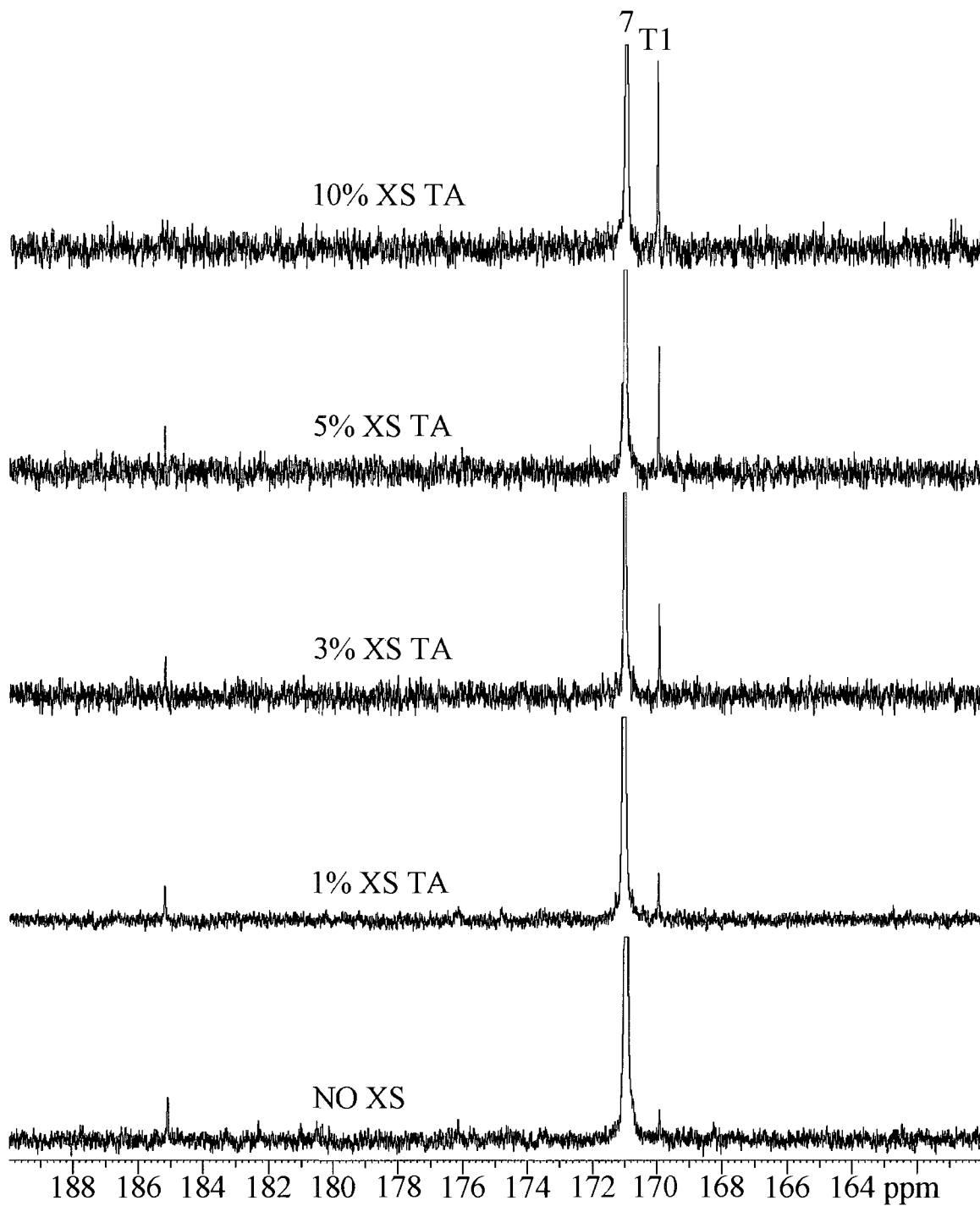
Figure 1.12. Carbonyl region of solution ^{13}C NMR spectra for polymers synthesized

from starting materials containing 0, 1, 3, 5, and 10 mol-% excess terephthalic acid (XS

TA). Peak intensities are normalized with respect to backbone carbon **7**.
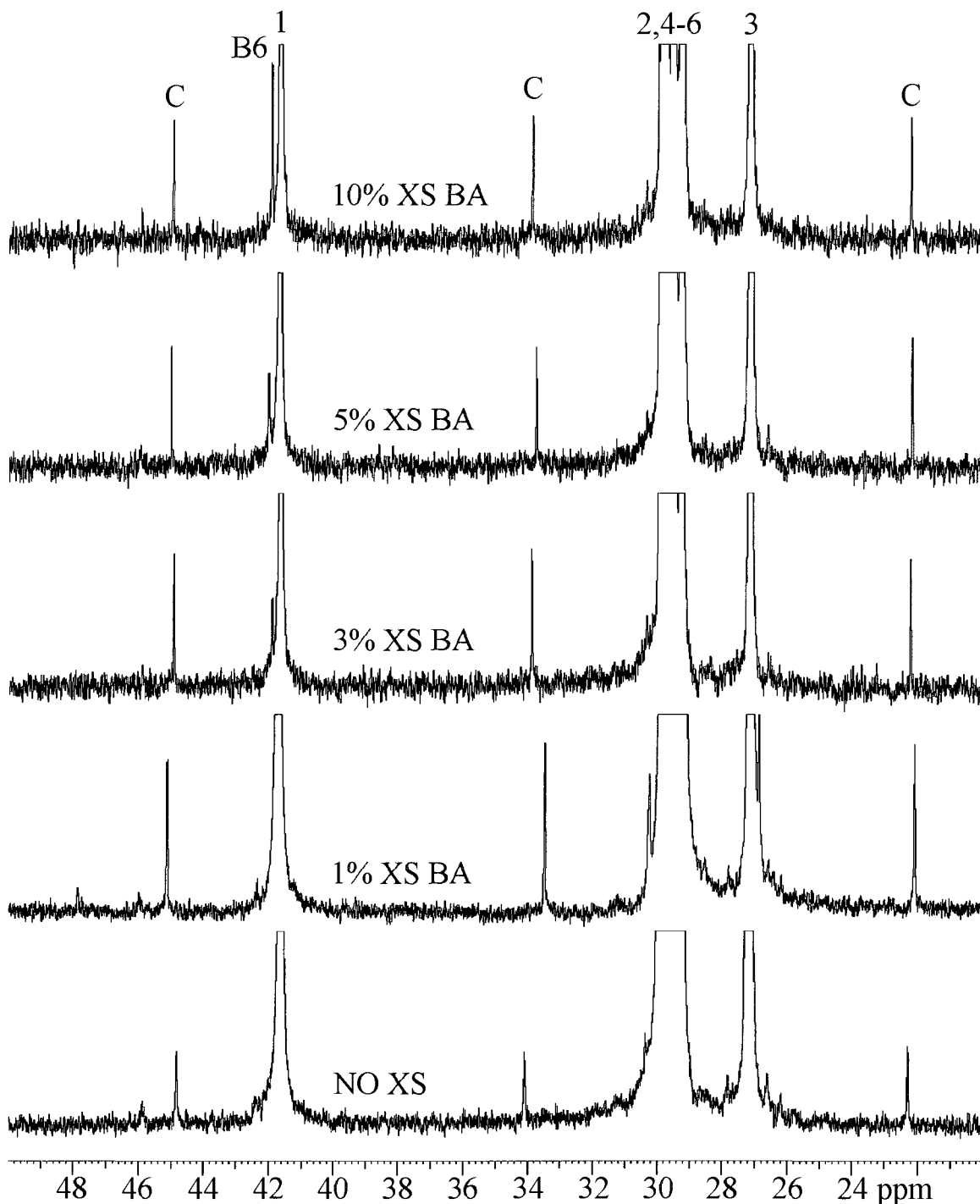
Figure 1.13. Aliphatic region of solution ^{13}C NMR spectra for polymers synthesized

from starting materials containing 0, 1, 3, 5, and 10 mol-% excess 1,12-diaminododecane

(XS BA). Peak intensities are normalized with respect to backbone carbon **1**.
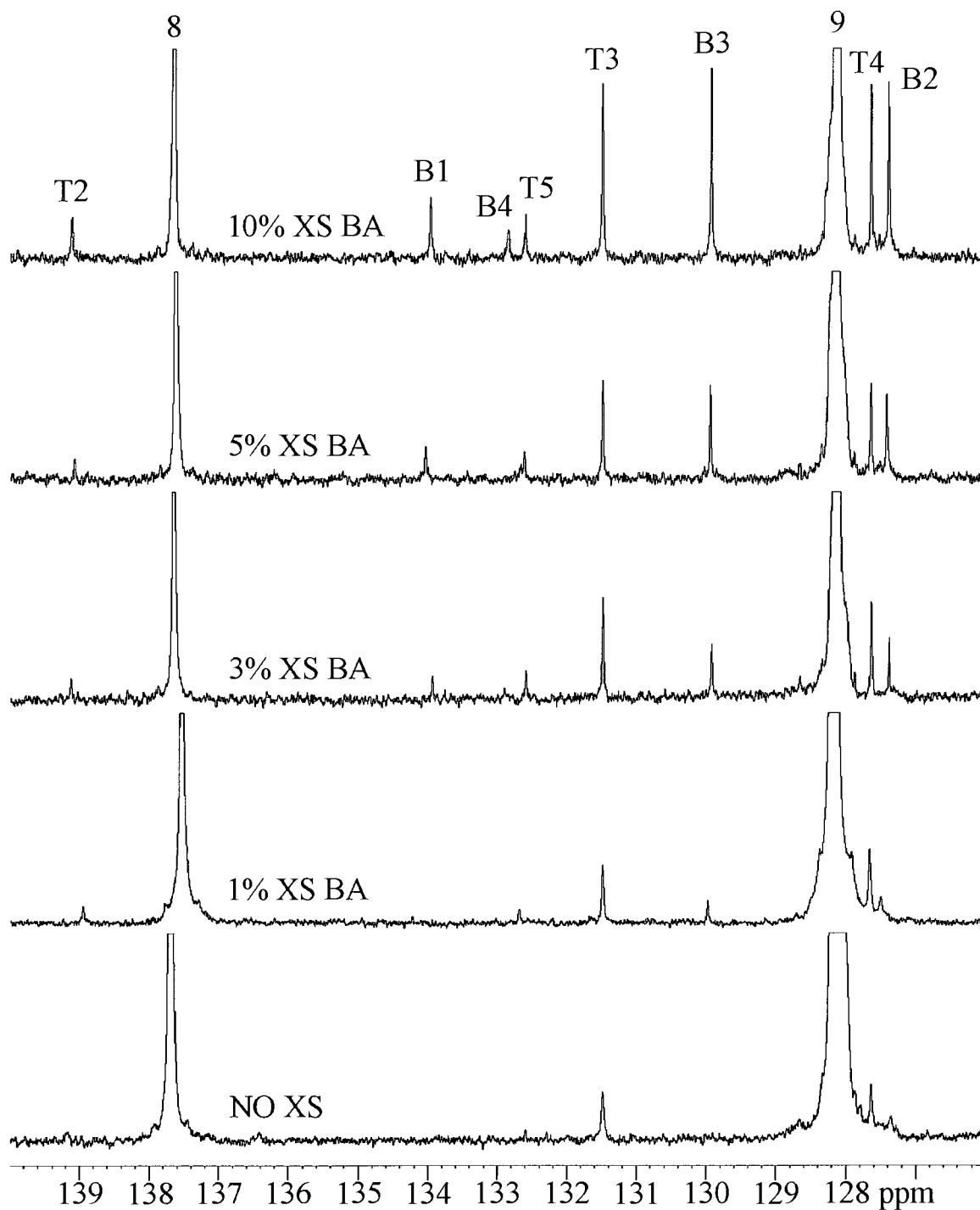
Figure 1.14. Aromatic region of solution ^{13}C NMR spectra for polymers synthesized from starting materials containing 0, 1, 3, 5, and 10 mol-% excess 1,12-diaminododecane (XS BA). Peak intensities are normalized with respect to backbone carbon **9**.
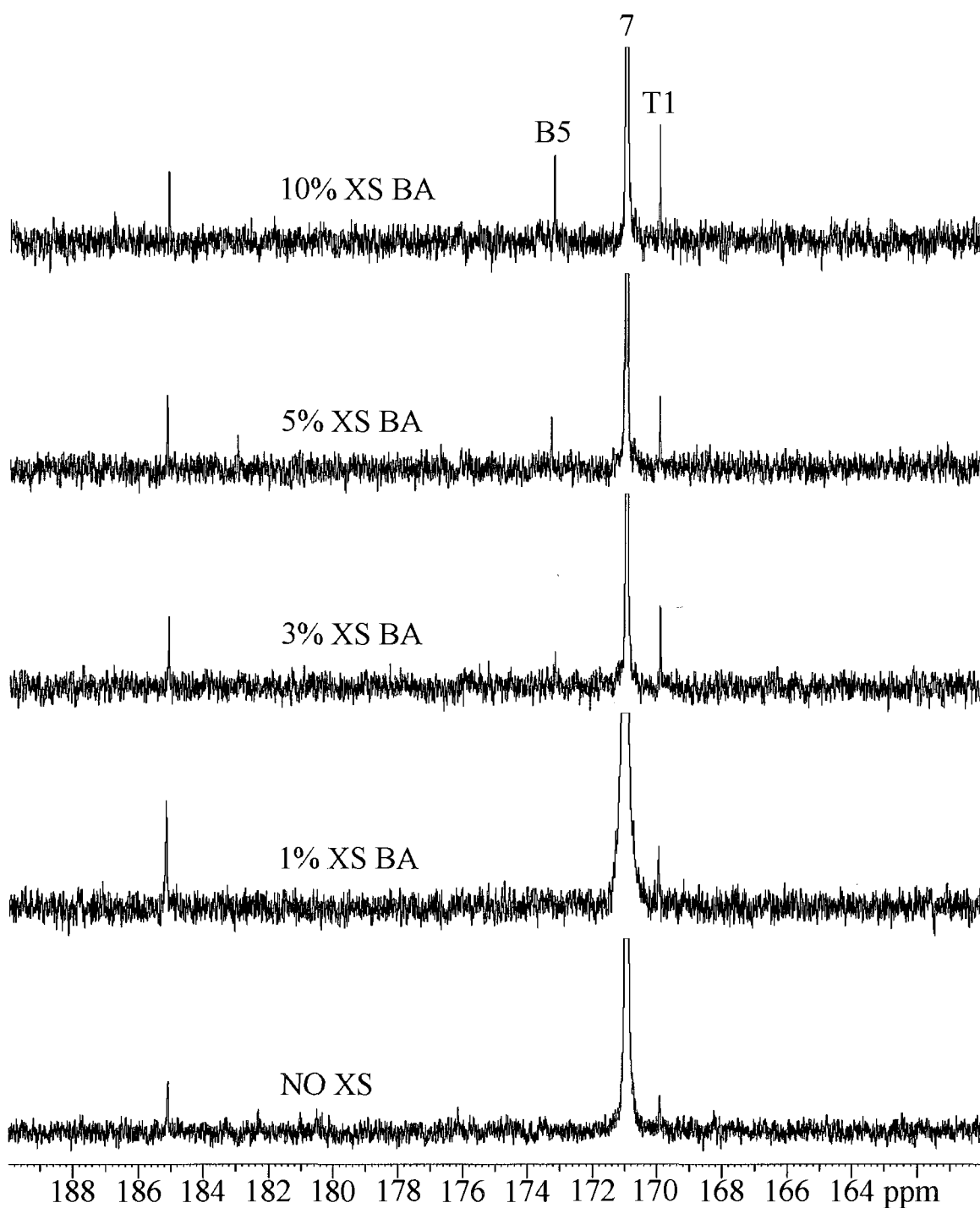
Figure 1.15. Carbonyl region of solution ^{13}C NMR spectra for polymers obtained from starting materials containing 0, 1, 3, 5, and 10 mol-% excess 1,12-diaminododecane (XS BA). Peak intensities are normalized with respect to backbone carbon **7**.

All NMR samples analyzed exhibited three equally intense peaks at 44.9 (**C**), 33.9 (**C**), and 22.2 (**C**) ppm which fluctuated between 2.3 and 6.3% (average 3.9%). The only apparent trend is that they are more pronounced for polymers containing excess BA (5.5% average intensity) as compared to those containing no excess (3.2% average intensity). However, the significance of this data is uncertain. These peaks are not consistent with NMR spectra of monomer and do not behave like end groups. Other possibilities include the presence of cyclical structures or *cis* amide repeat units. Figures 1.9, 1.12, and 1.15 show a peak at 185.2 ppm that also exhibits anomalous behavior. It is present in all spectra except for products formed using 10 mol-% excess diamine or diacid in their starting materials. Its identity is unconfirmed to date.

End Group Concentrations and Molecular Weights

End group concentrations relative to the polymer main chain peaks were calculated by NMR analysis using the equation;

$$[EG] = I_{EG}/[(I_1/2 + I_9/4)/2]$$

where $I_{EG} = I_{A1}$ or $I_{T3}/2$ or $I_{B3}/2$. Figure 1.16 displays a plot of total end group concentration [EG] and IV as a function of excess DA and TA. Note that the positive and negative x-axis values refer to the mol-% excess or deficiency of DA. For all samples, end group concentration is inversely proportional to IV. For example, the product synthesized with 10 mol-% excess TA has the lowest IV and the highest [EG]. As amount of excess TA is decreased from 10 to 0 mol-%, [EG] decreases and IV increases progressively. A similar trend is apparent as excess DA decreases from 10 to 3 mol-%. However, there is a large difference in IV and [EG] between samples containing 10 mol-% excess DA and TA. This deviates from traditional step-growth theory which predicts

that an equivalent imbalance of either the A-A or B-B monomer similarly affects

molecular weight. Further deviation from theory is apparent in the fact that products

synthesized with 1 and 3 mol-% excess DA had higher IVs than products of pure salt.
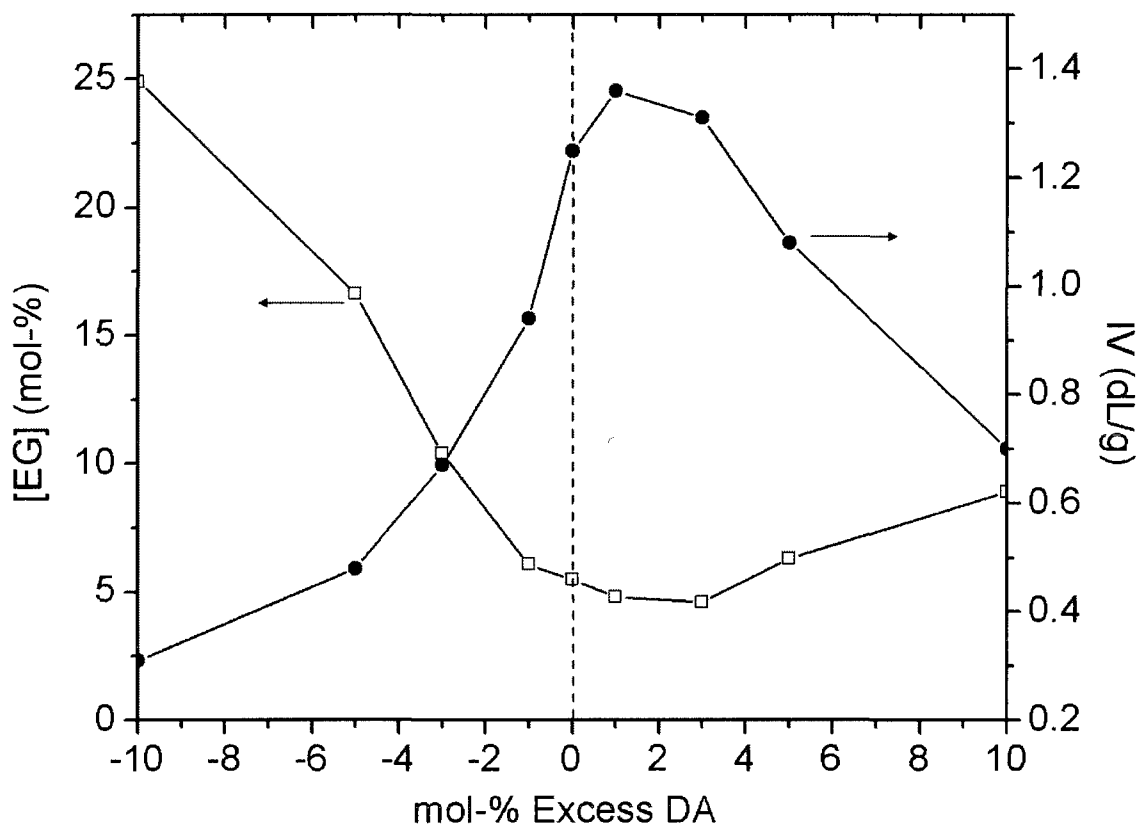
Figure 1.16. Total end group concentration by ^{13}C NMR (□) and IV (●) of PA-12,T

synthesized with excess DA (positive values) and excess TA (negative values of DA).
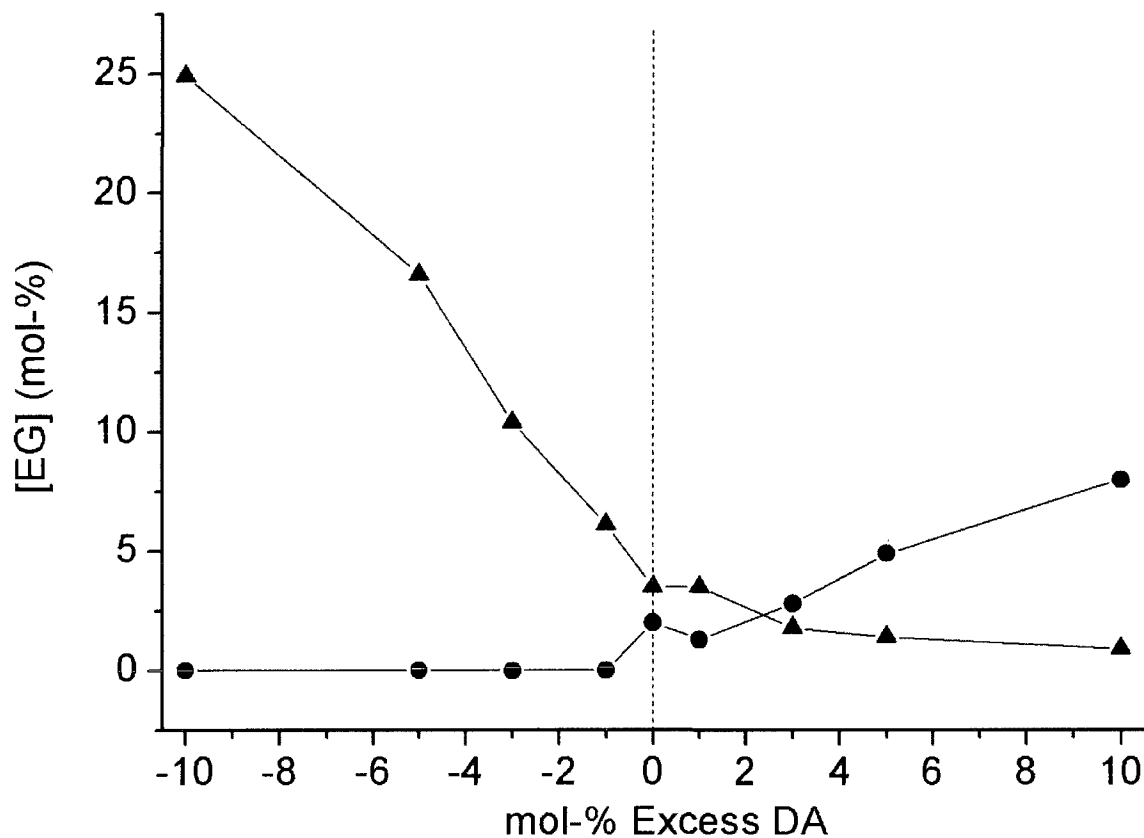
Figure 1.17: Acid (▲) and amine (●) end group concentrations of PA-12,T synthesized with excess DA (positive values) and TA (negative values)

Figure 1.17 shows the concentration of amine and acid end groups as a function of excess DA and TA. No amine end groups were observed for all concentrations of excess TA, therefore, these reactions have reached maximum attainable conversion. With excess TA, molecular weight advances to a point where DA is completely reacted or volatilized, resulting in polymer with total acid end groups. Higher molecular weight is obtained by decreasing amount of excess terephthalic acid, thus lowering acid (total) [EG].

Pure PA-12,T salt and excess DA products have both acid and amine end groups. These reactions have not reached full conversion and are still in an equilibrium state within the given polymerization conditions. The majority of end groups are acid at 1 mol-

% excess DA, while amine end groups are the majority at 3 mol-% DA. Recall that these compositions have the highest IV and the lowest total end group concentration. Interpolation of Figure 1.17 reveals that end group functionality would be balanced yielding the highest molecular weight with approximately 2.4 mol-% excess DA. Without determining the equilibrium constant specifically, qualitative observations show that the highest equilibrium molecular weight would be obtained close to this value. This data suggests that maximum molecular weight is achieved when the stoichiometry of the product is balanced, which is not necessarily the same as balancing the stoichiometry of the initial reactants. This is due to the volatilization of diamine from the reaction and IV and ^{13}C NMR have shown in agreement that adding between 1 and 3 mol-% excess diamine accounts for this loss, resulting in the highest molecular weight and most balanced end group functionality.

Total end group concentrations and IV for PA-12,T synthesized with excess BA and TA are presented in Figure 1.18. No amine end groups were detected in polymers synthesized with excess BA or TA. Therefore, reactions have reached total attainable conversion and the total end group concentration is the sum of terephthalic acid and benzamide end groups. As the initial concentration of excess BA and TA increased, the total end group concentration increased and IV decreased. The magnitude of the effects of BA and TA on IV and [EG] were identical on a molar basis despite their different functionality. Thus, the only difference observed between PA-12,T synthesized with excess BA and TA was end group functionality. An excess of 1 mol-% BA yielded polymer containing 71% acid and 29% benzamide end groups.

At 10 mol-% excess BA, the resulting polymer had 48% acid and 52% benzamide end

groups. Differences in the reactivity and polarity of these end groups can affect post

polymerization processes, dyeability[5] and interactions with fillers in composite

materials.[19]
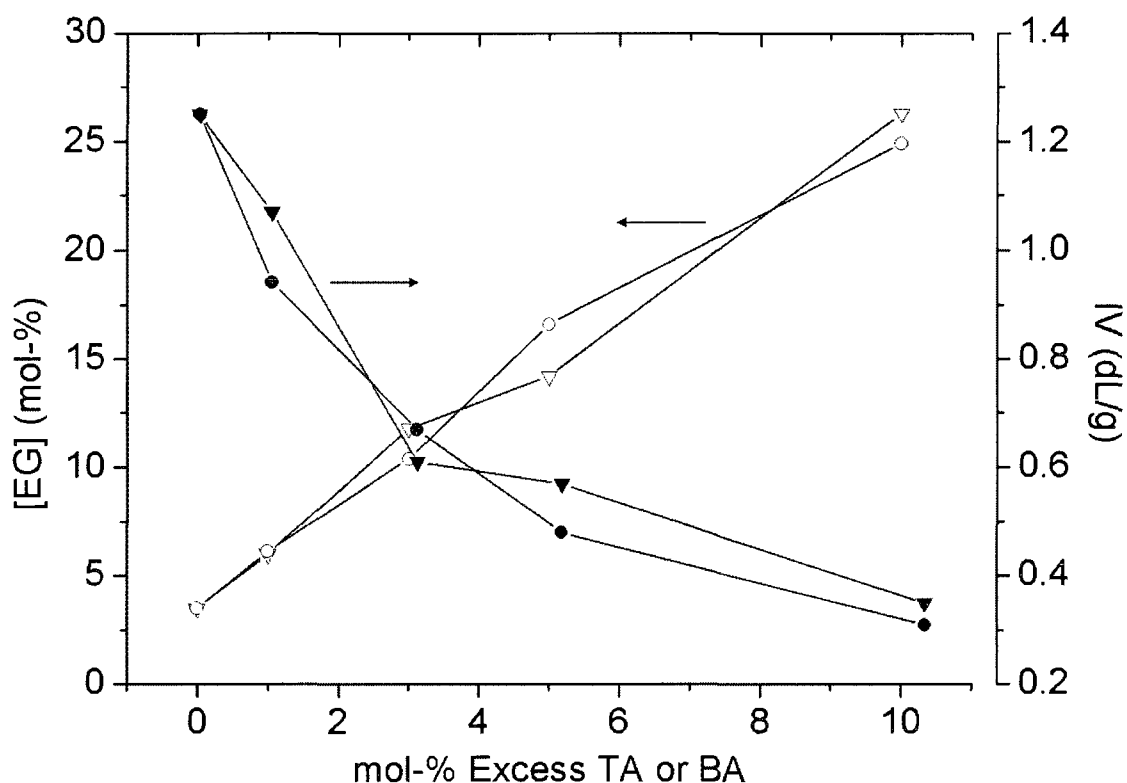
Figure 1.18. IV (solid) and total end group concentration (hollow) for PA-12,T

synthesized with TA ($\bullet$, $\circ$) and BA ($\blacktriangledown$,∇).

Number average molecular weights (M_n) were calculated by multiplying the

molecular weight of the repeat unit for PA-12,T (M_0 = 330.5 g/mol) by the average

degree of polymerization (DP) using the equation;

$$M_n \text{ (g/mol)} = M_0[(I_1/2 + I_9/4)/2] / [(I_{A1} + I_{T3}/2 + I_{B3}/2)/2]$$

The degree of polymerization was calculated by NMR analysis as the ratio of average

main chain repeat units to the sum of end group units. I_1 and I_9 represent the intensity of

amine and acid main chain peaks, respectively, while I_{A1}, I_{T3}, and I_{B3} respectively represent the intensity of amine, terephthalic acid, and benzoic acid end group peaks as assigned in Figure 1.1. M_n versus excess reactant is plotted in Figure 1.19. Similar trends in Figures 1.3 and 1.19 demonstrate strong agreement between IV measurements and M_n calculations based on NMR analysis. Both confirm that 1-3 mol-% excess DA yielded polymers with higher M_n and IV than the product of pure 12,T salt. Both M_n and IV decreased progressively above 3 mol-% excess DA and for all concentrations of excess BA and TA.
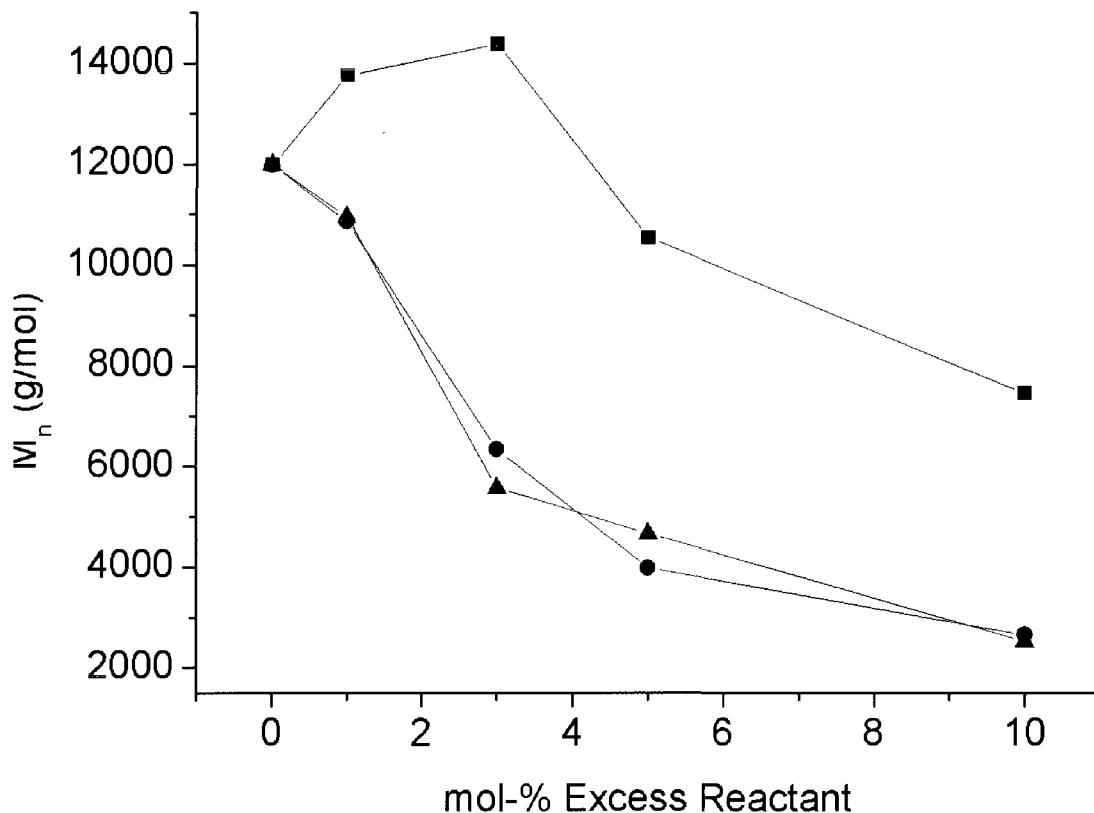
Figure 1.19. PA-12,T number average molecular weights calculated by NMR plotted as a function of mol-% excess 1,12-diaminododecane (■), terephthalic acid (●), or benzoic acid (▲).
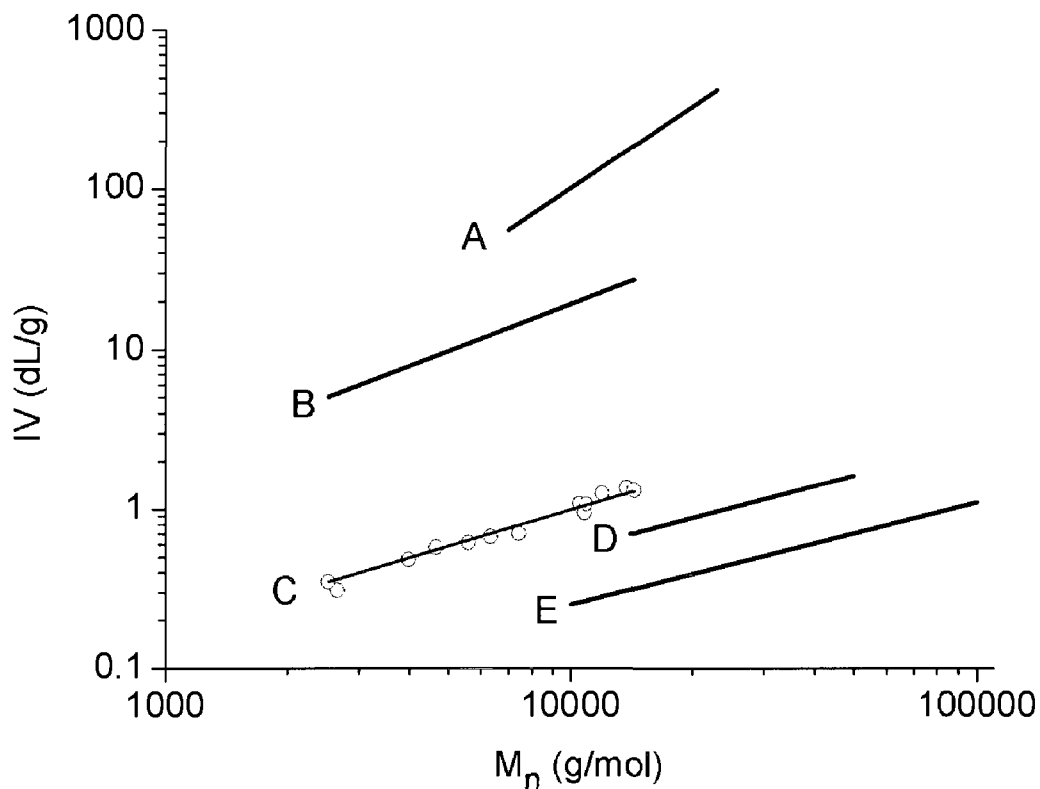
Figure 1.20. Log-Log plot of IV vs. Mn for: A) poly(p-benzamide) (96% sulfuric acid,

20°C)[21]; B) PA-6I (conc. sulfuric acid, 25°C)[22,23]; C) experimental data (○) and best fit

curve for PA-12,T(conc. sulfuric acid, 25°C); D) PA-6,6 (96% sulfuric acid, 25°C)[23]; E)

PA-12 (96% sulfuric acid, 25°C)[23].

Figure 1.20 shows a log-log pot of IV versus M_n with a linear trend for these

polymers. A best fit line was used to calculate Mark-Houwink constants of K=55.8*10^{-5}

dL/g and a = 0.81. The physical significance of these data is a tendency for the net

polymer system to behave more like flexible chains than rigid rods under these

conditions.[20] Sulfuric acid is not a theta solvent for these polymers; therefore plots are

only shown over the molecular weight range where the Mark-Houwink relationship has

been demonstrated to be accurate for each system.[21-23] IV of PA-12,T is 1-2 orders of

magnitude less than poly(p-benzamide) and PA-6,I over the range of molecular weights

studied. However, PA-12,T shows only a marginal increase in IV over completely aliphatic nylons of comparable molecular weights. For example, at a M_n of 14,300 g/mol, PA-6,6 has an IV of 0.70 g/dL (commercial grade), PA-12,T has an IV of 1.30 g/dL.

Conclusions

PA-12,T of varying molecular weights was synthesized by the melt condensation polymerization of 12,T salt with 0-10 mol-% excess 1,12-diaminododecane, terephthalic acid, or benzoic acid. Molecular weight differences as identified by intrinsic viscosity were in agreement with relative end group concentrations determined by ^{13}C NMR methods. Addition of 1 and 3 mol-% molar excess diamine increased the number average molecular weight of products to (~14,000 g/mol) compared to pure salt (12,000 g/mol). Additionally, it was seen that an inversion between the relative concentration of acid and amine end groups occurred between 1 and 3 mol-% excess DA. At approximately 2.4 mol-% excess DA, equal stoichiometry is expected to be obtained for products using these detailed polymerization conditions, producing PA-12,T of maximum equilibrium molecular weight. On a molar basis, addition of terephthalic acid or end capping with benzoic acid, decreased molecular weights to a similar degree. Molecular weights of all polymers calculated using ^{13}C NMR spectroscopy showed a linear trend on a log (M_n) - log (IV) plot. These were used to calculate with Mark-Houwink constants of $K=55.8*10^{-5}$ dL/g and $\alpha=0.81$. Since these values are based on single-point intrinsic viscosity measurements used to a great extent in semi-aromatic polymer patent literature, they should prove useful in determining the magnitude of molecular weight changes of similar monomer systems.

Acknowledgements

References

[1] Kohan, M.I. Nylon Plastics Handbook. Hanser Gardner Publications: Cincinnati, 1995.

[2] Keen, W.E.; Kirkaldy, D. (Imperial Chemical Industries). G.B. Patent 3,642,710, Feb. 15, 1972.

[3] Takeshi Sakahita, I.; Hashimoto, H.; Nakano, T. (Kuraray Co., Ltd.). U.S. Patent 4,607,073, Aug. 19, 1986.

[4] Howard, Ng. (DuPont Canada, Inc.). U.S. Patent 6355769, Mar. 12, 2002.

[5] Campbell, R.W. (Phillips Petroleum Company). U.S. Patent 3,843,611, October 22, 1974.

[6] Rulkens, R.; Crombach R.C.B. (DSM). U.S. Patent 6,747,120, June 8, 2004.

[7] Chapman, R.D.; Pickett, Jr, O.A.. (Monsanto Company). U.S. Patent 3,917,561, Nov. 4, 1975.

[8] Tamura, K.; Oka, H.; Wantabe, K.; Matsunga, S. (Kuraray Co., Ltd.). U.S. Patent 6,156,869, Dec. 5, 2000.

[9] Mok, S.L.; Pailagan, R.U. (E.I. Du Pont de Nemours and Company). U.S. Patent 5,378,800, Jan. 3, 1995.

[10] Campbell, R.W. (Phillips Petroleum Company). U.S. Patent 3,839,296, Oct. 1, 1974

[11] Akkapeddi, M. K.; Cummings, M. F.; Dege, G. J. (Allied Signal). U.S. Patent 5,191,060, Mar. 2, 1993.

[12] Cheng, P.P. (E.I. Du Pont de Nemours and Company). World Patent 2006/020845 A2, Feb. 23, 2006.

[13] Oka, H.; Kashimura, T.; Yokota, S.;Hayashihara, H. (Kuraray Co., Ltd.). U.S. Patent 5,670,608, 1997.

[14] Odian, G. Principles of Polymerization. John Wiley and Sons, Inc: New Jersey, 2004; 4th edition, Chapter 2, pp 74-78.

[15] Davis, R.D.; Jarrett, W.L.; Mathias, L.J. *Polymer* **2001**, 42, 2621.

[16] Davis, R.D.; Steadman, S.J.; Jarrett, W.L.; Mathias, L.J. *Macromolecules* **2000**, 33, 7088.

[17] Solomon, O. F.; Ciuta, I.Z. *J. Appl. Polym. Sci.* **1962**, 6, 683.

[18] Singletary, S.; Bates, R. B.; Jacobsen, N.; Lee, A. K.; Lin, G.; Somogyi, A.; Streeter, M. J.; Hall, H. K. *Macromolecules* **2009**, 42, 2336-2343.

[19] Youngjae Yoo, D. R. Paul. *Polymer* **2008**, 17, 3795-3804.

[20] Arpin, M.; Strazielle, C. *Polymer* **1977**, 18, 591.

[21] Brandup, J.; Immergut, E.H. Polymer Handbook. John Wiley and Sons, Inc: New York, 1989; 3rd edition, Section 7, pp 24-25.

[22] Cote, P.; Brisson, J. *Macromolecules* **1994**, 27, 7329-7338.

[23] Brisson, J.; Breault, B. *Macromolecules* **1991**, 24, 495-504.

CHAPTER II

EUTECTIC MELTING BEHAVOIR OF POLYAMIDE 10,T/12,T: 6,T

COPOLYTEREPHTHALAMIDES

Abstract

Semi-aromatic polyterephthalamides 10,T and 12,T were synthesized with 0-60 wt-% PA-6,T comonomer by melt condensation polymerization. Molecular weights of the copolymers ranged from 12,000 to 27,000 g/mol and all produced tough melt-pressed films. The substituted aromatic carbon of the ^{13}C NMR spectra revealed that comonomer sequences are statistical, e.g., 50:50 wt-% PA- 12,T, 6,T copolymer had 12,T-12,T:12,T-6,T:6,T-6,T sequence ratios of approximately 1:2:1. Copolymers of both PA-10,T and 12,T exhibited a eutectic melting point at 30-wt% PA-6,T, with melting points decreasing linearly from 315 and 292 °C to 280 and 272 °C, respectively. Melting enthalpies showed a similar depression at 35 wt-% PA-6,T. Although PA-10,T/12,T and PA-6,T are not co-crystalline, no wholly amorphous samples were observed at any composition. WAXD displayed three regions of diffraction patterns: 1) sharp PA-10,T crystal diffractions from 0-20% PA-6,T, 2) broad amorphous scattering between 25-45% PA-6,T, 3) sharp diffraction peaks from 50-60 wt% PA-6,T. The Tg of PA-10,T and 12,T, observed by DMA, were 147 and 137 °C, respectively. At 15 wt% PA-6,T, both PA-10,T and 12,T showed a second, higher T_g phase at 190 and 182 °C, inferring phase separation. At 50% PA-6,T, a single T_g was observed at 151 and 144 °C for PA-10,T and PA-12,T respectively. Differences in storage modulus below T_g (100 °C) were negligible, while samples with lower crystallinity (30 wt-% PA-6,T) showed an approximate 40% decrease in storage modulus at 200 °C.

Introduction

Semi-aromatic polyamides combine high melting temperatures and heat resistance of wholly aromatic polyamides (e.g. Kevlar poly p-phenylene terephthalamide) with the melt proccessability of aliphatic polyamides (nylon 6,6). Much research has focused on semi-aromatic polyamides synthesized using aliphatic diamines and terephthalic acid.[1] With short aliphatic diamines (2-7 CH_2's), melting temperatures surpass the thermal decomposition temperature of polyamides, thus making melt processing impractical. For example, the melting points of PA-4,T and PA-6,T are 430 and 370 °C, respectively.[2] Increasing the length of the aliphatic diamine, the melting point is lowered into a processable range. For instance, the melting points of PA-9,T, PA-10,T, PA-12,T[3] and PA-18,T[4] are approximately 309, 315, 295 and 245 °C, respectively. Semi-aromatic polyamides also have glass transition temperatures ranging from 100 – 140 °C (as observed by DSC), rendering them suitable for applications below these temperatures.

Comonomers are commonly used in semi-aromatic polyamides to alter properties such as melting temperature, processability, and optical clarity.[1] The ability of monomer to co-crystallize is determined by plotting polymer melting temperature versus copolymer composition. If melting temperatures do not display a local minimum as a function of composition, the comonomers are said to be isomorphous. Isomorphism of adipic acid and terephthalic acid in PA-6,T, 6,6 copolymers is well known.[5,6,7] The explanation of their co-crystallization is that the length between amide groups of adipic acid and terephthalic acid units are similar, thereby allowing entrance into the same crystal structure. Alternatively, when a local minimum, or eutectic point, is observed, the comonomers are not co-crystalline and thus do not fit into the same crystalline lattice.

Here the comonomer acts an impurity, thus decreases the perfection and melting point of the formed crystals. This is observed in copolyamides of PA-6,T and poly(hexamethylene isophthalamide) (PA-6,I) and PA- 6, 6,T.

Research on PA-10,T copolymers has been limited to copolymerizations involving caprolactam[8] and adipic acid[6]. It has been demonstrated that adipic acid and terephthalic acid co-crystallize when polymerized with decamethylene diamine showing melting point versus composition trends similar to that of PA-6,T, 6,6 copolymers. No literature currently exists covering the copolymerization of PA-10,T of 12,T with other linear diamines. A single reference describes semi-aromatic copolyamides synthesized using terephthalic acid and a combination of linear aliphatic diamines.[9] It was found that copolyamides of PA-4,T and 6,T display a depression of melting temperature with composition, but maintain some level crystallinity throughout all compositions studied.

In the present study, copolymers of PA-10,T and 12,T were synthesized with PA-6,T via melt condensation polymerization. Polymers were characterized using high resolution ^{13}C NMR spectroscopy for composition analysis and intrinsic viscosity for molecular weight determination. Differential scanning calorimetry and dynamic mechanical analysis were used to examine the thermal properties of the synthesized copolymers, while wide-angle x-ray scattering provided information concerning the effect of composition on crystallinity.

Experimental

Materials

Terephthalic acid, 1,10-diaminodecane, 1,12-diaminododecane, and 1,6-diaminohexane (HMDA) were purchased from Aldrich. Terephthalic acid and 1,6-diaminohexane were used as received. 1,10-Diaminodecane, and 1,12-diaminododecane were sublimed at 70 °C and dried at room temperature under vacuum before use. N,N-Dimethylacetamide (DMAc) and triethylamine were distilled from barium oxide onto molecular sieves before use. Concentrated sulfuric acid (96%) for viscosity measurements was purchased from Aldrich and used as received. Solutia provided PA-6,T salt, siloxane antifoam, and a commercial antioxidant.

Synthesis

Polyamide (n, T) salt. Into a 2 L beaker, 1 L of deionized water, 1,10-diaminodecane (49.5 g, 0.287 mol) and terephthalic acid (42.3 g, 0.285 mol) were added and the slurry was heated to a boil. Additional water was added and brought to boil to yield a supersaturated clear salt solution. The hot salt solution was then added to a 2 L beaker containing 500 mL of reagent alcohol and cooled to room temperature, followed by cooling in a freezer. The precipitate was then filtered and washed with reagent alcohol. The resulting 10,T salt was formed in quantitative yield (95 %). PA-12,T salt was prepared in a similar manner. All terephthalic acid salts were precipitated from water into reagent alcohol and dried before use. PA 12,T, 10,T, and 6,T salt melting temperatures were 271.9, 271.6, and 281 °C respectively, with melting enthalpies of between 430 and 450 J/g.

Melt condensation of polyamide (n,T) and copolymers. Polyamide (n,T) salt, 3 mol-% excess diamine, and 0.5 wt-% antioxidant were weighed and mixed with a mortar and pestle. The solid mixture was then added to a test tube and approximately 50 wt-% deionized water was added to create a slurry. Twelve test tubes were loaded into a Parr reactor, which was then sealed and purged with nitrogen. Heating steps were programmed into the reactor controller unit and monitored with a thermocouple placed in one of the test tubes. The reactor was surrounded by insulation to improve heating control. Nitrogen pressure was controlled manually and measured by a gauge on the reactor head. Predetermined temperatures provided signals for pressure changes. With approximately 125 kPa nitrogen pressure and a 200 °C set point, the sample temperature remained at 125 °C until all water evaporated. At 150 °C the pressure was elevated to 1724 kPa. At 280 °C the pressure was released and the temperature was allowed to rise and hold at 310-315 °C for 15 minutes with purging nitrogen.

Solution polymerization of polyamide 6,T (PA-6,T). HMDA (10.98 g, 0.095 mol) and triethylamine (27 mL, 0.194 mol) were dissolved in 230 mL of DMAc and added to a glass Waring blender. The blender was turned on high and 60 mL of DMAc with terephthaloyl chloride (19 g, 0.094 mol) was added as quickly as possible. A white precipitate immediately formed and followed by a large increase in viscosity. After 5 minutes, the precipitate was filtered and washed with acetone followed by water, giving PA-6,T (20.7 g, 90%).

Sample Preparation

Solid polymers obtained from the test tubes immersed in liquid nitrogen for approximately 10 minutes were ground using a Waring blender with a stainless steel

mixing jar. The pellets were then dried at 80 °C under vacuum for 24 hours, and placed in a desiccator until further characterization.

Dry pellets were then compression molded into 0.8 or 0.3 mm films at a temperature approximately 10-20 °C above the melting temperature of the polymer. The pellets were placed between two woven Teflon sheets and held at this temperature between two hot plates for 3 minutes with no pressure. For an additional 2 minutes, the film was pressed with 2700 kPa. Hot plates were then taken from the press and immersed in a room temperature water bath. For a higher degree of supercooling, films were removed from the hot plates and placed underneath a room temperature steel plate. Films were dried at 80 °C under vacuum for 12 hours. Annealing was performed at 200 °C for 12 hours under vacuum.

Characterization

Nuclear magnetic resonance spectroscopy (NMR). NMR samples having a 10 wt-% polymer concentration was prepared using a 3:1 volume ratio of hexafluoroisopropanol (HFIP) to $CDCl_3$. Preparation was performed by first dissolving pellets in HFIP, followed by addition of $CDCl_3$. Solution ^{13}C spectra were collected on a Varian $^{UNITY}INOVA$ NMR spectrometer operating at a frequency of 125.7 MHz. Routine acquisitions were obtained using a 1.3 second acquisition time, a 45° pulse width of 2.9 μs, and a 1 second recycle delay. The number of accumulate transients ranged from 15,000 to 30,000, involving 12-24 hour collection times. Spectra were recorded at 25°C. Data was zero-filled up to 256k points and filtered with 1 Hz of line broadening prior to application of Fourier transformation. Baselines were corrected using a 10th order polynomial.

Viscometry. Solutions containing 0.5 g/dL of polymer in concentrated sulfuric acid were prepared by adding 0.25 grams of polymer and 25 mL of concentrated sulfuric acid into a 50 mL flask. After 12 hours of mixing via magnetic stirring, the solutions were diluted with an additional 25 mL of sulfuric acid, and stirring continued for another 12 hours. Solutions were visually inspected for gelling, and passed through a funnel packed with glass fiber if gel was present. Measurements were obtained using a Cannon viscometer in a 25 °C controlled water bath. The viscometer was washed with sulfuric acid and a portion of the next sample to be tested before measurements were recorded. Flow times were an average of three tests with that agree within +/- 0.2 seconds. Using flow times of concentrated sulfuric acid and polymer solution were used to calculate the specific and relative viscosities. Single point intrinsic viscosities were then determined using Solomon and Ciuta relationship;

$$[\eta] = [(2^*(\eta_{sp} - \ln(\eta_{rel})]^{1/2})]/C$$

where, η_{sp} is specific viscosity, η_{rel} is relative viscosity, and C is concentration.[10]

Differential scanning calorimetry (DSC). Polymer melting temperatures were analyzed using a TA Instruments 2920 DSC. Scans were taken at a heating rate of 10 °C/min. Data from first and second heating scans were collected. Samples were heated approximately 10-20° C above their melting temperature, air cooled to room temperature, and heated a second time to 350° C.

Wide-angle x-ray scattering (WAXD). WAXD was performed on a Rigaku Ultima II x-ray diffractometer. Data was collected from 3-40° 2θ at a rate of 2 °/min. Samples were annealed at 100 °C for 12-24 hours prior to analysis to achieve maximum attainable crystallinity.

Dynamic mechanical analysis (DMA). Tensile mode DMA was obtained using a Thermal Analysis Q800 series instrument. Samples of 0.8 mm thickness were prepared by melt pressing, followed by annealing and drying at 200° C prior to testing. Data was collected from 30-250 °C at a heating rate of 2° C/min with a 20 um amplitude, 0.05 N preload force, and 125% force track.

Results

Synthesis and Intrinsic Viscosity

Copolymers were synthesized from their corresponding diamine/terephthalic acid salts as shown in Figure 2.1. Figure 2.2 shows the temperature and pressure profiles of the melt condensation polymerization used to synthesize all copolymers.
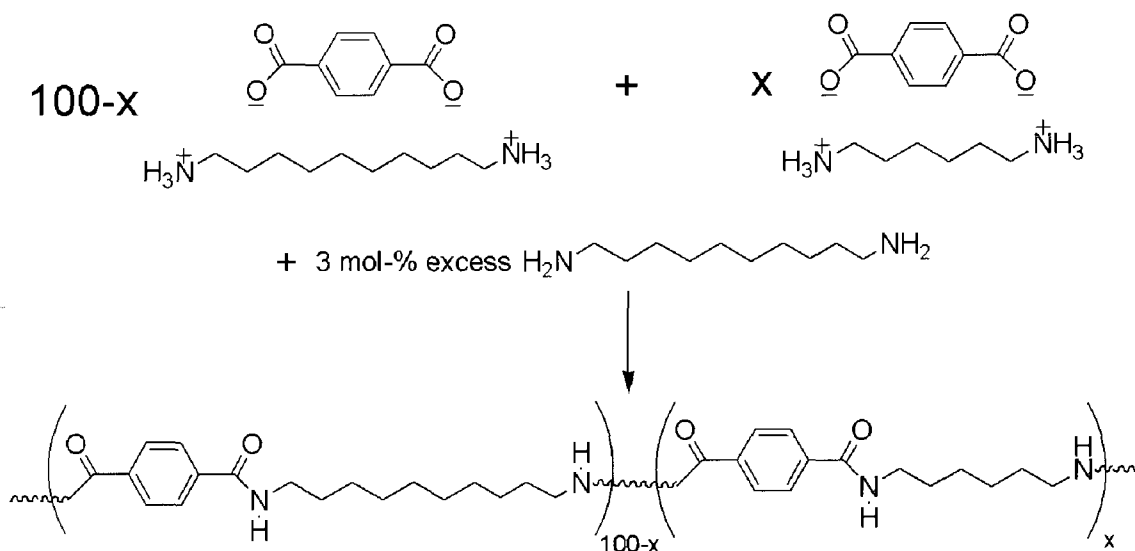
Figure 2.1. Synthetic scheme of PA-10,T:6,T copolymers, where x = 0-60 wt-%

The melt condensation polymerization was performed in three stages, the boiling, high pressure, and hold stage. Duration and pressure of each stage was determined by temperature of the reaction. The boiling stage ensures homogenization of the reaction mixture and very little polymerization occurs. At completion of boiling and sudden rise

of temperature, the pressure is increased to 1724 kPa. High pressure is maintained from

125-270 °C to mitigate the loss of diamine due to volatilization throughout this initial

stage of the polymerization. The pressure was released and the polymerization was

allowed to heat to maximum temperature. Stage three is the hold stage at maximum

temperature. Initially, higher polymerization temperatures and hold times were used, but

this process often resulted in polymers that were not soluble in sulfuric acid or amendable

to compression molding. In order to avoid this 'gelling', a lower maximum temperature

(315 from 330 °C) and polymerization time (15 from 30 minutes) were used. This yielded

homo and copolymers that were soluble in both sulfuric and dichloroacetic acid, and were

suitable for compression molding into films for testing.
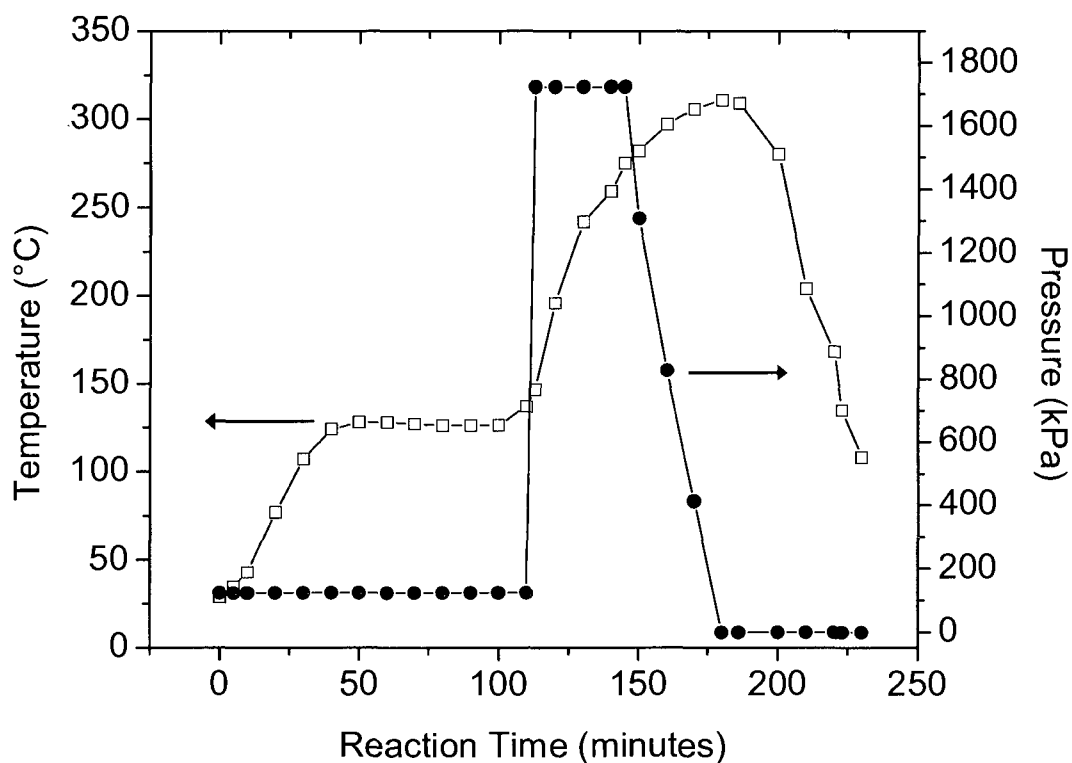
Figure 2.2. Melt condensation polymerization temperature and pressure profiles

In studies published separately, it was found that PA-12,T synthesized with 1 and 3 mol-% excess 1,12-diaminododecane had the lowest total end group concentration, the most balanced acid/amine end groups, and the highest molecular weights, under identical melt polymerization conditions.[11] Therefore, in order to obtain suitable molecular weights for copolymer analysis, 3-mol% deca or dodecamethylene diamine was added to each reaction. Single point intrinsic viscosities were determined to estimate relative number average molecular weights between copolymer samples. IV values for several of the copolymers studied are given in Table 2.1.

Table 2.1. Intrinsic viscosities and 1st heating DSC melt temperatures of homo and copolymers

Feed Ratio (PA-n,T:PA-6,T)	PA – 10,T			PA-12,T		
	IV	M_n^a (g/mol)	T_m (°C)	IV	M_n^a (g/mol)	T_m (°C)
100:0	1.68	19700	327	1.14	12200	295
85:15	1.41	15900	316	1.21	13100	287
70:30	1.26	13800	283	1.24	13500	274
50:50	1.68	19700	324	2.17	27000	328

^{a} K = 0.000558 dL/g and α=0.81 in 96% H_2SO_4 at 25 °C

Number average molecular weights for PA-12,T:6,T and PA-10,T:6,T copolymers were estimated from Mark-Houwink constants developed for PA-12,T homopolymer. Assuming that the solution properties of PA-10,T, 12,T and 6,T are similar, an estimate of M_n for the copolymers was determined using the equation;

$$[\eta] = 0.000558(dL/g)*(M_n)^{.81}$$

Note that these constants were developed using single-point IV values, and this relationship is only applicable for 0.5 g/dL concentrations dissolved in 96% concentrated H_2SO_4 at 25 °C.

There are two effects that create M_n differences in the copolymers; differential diamine volatility and the physical state of the polymer during the reaction. Excess diamine is required in order to obtain balanced stoichiometry and the amount of excess needed is a function of the volatility of the diamine during the polymerization. Since, hexa-, deca-, and dodecamethylene diamine have different melting points and vapor pressures, using a constant 3 mol-% excess diamine for all copolymer compositions will not result in the same stoichiometric balance under identical polymerization conditions. For example, PA-12,T, 85:15 and 70:30 PA-12,T, 6,T had intrinsic viscosities of 1.14, 1.21, and 1.24, respectively. Increasing the amount of PA-6,T comonomer has a greater impact on stoichiometric imbalance, because a higher fraction of the more volatile HMDA (compared to deca and dodecamethylene diamine) is present. If equal molecular weights were desired, the amount of excess diamine would need to be increased corresponding to the amount PA-6,T comonomer in order to compensate for differential volatility of the two diamine monomers.

The main cause of molecular weight differences is the physical state of the polymer during the reaction, as determined by the relationship between the crystalline melting temperature of the polymer and the maximum reaction temperature. Table 1 lists the DSC first heating melting temperatures of several of the copolymers. Their corresponding DSC thermographs are presented in Figure 2.3. The 1st heating DSC data is related to the crystalline state of the polymer formed from the reaction. Comparison of the IV and DSC data show that when the melting temperature of the polymer is higher than the maximum process temperature, the intrinsic viscosity is notably higher. The melting temperatures of PA-10,T (327 °C), 50:50 10,T:6,T (324 °C) and 50:50 12,T:6,T

(328 °C) are substantially higher than the final reaction temperature of 315 °C. These polymers also have the highest intrinsic viscosities (1.68, 1.68, and 2.17) and molecular weights (19,700, 19,700, and 27,000). Comparison of a molten (PA-12,T – T_m = 295 °C) and crystallized polymer (50:50 PA-12,T, 6,T – T_m = 328 °C) shows a near doubling of intrinsic viscosity from 1.14 to 2.14 dL/g. This phenomenon is known as solid state polymerization. Step-growth polymerizations proceed via the equilibrium, P_1 + P_2 □ P_3 + B, where P_1 and P_2 are small molecule reactants or polymer end groups, P_3 is a higher molecular weight chain, and B is water.[12] If polymer (P_3) is crystallized from the reaction mixture, the equilibrium of the molten state is changed. Since end groups do not participate in crystallization, the concentration of reactants (P_1 and P_2) is increased, and the reaction proceeds to higher molecular weight materials (P_3).

Despite the M_n differences, the copolymers could be compression molded into films were tough. This implies all copolymers are above the critical molecular weight and thus molecular weight variations of the following results are negligible. It is noteworthy to mention that the compression molding of the 50:50 PA-12,T, 6,T (the highest M_n) was the most difficult, requiring much a higher temperature and pressure compared to the other copolymers. Semi-aromatic polyamides are known have markedly higher melt viscosities than purely aliphatic polyamides, and an IV of 2.16 ($M_n \sim$ 27,000) may approximate an upper limit in regard to the processability of these materials.
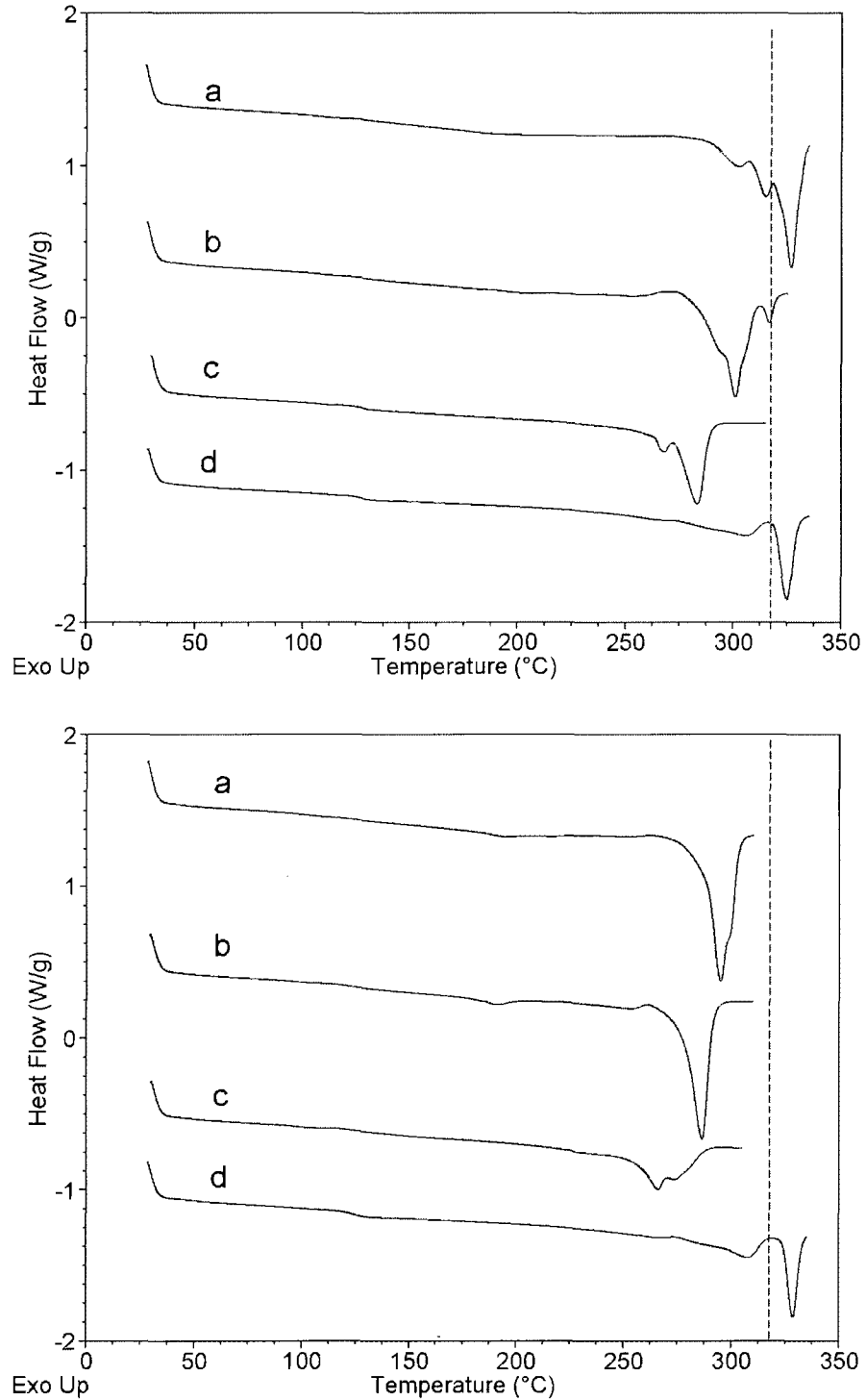
Figure 2.3. First heating DSC thermographs of PA-10,T (top) and PA-12,T (bottom)

with (a) 0, (b) 15 wt-% (c) 30 wt-%, and (d) 50 wt-% PA-6,T (vertical line represents the

maximum reaction temperature).

High Resolution Solution ^{13}C NMR Spectroscopy

High resolution NMR spectroscopy was used to determine copolymer composition and comonomer distribution. The ^{13}C NMR spectra for PA-12,T and PA-10,T are shown in Figures 2.4 and 2.5. General peak assignments for PA-12,T are as follows (see labels on Figure 2.4): carbonyl (1) – 170.8 ppm, substituted aromatic carbons (2) – 137.7 ppm, aromatic carbons (3) – 128.0 ppm, α-amide carbon (4) – 41.7 ppm, methylene carbons (5-9) – 30.0, 29.9, 29.7, 29.4, and 27.3 ppm. General peak assignments for PA-10,T are as follows (see labels on Figure 2.5): carbonyl (1) – 170.8 ppm, substituted aromatic carbons (2) – 137.7 ppm, aromatic carbons (3) – 128.0 ppm, α-amide carbon (4) – 41.6 ppm, methylene carbons (5-8) – 29.8, 29.6, 29.4, and 27.2 ppm.

Analysis of the PA-10,T/12,T, 6,T copolymers displays multiple peaks of carbon atoms 1, 2, 3, and 4 as labeled in Figure 2.4 and 2.5. Figures 2.6 shows expanded regions of the α-amide carbon (4) and substituted aromatic carbon (2) of PA-12,T, PA-6,T, and several of copolymers. Slight variations in sample viscosity and solvent caused small shift changes; therefore peaks were aligned based on the α-amide carbon. The α-amide carbon shows two distinct peaks representing the fraction of PA-12,T and PA-6,T in the copolymer, ensuring that resulting polymer corresponds to the monomer feed ratio. Note that samples were prepared in wt-%, e.g. 50:50 wt-% is approximately 45:55 mol-% PA-12,T, 6,T. This is significant since NMR spectral intensities reflect molar compositions.
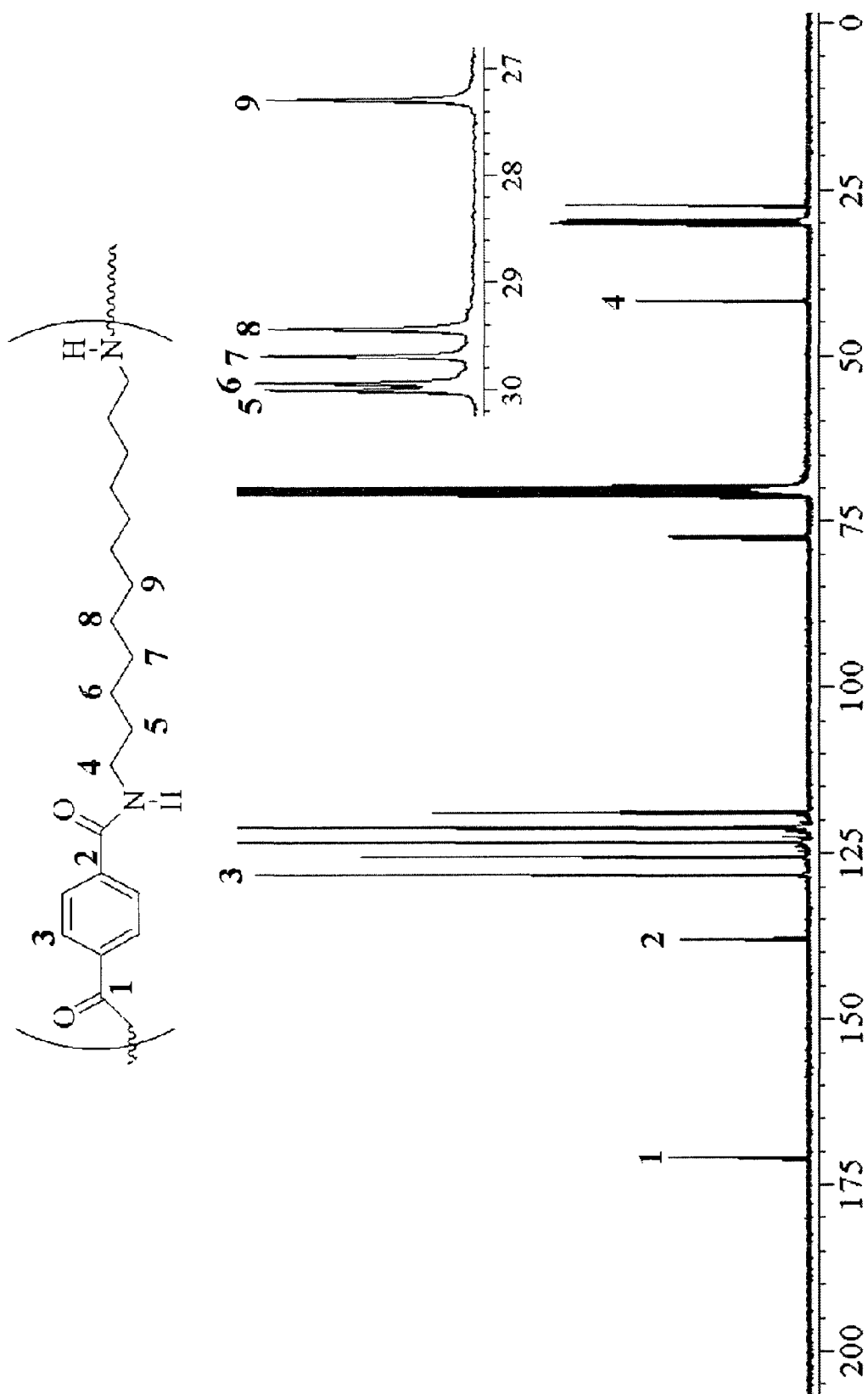
Figure 2.4. PA-12,T ^{13}C NMR spectrum

52
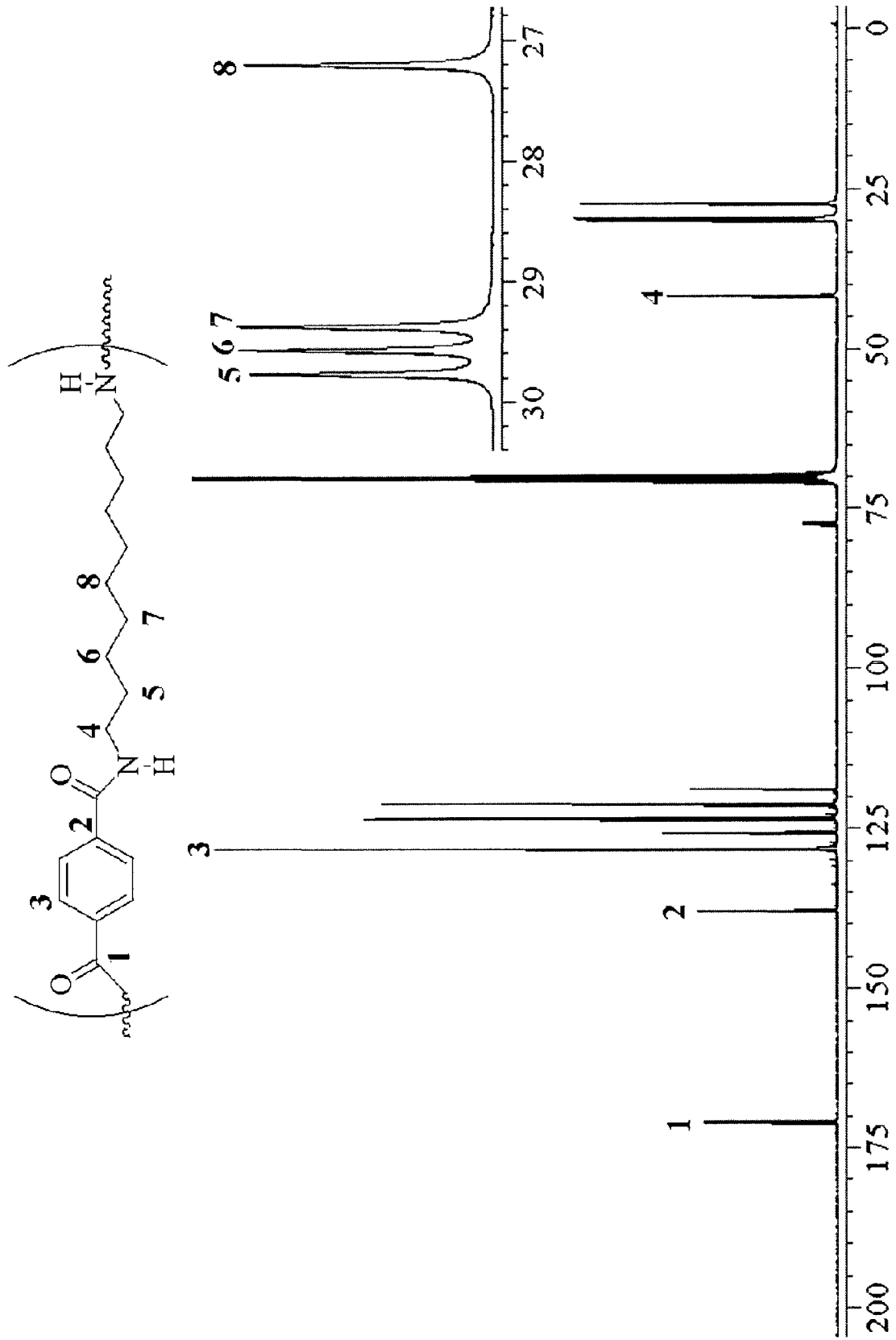
Figure 2.5. PA-10,T ^{13}C NMR spectrum

In addition to the substituted aromatic carbon peaks (Figure 2.6, left) for PA-12,T and 6,T at 137.74 and 137.62 ppm respectively, two new peaks appear for all copolymers. The new peaks are due to the formation of PA-12,T – PA-6,T alternating sequences. This is further confirmed by comparing the 50:50 wt-% copolymer and a 50:50 wt% mixed solution of the two homopolymers shown in Figure 2.7. The physical mixture of the two homopolymers displays two chemical shifts for the substituted aromatic carbon, whereas the 50:50 copolymer has four chemical shifts (Figure 2.7, a and b). The new peaks (c and d) are due to PA-12,T-PA-6,T alternating sequences, having identical peak heights and representing one carbon each. This sequence information gives insight to the randomness of the copolymers.[13] For example, the 50:50 wt-% PA-12,T, 6,T copolymers, the ratio of 12,T-12,T:12,T-6,T:6,T-6,T units is approximately 1:2:1, ensuring that the polymerization yields completely random, statistical copolymers.

The relative amounts of PA-12,T, PA-6,T, and PA-12,T-PA-6,T sequences formed by varying PA-6,T content of the copolymer from 15 to 50 wt-% is shown in Figure 2.6 (bottom left). At 15 wt-% PA-6,T (Figure 2.6b), a short broad peak between the chemical shifts for pure PA-6,T and the 12,T-6,T unit is present. Comparison with the corresponding peak of the PA-12,T – PA-6,T sequence indicates little if any pure PA-6,T exits at a 15 wt-% loading. At 30 wt-% PA-6,T, the peak due to pure PA-6,T sequences appears, but the number of these sequences are still small as compared to the 12,T and 12,T-6,T sequences. At 50-wt% PA-6,T, the peak for pure PA-6,T sequences is increased to approximately the same number at pure 12,T units and half that of 12,T-6,T sequences, typical of a random melt condensation polymerization. Since crystallinity is dependent on regularity of the polymer structure, the behavior of the substituted aromatic carbon

should provide additional chemical information to help characterize the physical eutectic

melting property of the copolymers in question.
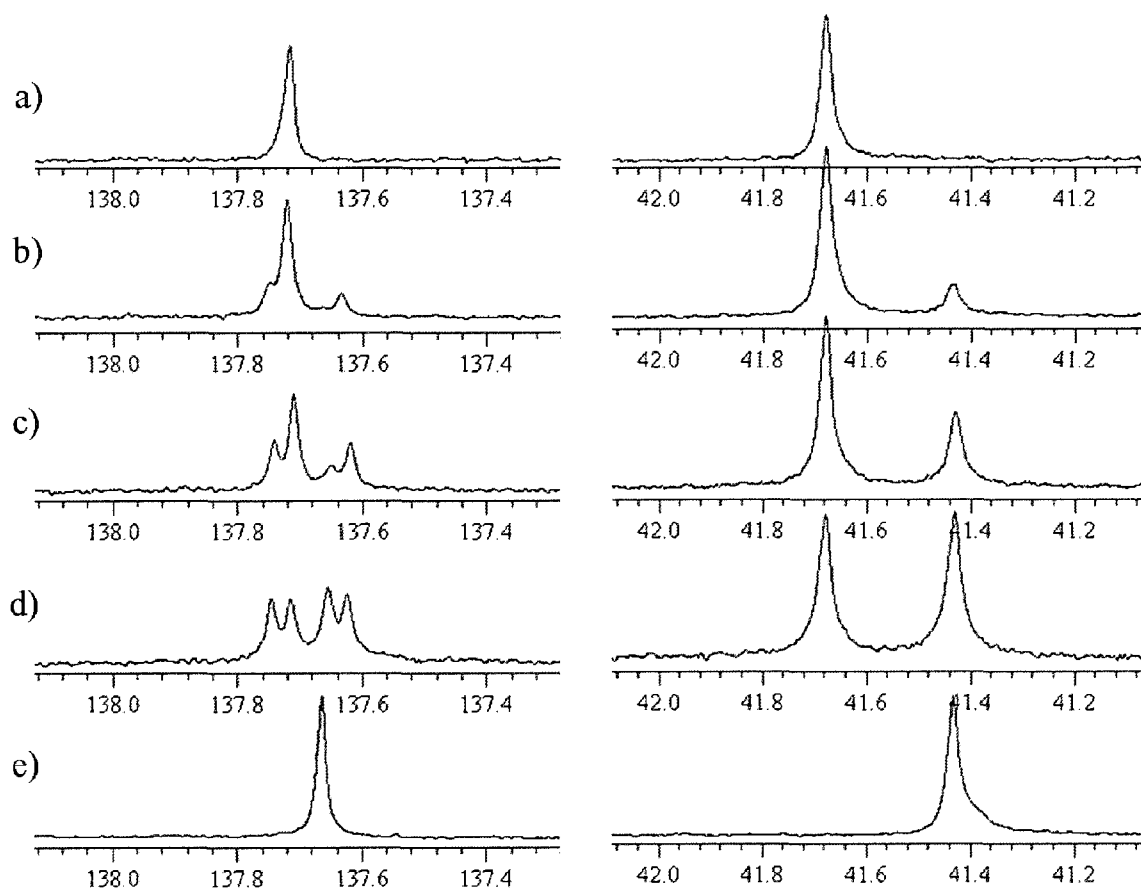
Figure 2.6. Expanded ^{13}C spectrum of substituted aromatic and α-amide carbon of a) PA-12,T, b) 85:15 wt-% PA 12,T, 6,T, c) 70:30 wt-% PA 12,T, 6,T, d) 50:50 wt-% PA 12,T, 6,T, and e) PA-6,T.
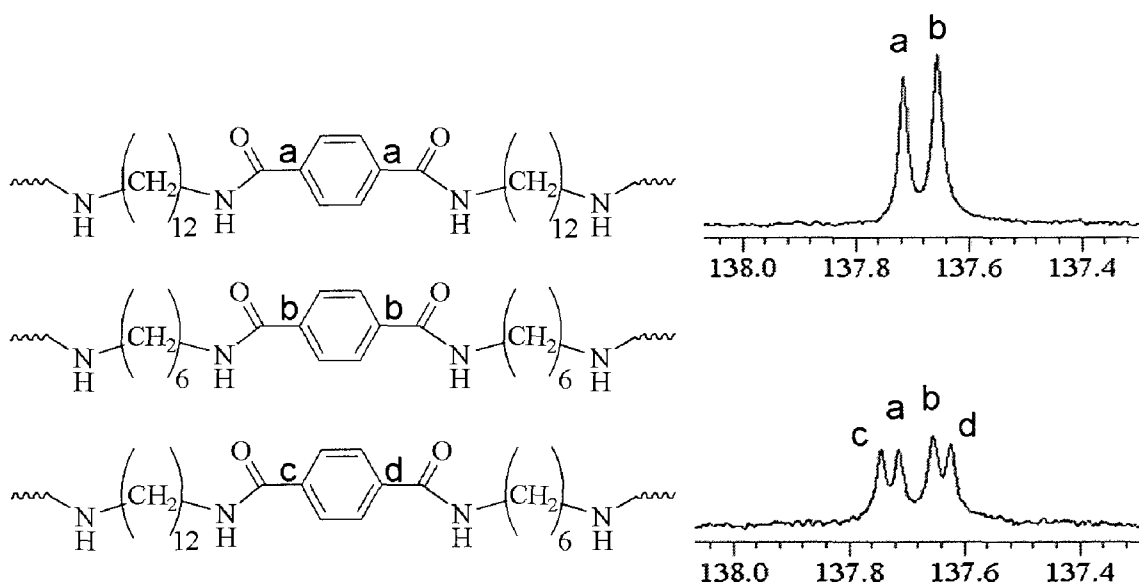
Figure 2.7. Peak assignments of substituted aromatic ^{13}C NMR chemical shifts of the

50:50 PA- 12,T, 6,T copolymer and a 50:50 mixture of the two homopolymers.

Thermal Characterization

A select series of second-heating DSC thermograms of PA-10,T, 6,T (Top) and

12,T, 6,T (Bottom) copolymers are shown in Figure 2.8. Melting temperatures and

enthalpies versus wt-% PA-6, T are plotted in Figure 2.9. PA-10,T and PA-12,T

homopolymers have melting temperatures of 315 and 292 °C, respectively. Copolymers

initially show a linear decrease in melting temperature with increasing PA-6,T

comonomer content, with the lowest melting temperatures of 280 and 272 °C observed

for PA-10,T, 6,T and 12,T, 6,T copolymers at 30 wt-% PA-6,T, respectively. Similarly,

melting enthalpies of both sets of copolymers show a linear decrease with increasing PA-

6,T comonomer. Melting enthalpies of PA-10,T, 6,T and PA-12,T, 6,T copolymers a

minimum at 35 and 30 wt-% PA-6,T, respectively, decreasing from 70 to 24 J/g for PA-

10,T, 6,T and 60 to 26 J/g for PA-12,T, 6,T copolymers. In addition, the melting

endotherms of copolymers containing 30 wt-% PA-6,T are very broad compared to those of their respective homopolymers.

The data indicates that PA-10,T/12,T and PA-6,T are not co-crystalline. The 6 or 8 carbon difference in the diamine portion of the repeat unit increases the length between amides, and therefore inhibit entrance of the PA-6,T repeat unit into PA-10,T/12,T crystal structure. The decreasing melting temperatures up to 30-wt% PA-6,T are consistent with the formation of smaller, less perfect crystals, while the decrease in melting enthalpies are due to the overall decrease in the amount of crystallinity. Here PA-6,T sequences up to 30-wt% act as impurities, and inhibit the formation of PA-10,T or PA-12,T crystals. ^{13}C NMR spectroscopy has shown that with 15-wt% PA-6,T, most PA-6,T units are statistically incorporated in PA-6,T-PA-12,T alternating units and not purely PA-6,T sequences. This maximizes the number of irregularities in the polymer chain, and therefore has a negative effect on crystal content as well as size and perfection, which is consistent with the copolymer melting behavior. The broadening of the melting endotherms is also associated with a larger distribution of crystal size and perfection. Compression molded films at these compositions have an increased clarity with PA-6,T content, further signifying a reduced crystallinity as depicted in Figure 2.10.

The eutectic point for PA-10,T, 6,T and PA-12,T, 6,T copolymers is 30 wt-% PA-6,T. Note that a totally amorphous composition may lie in the vicinity of 30 wt-%. Increasing PA-6,T comonomer content above 30 wt-%, increases the melting temperature in a manner that is independent of the comonomer PA-10,T or 12,T. PA-6,T comonomer content from 30 wt-% to 35 wt-% of PA-10,T, 6,T yields a copolymer with a higher melting temperature but a lower melting enthalpy. If the decrease in enthalpy was a

further reduction of the size PA-10,T crystals, a corresponding decrease in melting temperature would result. Since the melting temperature is increased rather than decreased, this indicated the onset of PA-6,T crystal formation. NMR results have shown that at 30 wt-% PA-6,T pure PA-6,T sequences are being formed. Although the crystalline melting temperature of PA-6,T homopolymer is 372 °C, the PA-6,T crystals formed at 35 wt-% in the copolymers have reduced size and perfection, and thus reduced values. Increasing from 30 wt-%, the PA-10,T, 12,T and alternating sequences now act as defects to the formation of PA-6,T crystals. This effect is reduced as the amount of PA-6,T comonomer increased. Melting temperature of PA-10,T , 6,T and PA-12,T, 6,T copolymers are increased from 272 and 280 at 30 wt-% PA-6,T to 325 °C and 320 °C at 60 wt-% PA-6,T, respectively. The rise of the melting temperature is similar in both copolymer sets studied, further confirming the formation of PA-6,T crystals. In addition, melting enthalpies show a corresponding increase exceeding PA-6,T content past 35-wt%.
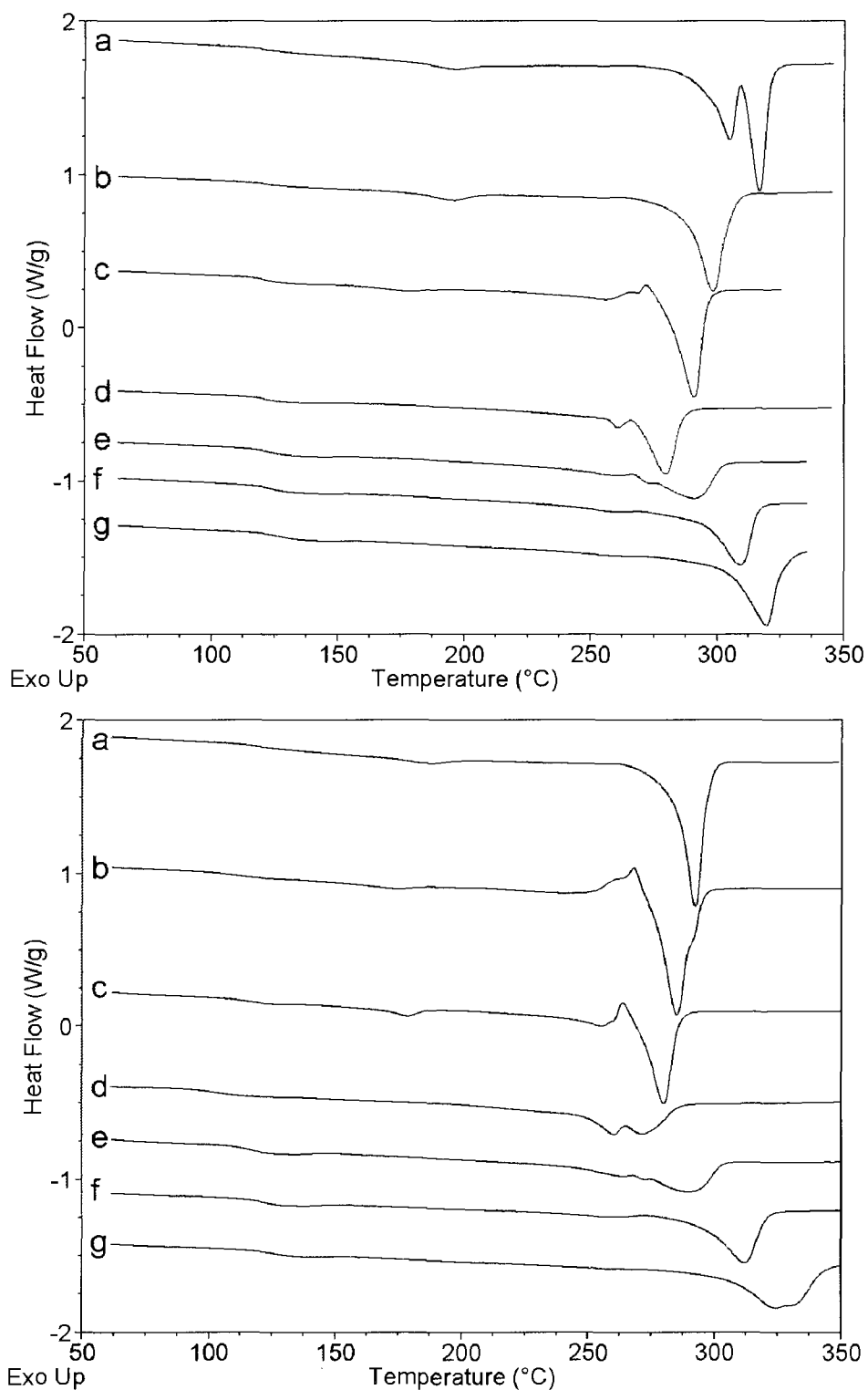
Figure 2.8. Second-heating DSC thermographs of PA-10,T (top) and PA- 12, T (bottom)

containing 0 (a), 10 (b), 20 (c), 30 (d), 40 (e), 50 (f), and 60 (g) wt-% PA 6,T.
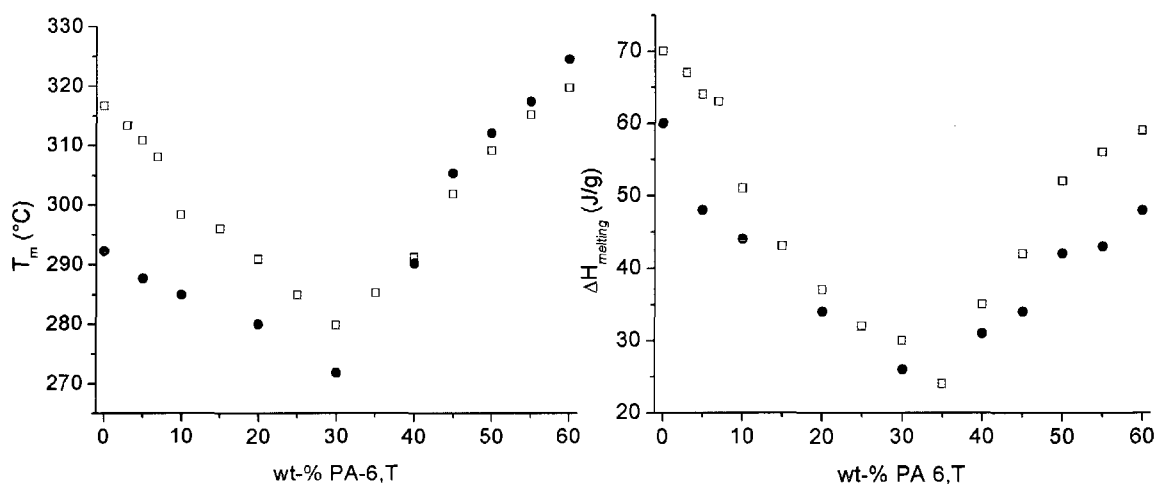
Figure 2.9. Second-heating DSC melting temperatures (left) and enthalpies (right) of PA-10,T (□) and PA-12,T (●) versus wt-% PA-6,T.
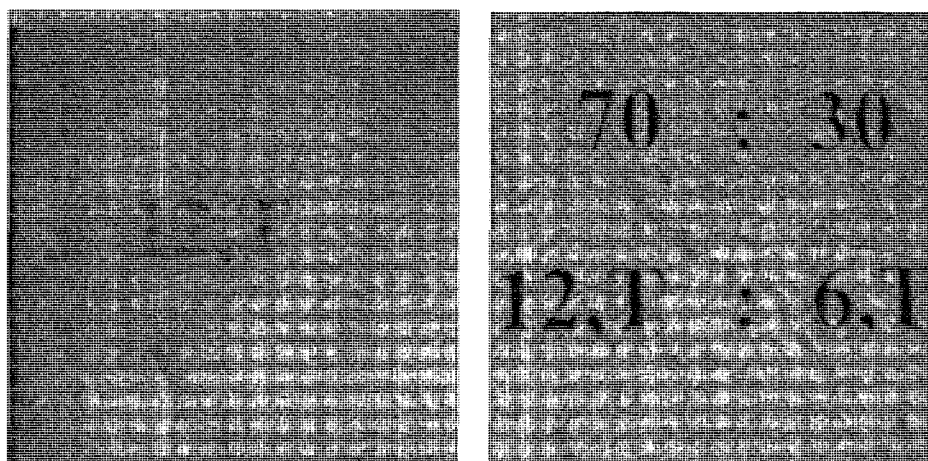
Figure 2.10. Compression molded films of PA-12,T and 70:30 wt-% PA-12,T,6,T copolymer displaying increased optical clarity

It is noteworthy to mention that copolymers from 60% PA-6,T displayed phase separation producing phases that have melting points of approximately 350 °C. The degree of phase separation was found to be affected by the heat treatment of the polymer. For example, compression molding of the 40:60 10,T, 6,T copolymer produced a film with different regions of clarity. Figure 2.11 shows compression molded films of the 40:60 PA-10,T, 6,T copolymer. Blotches were large enough to separate by regions of

clarity. Figure 2.12 shows first heating DSC thermographs of a relatively (a) white and

(b) clear spot of the compression molded film, along with second heating curves of

material from the melt polymerization and a DSC annealed sample. The vertical line at

240 °C on the graph represents molding and annealing temperatures.
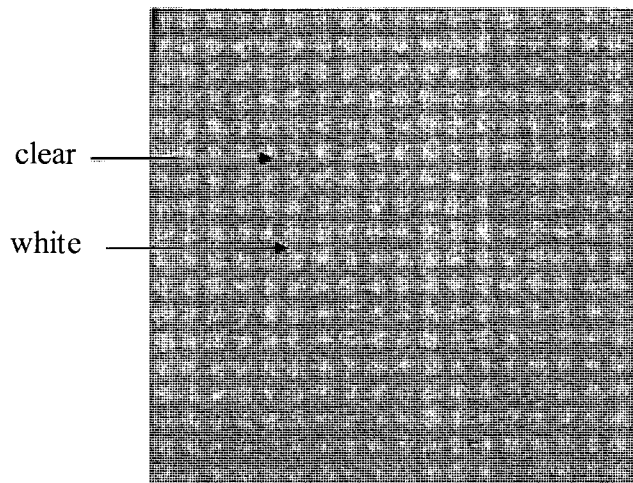
clear

white

Figure 2.11. Blotchy compression molded films of the 40:60 PA-10,T,6T copolymer

Figure 2.12 shows that the white sections (a) of the blotchy film have a larger

melting enthalpy, corresponding to a higher melting phase as compared to the clearer area

(b) of the film. It appears that compression molding at 340 °C induces phase separation

and/or annealing of this higher melting phase, resulting in the blotchiness of the film. To

confirm that annealing of the higher melting phase is occurring during compression

molding, DSC annealing of the bulk reaction material at 340 °C was performed for 30

minutes. The control sample (c) was bulk reaction material that was heated to 340 °C and

immediately air cooled. The annealed sample displayed a higher melting peak that was

approximately five times larger than that of the un-annealed sample, confirming that

phase separation and annealing is occurring during melt pressing of the 40:60 PA-

10,T,6,T copolymers. Since there was no mixing and the maximum reaction temperature

was 316 °C, this phase separation could be a result of the crystallization of PA-6,T rich

phases during the reaction. If crystallization during the reaction occurs, the randomness

of the resulting polymer would be directly affected, thus producing the observed

multiphase system. Since this topic is currently unexplored in SAPT literature, further

investigations are needed confirm these results.
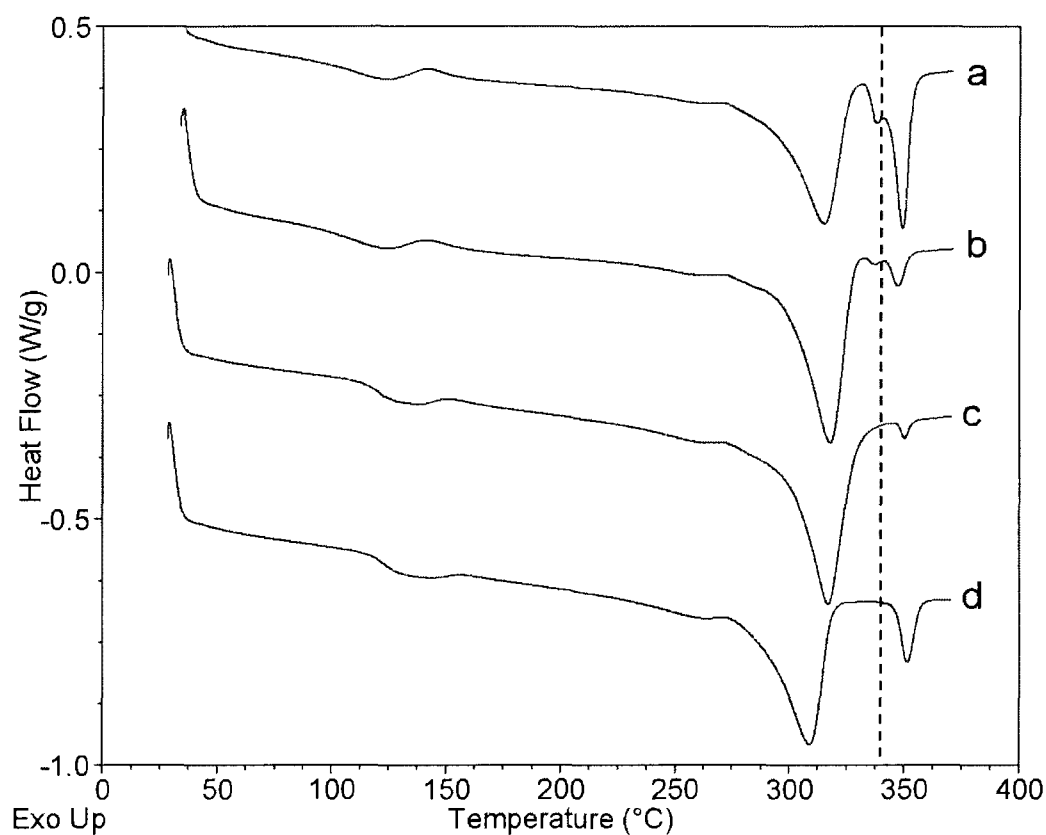
Figure 2.12. DSC thermographs of white (a) and clear (b) regions of compression

molded film, and unannealed (c) and annealed (d) non-compression molded samples of

the 40:60 wt-% PA-10,T, 6,T copolymer (vertical line represents compression molding

and DSC annealing temperature).

Melting point trends have shown that PA-6,T comonomer is not co-crystalline

with PA-10,T or PA-12,T, although no wholly amorphous samples were observed. X-ray

diffraction patterns was used examine the types of crystalline regions formed with

addition of the PA-6,T comonomer. Copolymers of PA-10,T with 0-60 wt-% PA-6,T are

shown in Figure 2.13. For brevity, WAXD trends of PA-12,T, 6,T copolymers are

omitted, but show similar diffraction patterns with increasing PA-6,T content. Diffraction

patterns of PA-10,T and 12,T compression molded films display sharp diffraction peaks

at approximately 19.5, 20.5 and 20 ° two theta. Note that the PA-6,T diffraction pattern

was obtained from a powder, whereas all others are from compression molded films.

Three regions of diffraction patterns were observed:

- *0-20 wt-% PA-6,T* – Sharp diffraction peaks of PA-10,T broaden and their

  intensity decreases, falling into the amorphous halo when the PA-6,T content to

  20%. All diffraction peaks are consistent with PA-10,T homopolymer diffraction

  patterns. This confirms that the addition of low levels of PA-6,T disrupt PA-10,T

  crystal formation, and new types of crystals are not formed.

- *25-45 wt-% PA-6,T* – No sharp diffraction peaks are observed between 25-45 wt-

  % PA-6,T, although DSC shows melting enthalpies between 24-30 J/g. The

  absence of sharp diffraction peaks, is due to the low crystallinity of the samples,

  while the broad amorphous scattering prevails. Increasing from 25 to 45 wt-%, the

  width of this broad diffraction increases from that of PA-10,T to PA-6,T. At 40-

  45 wt-% peaks corresponding to PA-6,T crystals are forming, but are still in

  minority to the amorphous phase. This is in agreement with the DSC

thermographs which indicate an increase in melting enthalpy after 35 wt-% PA-6,T.

- *50-60 wt-% PA-6,T* – The reappearance of sharp diffraction peaks is observed between 50 and 60 wt-% PA-6,T similar to those PA-6,T homopolymer synthesized by solution polymerization. This further confirms that past the eutectic point, PA-6,T crystals are being formed.
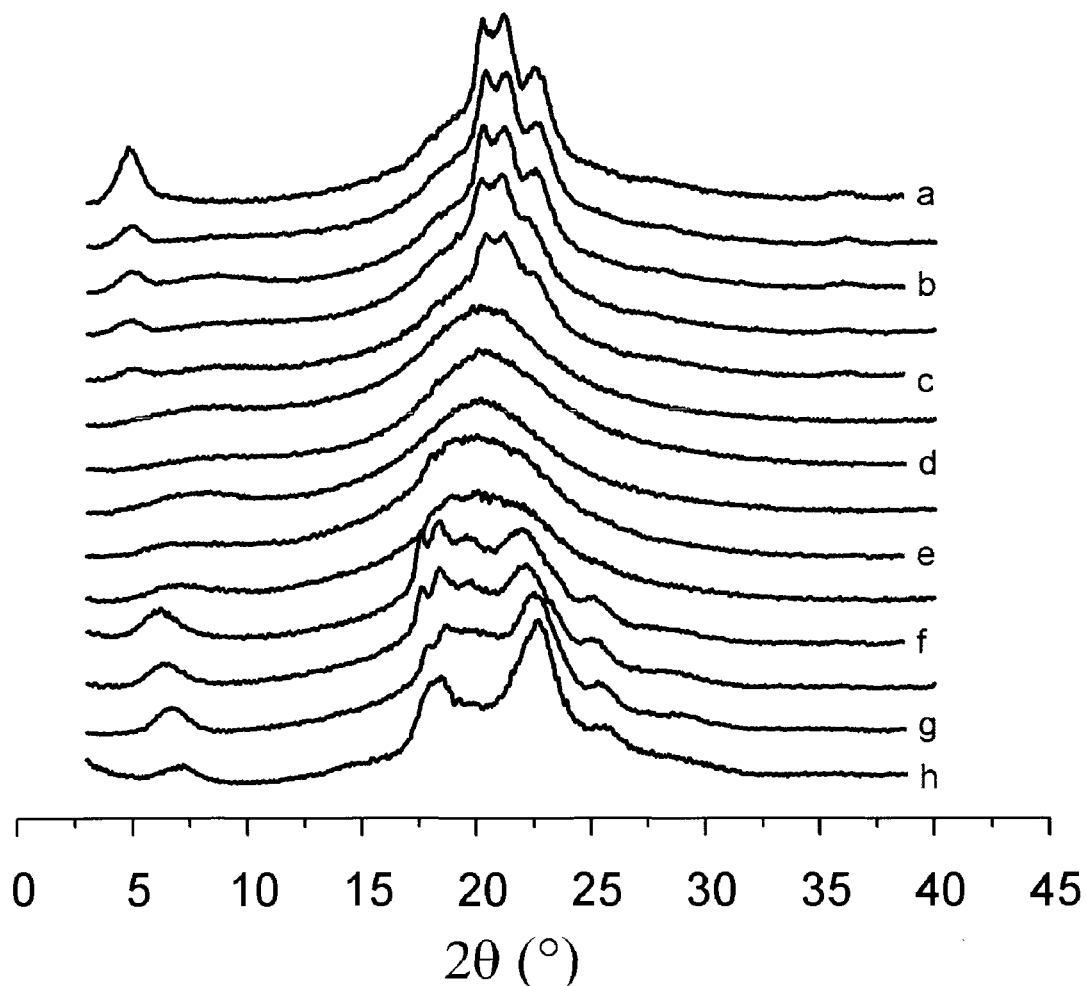
Figure 2.13. X-ray diffraction patterns of PA-10,T (a) containing 10 wt-% (b), 20 wt-% (c), 30 wt-% (d), 40 wt-% (e), 50 wt-% (f), and 60 wt-% (g), PA-6,T (100% PA-6,T(h)).

(5-wt-% PA-6,T increments)

Figure 2.14 displays the tan δ of compression molded and annealed copolymer films obtained from dynamic mechanical analysis. All the DMA data, including the storage modulus at 100 and 200 °C and the maximum tan δ is summarized in Table 2.2. The glass transition temperature (T_g), as determined by the tan δ maximum for PA-10,T and PA-12,T were found to be 147.7 and 137.3 °C, respectively. PA-12,T has two additional flexible methylene groups per mole of repeat unit when compared to that of PA-10,T, thus decreasing the amide density and T_g.

Comonomer composition has been shown to influence the amount of crystallinity and the types of crystals formed due to the variation of comonomer sequences formed. This consequently impacts the composition of the amorphous phase. Both PA-10,T and 12,T with 15 wt-% PA-6,T display a small second transition at approximately 190 and 182 °C respectively. This is consistent with the formation of a second phase. Although there exists no data in the literature describing the miscibility of these polymers, this work suggests that at 15 wt-% PA-6,T phase separation may occur, resulting in a higher T_g phase. WAXD has shown that 6,T segments do not participate in crystallization at 15 wt% PA-6,T. With this exclusion from the crystalline domain, the local content of PA-6,T in the amorphous domain is increases upon crystallization of the 10,T or 12,T sequences. This result creates a concentration and distribution of sequences that favor phase separation. At 30 and 50 wt-% PA-6,T this shoulder disappears, but an overall increase in T_g is observed. Due to lack of crystallinity at these PA-6,T levels, the tan delta signal is larger compared to the homopolymers. The slight increase in T_g is due to the increase of more rigid 6,T segments in the amorphous domain.
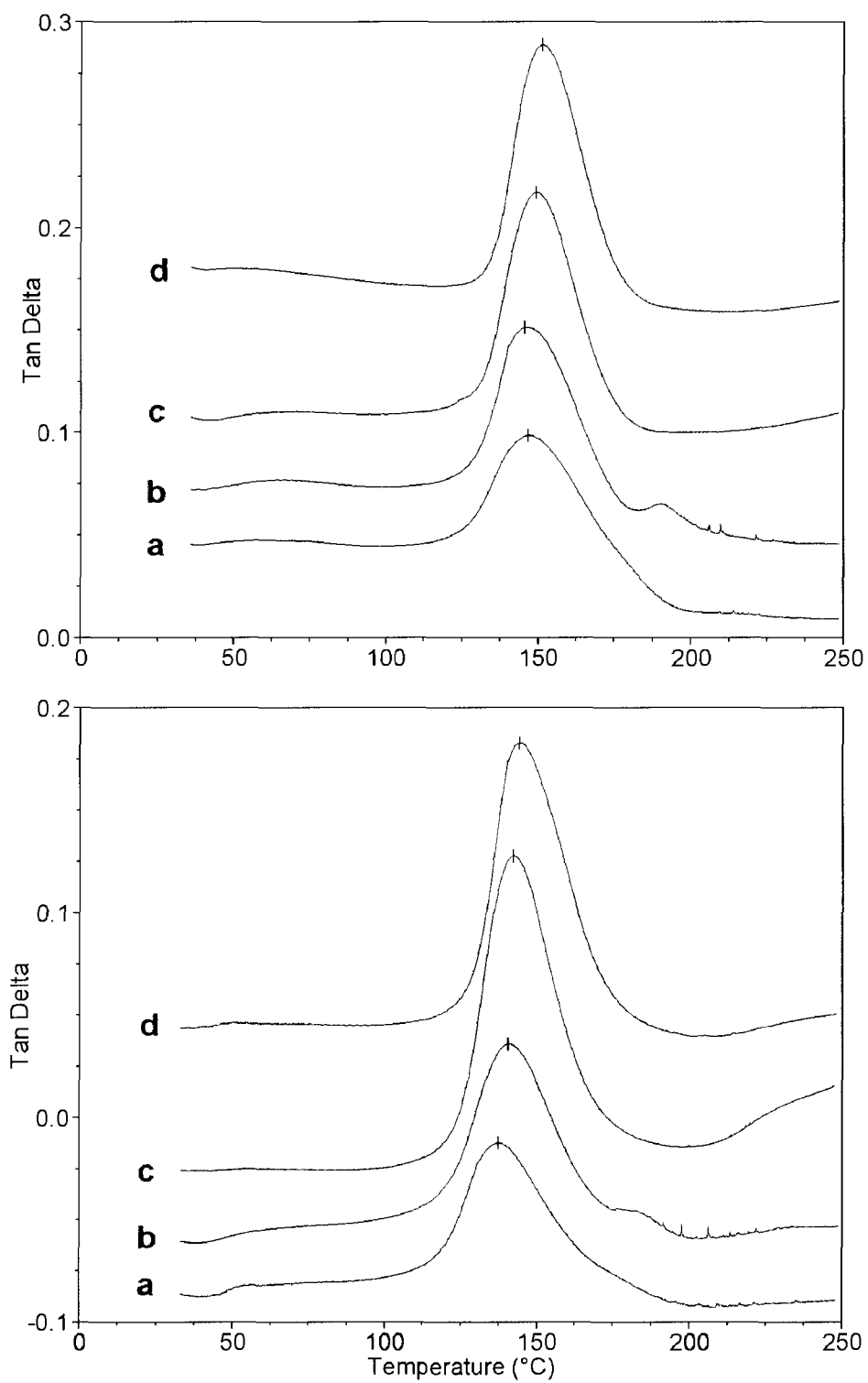
Figure 2.14. Tan delta of PA-10,T (Top) and PA-12,T (Bottom) with 0 (a), 15 (b), 30 (c),

and 50 (d) wt-% PA-6,T

Table 2.2. Storage modulus, maximum tan δ and melting enthalpies for PA-10,T, 6,T and

PA-12,T, 6,T copolymers

	E' at 75 °C (MPa)	E' at 200 °C (MPa)	tan δ_{max}	$\Delta H_{melting}$ (J/g)
PA – 10,T	1740	470	148	70
15 wt-% PA 6,T	1810	330	146	43
30 wt-% PA 6,T	1790	260	149	30
50 wt-% PA 6,T	1820	260	149	52
PA – 12,T	1730	450	137	60
15 wt-% PA 6,T	1600	360	140	38
30 wt-% PA 6,T	1660	240	142	26
50 wt-% PA 6,T	1750	280	144	42

While the differences in the storage modulus below T_g (75 °C) are negligible, the modulus above T_g (200 °C) is significantly lower for less crystalline samples. For example, the modulus at 200 °C for PA-12,T is 450 MPa while the 70:30 PA-12,T, 6,T copolymer has a modulus of 240 MPa at that temperature. Crystals act as reinforcing agents by tying the chains together and are independent of the glass transition, therefore the modulus above T_g is a function of the degree of crystallinity. Thus, the decrease in the storage modulus and enthalpy from the homopolymer to 30 wt-% PA-6,T can be properly deduced as reduction of the degree of PA-12,T crystallinity. This is in correlation with WAXD, where the diffraction peak intensity and sharpness decreased with increasing PA-6,T content.

While the melting enthalpy of the 50 wt-% PA-6,T copolymers recover from the eutectic point, the storage modulus above T_g does not. For example, the melting enthalpies of the 30:70 and 50:50 PA-12,T, 6,T copolymers are 26 and 42 J/g respectively, and their moduli above T_g are 240 and 280 MPa, respectively. Additionally, the 15:85 copolymer has a lower melting enthalpy, but a 20% larger modulus at 200 °C.

Therefore, the rise in melting enthalpy from 30 to 50 wt-% PA-6,T is not solely due to the increase of the degree of crystallinity, but also corresponds to the change of crystal form from PA-12,T to PA-6,T, since the theoretical melting enthalpy of a perfect PA-6,T crystal is higher. This is in agreement with WAXD data, where the PA-12,T crystals at 15 wt-% PA-6,T are much sharper than those for PA-6,T crystals and 50 wt-% PA-6,T. Interpretation of the enthalpy data as the degree of crystallinity can be misleading because there is the change of enthalpy associated wit new crystal formation.

Discussion

Copolyamide crystallization behavior is a result of amide distance and orientation symmetry. For example, PA-6,6, 6,T copolymers exhibit co-crystalline (isomorphic) behavior because they are both A-A B-B, even-even monomers and the distance between amide groups of adipic and terephthalic acids have only a 0.3 angstrom difference.[5] Therefore, they display linear trend of melting temperature as function of PA-6,T comonomer content. This data is shown Figure 2.15, along with PA-12,T (10,T) – 6,T and several other PA-6,T copolymers[1,9] as a function of PA-6,T comonomer content.

PA-10,T(12,T) – 6,T, PA-6,I, 6,T, PA-4,T, 6,T, and PA-6, 6,T copolymers are not isomorphic, displaying a minimum of melting temperature as a function of composition. Figure 2.15 shows that the eutectic melting behaviors of these copolyamides are distinct in terms of the location and depth of the curve. For instance, PA-10,T(12,T)-6,T copolymers display a smaller melting point depression which occurs at higher amounts of PA-6,T, compared to PA-6, 6,T copolymers. At the eutectic point, the decrease in melting temperature from PA-6 homopolymer is 88 °C with 16 mol-% PA-6,T, while for PA-12,T, 6,T and PA-10,T, 6,T copolymers these values are 20 °C at

34 mol-% and 35 °C at 37 mol-%, respectively. This implies that PA-6,T disrupts PA-6 crystallinity to a greater extent than PA-10,T and PA-12,T. This behavior can be attributed to similarities in PA-10,T, 12,T, and 6,T repeat unit structures. Terephthalamide copolymers maintain a regular hydrogen bonding orientation and all have an even number of carbon atoms between amide bonds. Alternatively, PA-6 includes a reverse amide bond due to the head to tail linkage of the A-B structure. Therefore, addition of PA-6,T has a larger effect on the eutectic meting behavior of PA-6, 6,T copolymers.
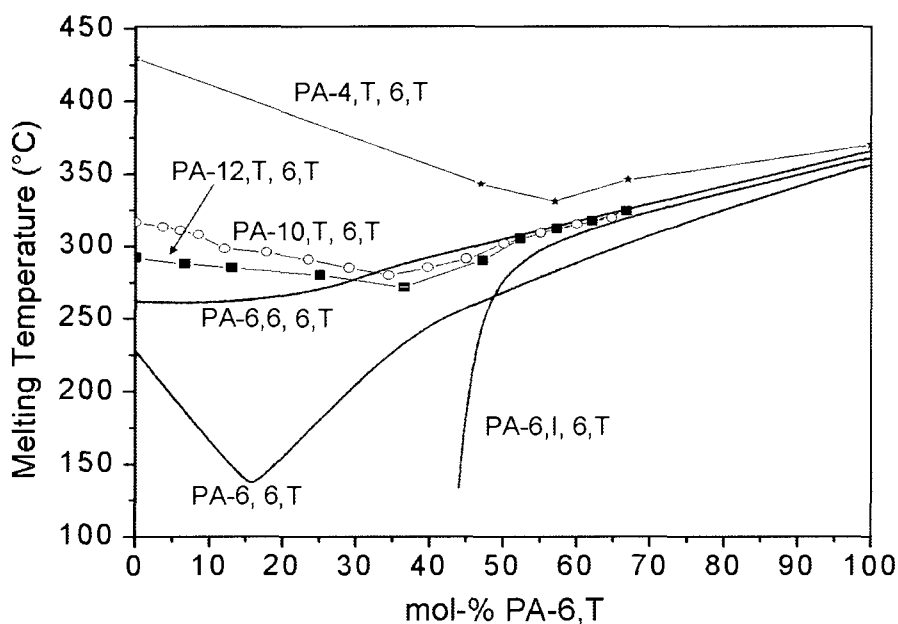
Figure 2.15. PA-10,T(12,T) – 6,T copolymer melting data overlaid with several additional PA-6,T copolymers versus mol-% PA-6,T

PA-6,I is amorphous due its kinked nature and its copolymers display a absence of crystallinity up to 43 mol-% PA-6,T. Both the length and orientation between amide bonds is affected by inclusion of the isophthalamide structure. The data shows the PA-6,T crystals can have exceedingly low melting temperatures (< 250°C), however eutectic behavior of fully terephthalamide polymers do not show such reduced melting points for

the onset of PA-6,T crystallinity. For example, PA-10,T, 6,T, 12,T, 6,T copolymers have lowest melting points of 281 and 270 °C respectively even despite having different lengths between amide bonds. Therefore, the symmetry of the aromatic substitution plays the major role in determination of shape of the eutectic melting temperature trends. Additionally, PA-4,T, 6,T copolymers have a similar shape as the PA-10,T, 6,T and 12,T, 6,T copolymers. Since, PA-6,T is the lower melting component, the eutectic point occurs at higher PA-6,T concentrations. Distinct from the isophthalamide copolymers, terephthalamide species maintain a symmetrical amide bond orientation in both homo and alternating segments. Their unique melting point trend may be associated with the ability of alternating units to crystallize or participate in homopolymer crystal formation in the eutectic well. Thus, they do not display a large reduction in melting point of PA-6,T crystals as seen in PA-6,I, 6,T copolymers.

The melting behavior of PA-6,6, 6,T and PA-10,T(12,T), 6,T copolymers exceeding 50 mol-% PA-6,T are similar. By definition, the melting temperature of isomorphic copolymers is a function of crystal composition with no loss of crystallinity, while non-isomorphic crystalline melting temperature is a function of crystal amount and size. For instance, the density PA-6,6, 6,T isomorphic copolyamides were found to rise with increasing PA-6,T content[5], whereas PA-10,T(12,T), 6,T copolymers were found to have reduced crystallinity with PA-6,T content based on DSC and DMA. Interestingly, PA-6,6, 6,T and PA-10,T(12,T) – 6,T copolymers exceeding 50 mol-% PA-6,T have crystals that differ in composition, amount, and size, but have the same melting temperature.

Conclusions

Melt condensation polymerization of PA 10,T and 12,T with PA-6,T comonomer has been demonstrated to produce statistical copolymers. The ^{13}C chemical shift of the substituted aromatic carbon is sensitive to the comonomer connectivity at different compositions, providing key chemical information in describing the physical changes of the above mentioned copolymers. It was found that at 15 and 30 wt-% PA-6,T little pure PA-6,T sequences exist, and the majority of the PA-6,T comonomer is found in PA-10,T (or 12,T) – PA-6,T alternating sequences. Since the comonomers are not co-crystalline, PA-10,T (or 12,T) – PA-6,T alternating units act as impurities that deter the formation of PA 10,T (12,T) crystals. This is supported by a decrease in melting temperature and enthalpy by DSC, the loss of sharp x-ray diffraction peaks up to 30 wt-% PA-6,T, and the increased clarity of compression molded films. However, at PA-6,T content greater 30-wt% increases the melting temperature of the corresponding copolymer in a manner independent of the comonomer. Past the eutectic point, pure 6,T sequences become sufficiently abundant for themselves to crystallize. NMR analysis confirmed the increase pure PA-6,T sequences being formed at 50 wt-% PA-6,T. X-ray diffraction at this composition also displayed sharp diffraction peaks that correspond to PA-6,T crystals. It has been demonstrated that melting temperatures and amount of crystallinity can be tuned by changing the amount of PA-6,T comonomer of PA-10,T, 6,T and PA-12,T, 6,T copolymers. These properties will affect the processability, optical clarity, and solvent resistance of the resulting polymer, while maintaining the notably higher glass transition temperatures than aliphatic polyamides.

Acknowledgments

References

[1] Kohan, M.I. *Nylon Plastics Handboook*. 1995 Carl Hanser Verlag, Munich Vienna NewYork. Pages 372-374 and 594-599

[2] Shashoua, V.E.; Eareckson, W.M. *J. Poly. Sci.*, **1959**, 40, 343-358.

[3] Morgan, P. W.; Kwolek, S. L. *Macromolecules*. **1975**, 8, 2, 104-111.

[4] Kaitian X.; Jarrett, W.; Mathias L. J. *Polymer Preprints* **2005**, 46, 1, 789.

[5] Edgar, O. B.; Hill R. *J. Polymer Sci.* **1952**, 8, 1.

[6] Yu, A.J.; Evans, R.D. *J. Poly Sci.* **1960**, 42, 249-257.

[7] Harveym E. D.; Hybart, F. J. *Polymer* **1971**, 12, 711-716.

[8] Liu, H.; Yang, G.; He, A.; Wu, M. *J. Apl. Poly Sci.* **2004**, 94, 819–826.

[9] Rulkens, R.; Crombach R.C.B. (DSM). U.S. Patent 6,747,120, June 8, 2004.

[10] Solomon, O. F.; Ciuta, I.Z. *J. Appl. Polym. Sci.* **1962**, 6, 683.

[11] Novitsky, Theodore, Lange, Chris. Mathias, L.J. Osborn, S.; Manning, S.; Ayotte, R. *J. Apl. Poly. Sci.* **2009**, Article in Press.

[12] Vouyiouka, S.N.; Karakatsani, E.K.; Papaspyrides, C.D. *Prog. Polym. Sci.* **2005**, 30, 10–37.

[13] Aerdts, A. M.;. Eersels, K. L. L; Groeninckx, G. *Macromolecules.* 1996, *29,* 1041-1045.

CHAPTER III

ONE-POT SYNTHESIS OF PA-12,T - PA-6 BLOCK COPOLYMERS USING CaCl$_2$

Abstract

PA-12,T-PA-6 block copolymers were synthesized using a one-pot synthesis involving the step growth formation of PA-12,T macroinitiator using biscaprolactam terephthalamide and 1,12-diaminododecane in caprolactam followed by the anionic polymerization of the caprolactam. The effect of time, stoichiometry, and CaCl$_2$ concentration on the step growth polymerization was first studied, following the effect of CaCl$_2$ on the anionic polymerization. CaCl$_2$ has little effect on the step growth formation of the PA-12,T macroinitiator, but has a substantial effect on the anionic polymerization. At a constant 5 minute reaction time, reactions with CaCl$_2$ concentrations below 5 mol-% of caprolactam display complete conversion of the caprolactam into PA-6, while above 5 mol-% only show partial conversion. Intrinsic viscosities of these samples increase linearly from 0.72 to 3.59 dL/g with a decreasing CaCl$_2$ concentration, and in the absence of CaCl$_2$ a crosslinked material is produced. The amount of PA-12,T block transamidation was found to increase linearly with decreasing CaCl$_2$ concentration observed by quantitative ^{13}C NMR. Results show that both caprolactam conversion and transamidation are competing reactions and are both negatively affected with increasing CaCl$_2$ concentration. DSC and solubility of the resulting materials behave consistently with trends found in copolymer composition, structure, and molecular weight variations provided by the dramatic effects of CaCl$_2$ on PA-12,T macroinitiator anionic polymerization.

Introduction

Polyamide block copolymers have properties and morphologies that cannot be achieved by polymer blends. Unfortunately, the synthesis of polyamide-polyamide block copolymers is complicated using conventional methods due to transamidation of the amine endgroups leading to random backbone structures. For example, Groeninckx et al. have shown by ^{13}C NMR spectroscopy that melt mixing PA 6,I and PA 4,6 homopolymers for 90 minutes at 315 °C yields average block sequences of 8 PA-4,6 repeat units.[1]

Anionic polymerization (AP) of lactams offers alternative synthetic strategies to achieve better control in forming of polyamide block copolymers. Lactam AP is performed by using sodium hydride (or sodium caprolactam salt) as the initiator with an n-acyl caprolactam co-initiator. Two approaches have been reported in the literature to form block copolymers via anionic polymerization. The sequential addition of monomers in AP using twin screw extrusion has been extensively studied by White et al. They demonstrated that block copolymers can be formed by first initiating the anionic laurylactam (PA-12) followed by the sequential addition of caprolactam and caprolactone at various points into the extruder.[2] However, the variety of cyclic monomers is much less than linear polyamide monomers, limiting the applicability of this strategy.

Another means of forming block copolymers by anionic polymerization of lactams involves reactions coinitiated by n-acylcaprolactam based macroinitiators. This approach is advantageous because the macroinitiator can be synthesized by other polymerization methods, thereby making a wide variety of PA-6 block copolymers available. Such examples in the literature include; polybutadiene[3,4], polytetrahydrofuran[5],

polyisoprene[6], polyethylene oxide-polyisoprene[7], polyimides[8], polysiloxanes[9], and poly(butadiene-co-acrylonitrile)[10]. Here, it is essential for AP that the MI has n-acyl caprolactam functionalities, usually adding an extra functionality step in the synthetic scheme. One popular method of functionalization is to endcap with isocyanates by reacting diisocyanate with a hydroxy or amine functional MI. When the isocyanate functionalized MI is dissolved in caprolactam, the isocyanate endgroups react with caprolactam to create an the n-acyl caprolactam coinitiator. While this approach is applicable to afford many types of copolymers with cyclic amides, the synthesis of polyamide-polyamide block copolymers remains challenging.

This study investigates the synthesis of polyamide-polyamide block copolymers by utilizing a one pot method. Only one other study was reported to utilize a one pot approach.[11] The first step of the synthesis involves the solution step growth polymerization of biscaprolactam terephthalamide and 1,12 diaminododecane using caprolactam as a solvent. By utilizing basic principles of polyamide step growth reactions, PA-12,T MI systems with n-terephthaloyl caprolactam end groups were obtained.

AP was then performed using the PA-12,T MI and caprolactam solvent as the monomer. The effect of $CaCl_2$ on the AP of PA-12,T MI is a pivotal finding in this study. Without $CaCl_2$, the reaction produces a crosslinked material in less than one minute. The presence of $CaCl_2$ in the AP yields tractable materials, making the $CaCl_2$ concentration the main variable of this study. While, several effects of inorganic salts such as LiCl and $CaCl_2$ on the AP of lactams have been reported in literature, actual mechanisms are still unknown.[12] Reaction rates, enthalpy and free energy of caprolactam AP have been

shown to decrease with increasing $CaCl_2$ and LiCl concentrations by monitoring the heat of formation of the reaction under adiabatic conditions.[13] Generally, $CaCl_2$ and LiCl are stated to retard the kinetics of caprolactam AP. The goal of this study is to examine the effect of $CaCl_2$ on the one pot synthesis and to use this retarding effect to identify the steps leading to the eventual crosslinking of the material.

Experimental

Materials

Terephthaloyl chloride, caprolactam, 1,12-diaminodoecane, triethylamine, calcium chloride and sodium hydride were purchased from Aldrich. Terephthaloyl chloride was recrystallized from hexanes by first creating a saturated boiling solution, then filtering this solution to remove undissolved acid, reheated and cooled. Diaminododecane was sublimed at 70 °C and dried before use. Caprolactam was dried at room temperature under vacuum for 24 hours. Hexanes, benzene, and triethylamine were dried over molecular sieves. Sodium hydride (60% in mineral oil) was used as received. $CaCl_2$ was pre-dried at 130°C under vacuum for 24 hours. Vacuum was released under dry air and the $CaCl_2$ stored in a dessicator. Sodium hydride was pre-weighed into separate vials in a dry box purged with argon.

Synthesis

Biscaprolactam terephthalamide (BCT). A solution of terephthaloyl chloride (22.624g, 0.111 mol) in 250 mL of benzene was added drop-wise to caprolactam (31.523 g, 0.279 mol) dissolved in 410 mL of benzene and 77 mL of triethylamine in an argon purged 2000 mL round bottom flask. The solution became progressively yellow with addition of the acid chloride solution. Following a one hour addition, the solution was

then heated at 80 °C for two additional hours. The solution was allowed to cool to room temperature overnight. The solids were then filtered and washed with 100 mL of cold benzene, followed by water to remove the triethylamine hydrochloride salt. The resulting solid was then dispersed in water, filtered and dried in under vacuum at 80 °C. The resulting BCT (36 g, 90% yield) had a melt point of 207 °C and 100 J/g melting enthalpy.

PA-12,T macroinitiator (PA-12,T MI). Test tubes with magnetic stir bars and pre-dried $CaCl_2$ were dried at 130 °C under vacuum for 24 hours. Vacuum was released using dry air (pulled through desiccant) and test tubes were immediately purged with argon. In a typical experiment 1,12-diaminododecane (0.5 g, 0.0025 mol), BCT (0.9362 g, 0.0026 mol), and caprolactam (4.5454g, 0.0402 mol) were added to the test tube. Note that mol-% $CaCl_2$ refers to the molar ratio of $CaCl_2$ to mols caprolactam in the initial monomer feed. Dry argon purging was continued for approximately 5 minutes. The test tube was then immersed in a silicone oil bath at 200 °C. The reaction was held at 200 °C with stirring for 4 hours. The solid white material plug was then ground, and soxhlet extracted with methanol for 12-18 hours. The white PA-12,T powder was obtained in a quantitative yield.

PA-12,T – PA-6 block copolymers. AP was performed subsequent to the formation of PA-12,T macroinitiator with various levels of $CaCl_2$. After the 4 hour PA-12,T step growth polymerization time, sodium hydride (0.022 g, 0.00036 mol) was added to the reaction mixture. The tube was then hand shaken to ensure complete dispersion of the sodium hydride. Magnetic stirring was adjusted throughout the reaction. After 5 minutes at 200 °C, the test tube was removed from the silicone bath and immersed in ice water. Samples with 10% $CaCl_2$ were a viscous liquid after reaction and when cooled turned

into brittle, white solid. Using 1% $CaCl_2$, resulted in material that was opaque, tough, and solid after reaction. The products were either freeze ground in a blender or pelletized by hand, and soxhlet extracted with methanol for 18-24 hours. Polymer solutions (1 wt-%) in concentrated sulfuric acid were then passed through a glass wool packed filter and precipitated into water. Total water used to wash each sample was approximately 2 L. Air-dried samples were then ground and dried under vacuum at 90 °C.

Characterization

Intrinsic Viscosity (IV). Single point intrinsic viscosities of 0.5 g/dL of polymer solutions in concentrated sulfuric acid (96%) were obtained to analyze molecular weight variations. Polymer solutions were prepared by adding 0.25 grams of polymer and 25 mL of concentrated sulfuric acid into a 50 mL flask. After 12 hours of mixing using magnetic stirring, the solutions were diluted with an additional 25 mL of sulfuric acid, and stirring was continued for another 5-10 hours. Solutions were visually inspected for gelling, and passed through a funnel packed with glass wool if gel was present. Measurements were obtained using a Cannon viscometer in a 25 °C controlled water bath. The viscometer was washed with sulfuric acid and a portion of the next sample to be tested before measurements were recorded. Flow times were an average of three tests with that agree within +/- 0.2 seconds. Using flow times of concentrated sulfuric acid and polymer solution were used to calculate the specific and relative viscosities. Single point intrinsic viscosities were then calculated using Solomon and Ciuta relationship;

$$[\eta] = [(2*(\eta_{sp} - \ln(\eta_{rel}))]^{1/2})]/C$$

where, η_{sp} is specific viscosity, η_{rel} is relative viscosity, and C is concentration.

Nuclear magnetic resonance spectroscopy (NMR). NMR samples containing 10 wt-% polymer in a 3:1 volume ratio of hexafluoroisopropanol (HFIP) to $CDCl_3$ were prepared by dissolving pellets in HFIP, followed by addition of $CDCl_3$. Quantitative solution ^{13}C spectra were collected on a Varian ^{UNITY}INOVA NMR spectrometer operating at a frequency of 125.7 MHz. A 90° degree pulse width of 5.8 μs was used, with recycle delays for each sample equal to approximately 5 times the longest T_1 time. All spectra were recorded at 25°C with decoupling implemented only data acquisition. The number of transients required to achieve sufficient signal-to-noise for end group identification ranged from 5,000 to 18,000, depending on molecular weight. Data was zero-filled up to 128k points and filtered with 1 Hz of line broadening prior to application of Fourier transformation. Baselines were corrected using a 10th order polynomial.

Differential scanning calorimetry (DSC). Polymer melting temperatures were determined using a TA Instruments 2920 DSC. Scans were collected at a heating rate of 10 °C/min from 30 -310 °C followed by forced air cooling. Thermograms from first and second heating scans were acquired.

Solubility. Polymer solutions in formic acid were prepared at 1 wt-% concentration, shaken overnight, and visually inspected.

Results and Discussion

The one-pot synthesis of PA-12,T - PA-6 block copolymers occurs in two sequential steps. First, the solution polymerization of biscaprolactam terephthalamide (BCT) and 1,12-diaminododecane (DA) is carried out using caprolactam as the solvent. The molecular weight and endgroup functionality of PA-12,T is controlled using basic principles of PA-12,T synthesized by melt condensation outlined in Chapter I. The

second step of the synthesis involves the anionic polymerization of the caprolactam using the n-terephthaloyl moieties of the PA-12,T MI. This is the focus of the second section of this paper.

The two-step reaction without $CaCl_2$ produces crosslinked materials that are insoluble in H_2SO_4 or any other common polyamide solvent. The utility of this investigation is based on the finding that >1 mol-% of $CaCl_2$ produces tractable materials. Therefore, the effect of $CaCl_2$ on each step was investigated.

PA-12,T macroinitiator (MI)

The first step of the one-pot approach of the synthesis PA-12,T - PA-6 block copolymers is the step-growth reaction of BCT and DA to form PA-12,T (Figure 3.1). The reaction of DA with the n-terephthaloyl caprolactam carbonyl to displace caprolactam is favored. However, ^{13}C NMR spectroscopy reveals that 5-15% of the reactions consists of ring opening of the caprolactam carbonyl to form PA-12,6,T units in the resulting polymer (Figure 3.2). The α-amide carbon peak provides the clearest evidence of PA-12,6,T unit formation. The three chemical shifts at 41.59, 41.09, and 41.01, represent the pure PA-12,T, 6,T and 12,6 α-amide carbon atoms, respectively. The 6,T and 12,6 units are generated by the same reaction and therefore have identical heights. The expanded aliphatic region of the spectrum presented in Figure 3.2 clearly shows extra 1,12-diaminododecane peaks due to the PA-12,6,T units, providing further evidence of ring opening through the BCT monomer.

Figure 3.1. Synthesis of PA-12,T MI.
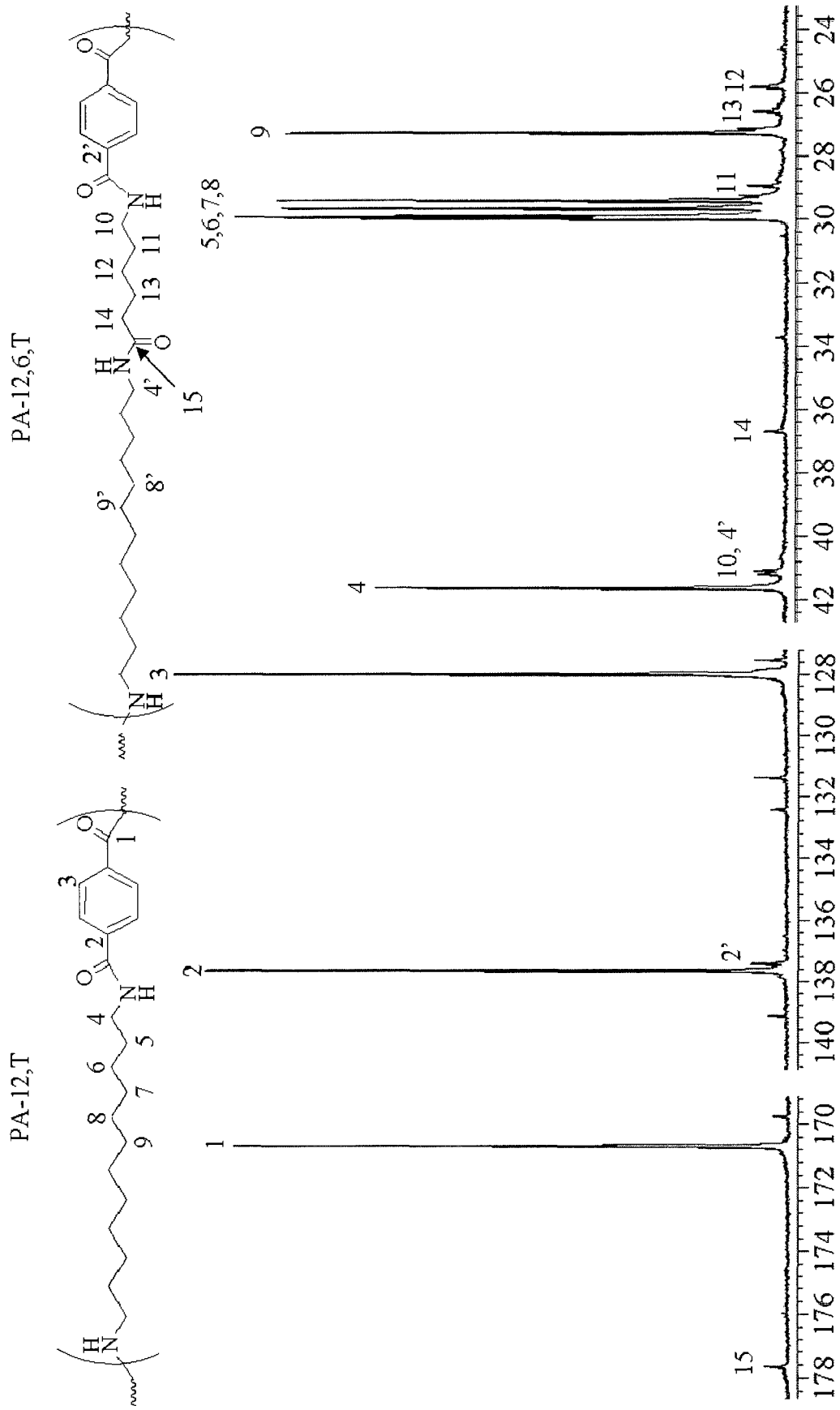
Figure 3.2. ^{13}C NMR spectrum of PA-12,T MI synthesized from BCT and DA with 10 mol-% CaCl$_2$ in caprolactam
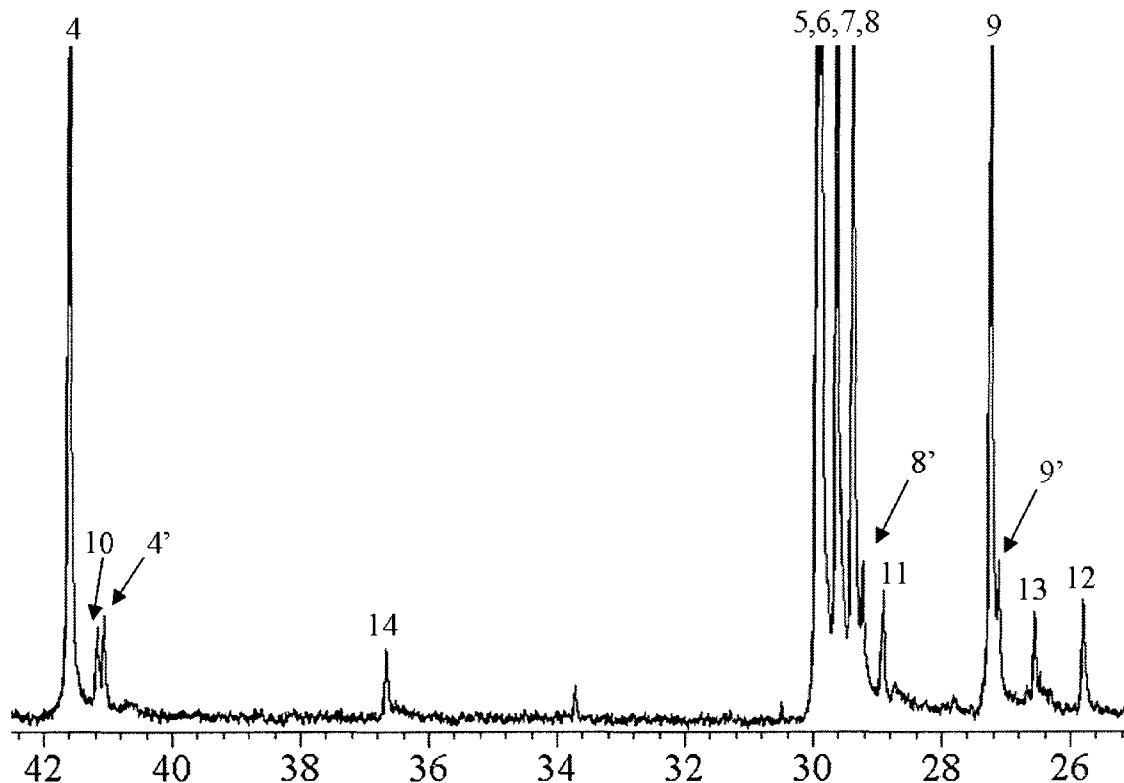
Figure 3.3. Expanded aliphatic ^{13}C NMR spectrum of PA-12,T MI from BCT and

DA with 10 mol-% $CaCl_2$ in caprolactam

Samples synthesized with 5 mol-% excess BCT and 5 mol-% $CaCl_2$ were soxhlet

extracted with methanol and precipitated from a sulfuric acid solution to remove the

caprolactam and $CaCl_2$. The ^{13}C NMR spectrum of the product shows that n-

terephthaloyl end groups are converted into terephthalic acid endgroups by hydrolysis. To

mitigate hydrolysis, a crude MI sample was washed with dry dichloromethane. The

carbonyl and aromatic ^{13}C NMR spectra of the dichloromethane extracted sample along

with the H_2SO_4 precipitated sample are presented in Figure 3.4. Peak broadening of the

dichloromethane extracted sample was observed because the $CaCl_2$ was not removed.

This caused complexation between polymer chains and sample thickening. The peak at

182.6 ppm is associated with n- acyl caprolactam species, shifted downfield by 0.6 ppm

from the BCT monomer. The n-acyl caprolactam peak is not observed in the H_2SO_4

precipitated sample, while the chemical shifts for terephthalic acid endgroups as

identified in Chapter I are seen in the spectrum. No peaks corresponding to amine

endgroups were observed at 42.3, 27.8 and 26.2 ppm.
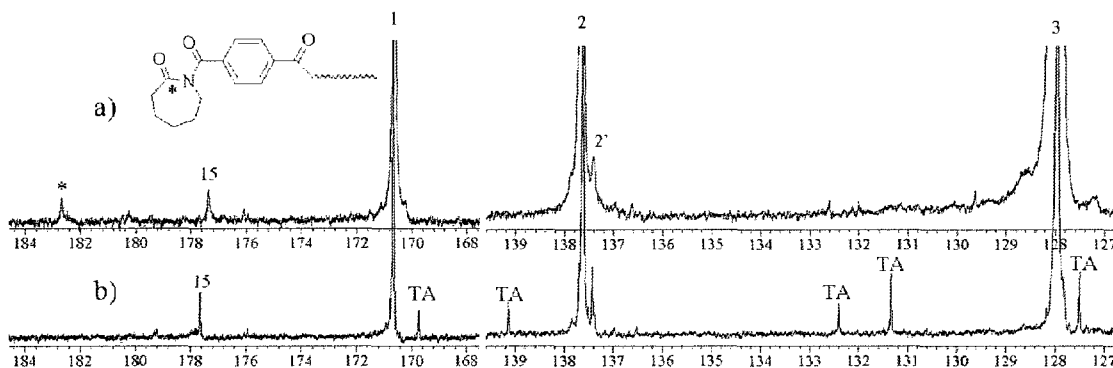
Figure 3.4. Carbonyl and aromatic ^{13}C NMR spectrum regions of a) dichloromethane

extracted and b) H_2SO_4 precipitated PA-12,T MI formed with 5 mol-% excess BCT and 5

mol-% $CaCl_2$

The concentration of anionic coinitiator (n-terephthaloyl caprolactam endgroups)

is a function of the molecular weight and endgroup functionality of the PA-12,T

macroinitiator (MI). Therefore, the effect of time, stoichiometry, and $CaCl_2$ concentration

of the step-growth formation of PA-12,T MI was studied. In each experiment, BCT, DA

and caprolactam were added to an argon-purged test tube with a predetermined amount of

$CaCl_2$. Solid polymer formed immediately upon melting of the caprolactam, trapping the

magnetic stir bar. Complete dissolution of all components and the onset of stirring

occurred at approximately 8-15 minutes for all reactions. Reaction temperatures (200 °C)

and MI concentration (15-wt-% caprolactam) were kept constant throughout all

experiments to ensure homogeneous solutions. With 5 mol-% $CaCl_2$, the solubility limit

of MI (BCT:DA = 1:0.95) was approximately 22 wt-% of caprolactam. If the temperature of this mixture is then lowered below ~190 °C, the MI started to precipitate. At the end of each polymerization, a clear viscous liquid was obtained. The white solid produced upon cooling was then ground, soxhlet extracted with methanol, and precipitated into water from a 1 wt-% H_2SO_4 solution. Table 3.1 lists the properties of MI synthesized with variations of polymerization time, stoichiometry, and $CaCl_2$.

Table 3.1. Properties of PA 12,T MI under various reaction conditions after soxhlet extraction and precipitation

Variable	Reaction time (hours)	BCT:DA	$CaCl_2$ (mol-% of Caprolactam)	IV (dL/g)	M_n[a]	DP
Reaction Time	1	1:0.98	3.5	0.75	7100	21
	2	1:0.98	3.5	0.74	7000	21
	4	1:0.98	3.5	0.77	7400	22
Stoichiometry (BCT:DA)	4	0.95:1	3.5	0.61	5500	17
	4	0.98:1	3.5	1.19	12700	38
	4	1:1	3.5	1.13	11900	36
	4	1:0.98	3.5	0.77	7400	22
	4	1:0.95	3.5	0.52	4500	14
$CaCl_2$	4	1:0.95	0	0.75	7100	21
	4	1:0.95	1	0.55	4800	15
	4	1:0.95	5	0.55	4800	15
	4	1:0.95	10	0.59	5300	16

[a] K = 0.000558 dL/g and a =0.81 in 96% H_2SO_4 at 25 °C

To determine the reaction time needed to ensure complete reaction of BCT and DA, identical polymerizations were run at 1, 2, and 4 hours. A stoichiometry of 1:0.98 BCT:DA, and $CaCl_2$ concentration of 3.5 mol-% were arbitrarily chosen. At 1, 2, and 4 hours at 200 °C, the intrinsic viscosity of the MI was 0.75, 0.74, and 0.77 dL/g, respectively. These values are identical within experimental error, and correspond to molecular weights of 7100-7500 g/mol based on Mark-Houwink solution constants developed for PA-12,T produced by melt condensation of terephthalic acid (TA) and

DA.[14] Although one hour appears to be a sufficient reaction time to complete the polymerization, four-hour experiments were chosen to ensure formation of a homogenous MI solutions for anionic polymerizations.

Keeping reaction time and $CaCl_2$ concentration constant, stoichiometry was then varied from 5 mol-% excess BCT to 5 mol-% excess DA. Figure 3.5 displays the change of intrinsic viscosity of the resulting polymer versus the reaction stoichiometry for the solution polymerization of BCT and DA in caprolactam and the melt polymerization of TA and DA. By adjusting the stoichiometry of the reaction to include 2 mol-% excess DA (BCT:DA = 0.98:1), MI with the highest intrinsic viscosity of 1.18 was observed, corresponding to a molecular weight of 12,700 g/mol. This result is due to the volatilization of the DA from the reaction, thereby altering stoichiometry by the nature of the polymerization conditions. This agrees with the data obtained from the melt polymerization of terephthalic acid and DA, where it was found that 1 and 3 mol-% DA yielded the highest molecular weight polymer and balanced amine and acid endgroups. Since amine endgroups do not initiate anionic polymerization, and may cause side reactions, e.g. transamidation, amine endgroups are not preferred for this study. Therefore, a stoichiometry of 5 mol-% excess BCT (BCT:DA = 1:0.95) was used for anionic polymerization to ensure complete n-terephthaloyl endgroups (Figures 3.1 and 3.4).
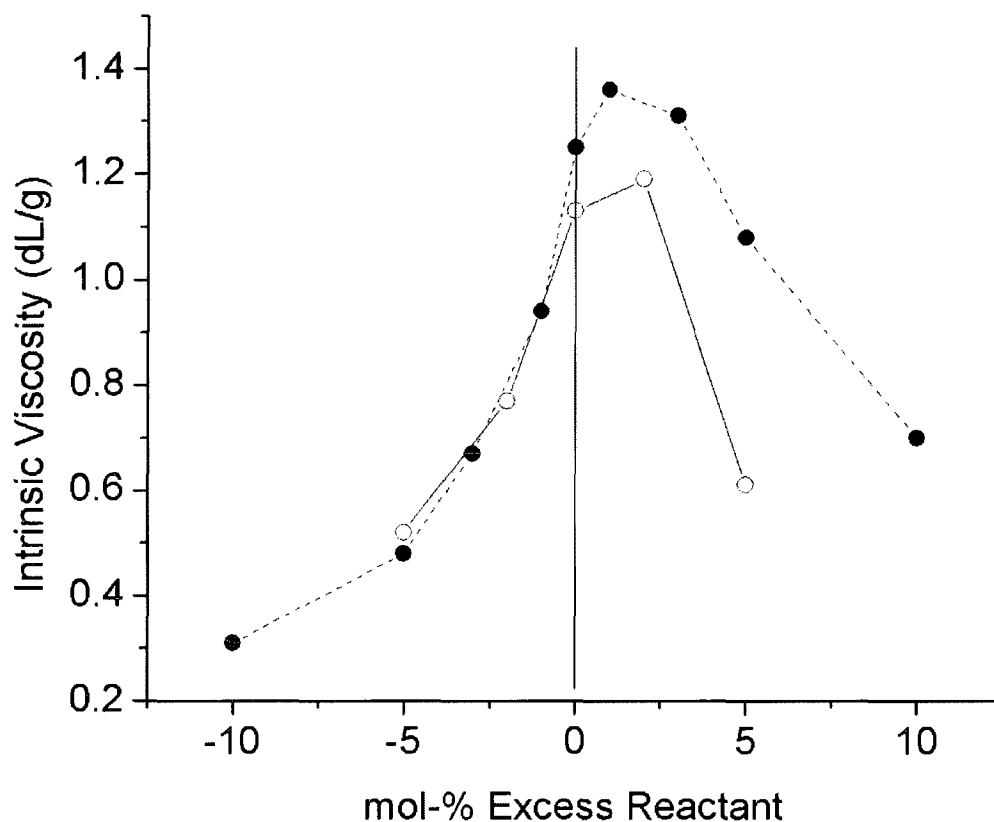
Figure 3.5. Effect of stoichiometry on (○) solution polymerization of BCT and DA in caprolactam and (●) melt polymerization of TA and DA. Negative values represent excess BCT or TA and positive values DA

Because this is a one pot reaction and $CaCl_2$ is present in both reactions it is important to examine its effect on the step-growth formation of the MI. The intrinsic viscosities of MI synthesized in the presence of 1, 5, and 10 mol-% $CaCl_2$ are 0.55, 0.55, and 0.59 dL/g respectively, with molecular weights of 4800-5300 g/mol. Table 3.2 displays DSC data of these samples, and DSC 1st and 2nd heating thermographs are presented in Figure 3.6. Generally, 1st heating melting temperatures display one sharp melting point. Since the samples were precipitated, the ability of the polymer chains to form more perfect crystals is greater due to increased mobility upon precipitation. Also, cold crystallization occurs between 100-105 °C, giving some indication of the glass

transition temperature of these materials. When cooling from the molten state and reheating, two melting temperatures were observed. Polyamides are known to have alpha and gamma crystal types, the alpha phase being a more perfect and higher melting crystal due to inter-chain and lamella symmetry. Due to the fast degree of supercooling (RT forced air cooling) from the melt and the rigid structure of PA-12,T compared to wholly aliphatic nylons, second heating curves display melting temperature for alpha and the less ordered gamma phases.

Table 3.2. DSC data of PA-12,T MI synthesized with various $CaCl_2$ concentrations

	1st Heating		2nd Heating			PA-6,T/ PA-12,T	wt-% PA-6
	T_m (°C)	$\Delta H_{melting}$	T_m^1 (°C)	T_m^2 (°C)	$\Delta H_{melting}$		
0	289.4	78.7	278.1	287.2	44.9	-	-
1	285.7	64.4	284.9	272.7	33.2	13.8	3.0
5	290.2	70.0	287.3	277.8	44.0	8.1	1.5
10	291.0	86.3	278.9	288.9	51.8	6.35	1.3

Figure 3.6. DSC 1st (left) and 2nd (right) heating thermographs of PA-12,T MI synthesized in caprolactam with (a) 0, (b) 1, (c) 5, and (d) 10 mol-% $CaCl_2$
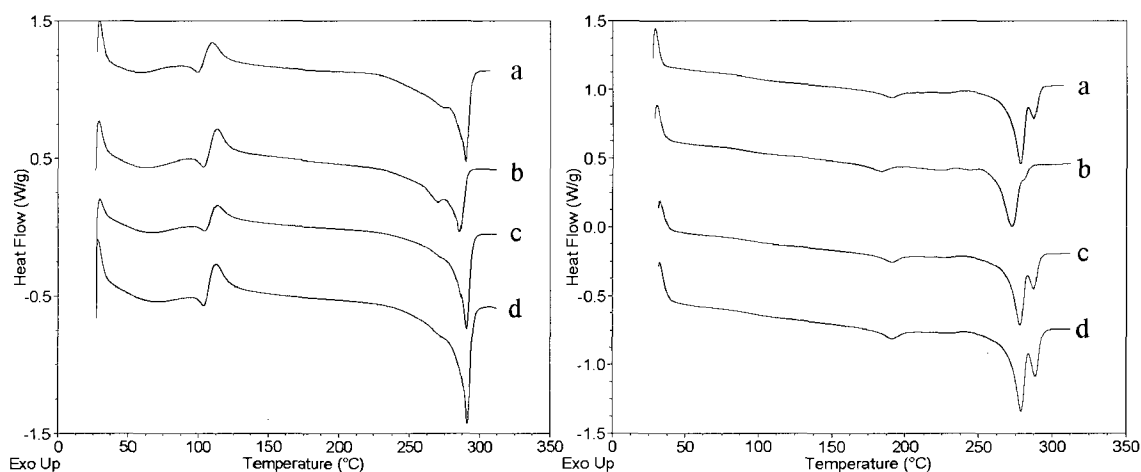
While $CaCl_2$ has little effect on the molecular weight of the PA-12,T MI, slight changes in the melting behavior were observed. It was found that increasing the amount

of $CaCl_2$ decreases the amount of PA-6 incorporated into the PA-12,T MI through ring opening of the BCT monomer. The amount of PA-6 incorporated was determined by integrating the PA-6,12,T and PA-12,T carbonyl peaks of the ^{13}C NMR spectra. The changes in melting temperature can be attributed to the amount of PA-6 incorporated, thus increasing the PA-6 amount decreases the melting temperature of the MI. It appears the PA-6 units are not co-crystalline with of PA-12,T crystals. PA-6 units act as irregularities, inhibiting the size and perfection of PA-12,T crystals, and thus decreasing the melting temperature and enthalpy. It is not surprising that co-crystallinity is not observed due to the differences hydrogen bonding orientation and length of the A-B PA-6 repeat unit and A-A B-B PA-12,T repeat unit. However, the amount of incorporation by using the BCT monomer is unexpected. The molar ratio of PA-12,T (Figure 3.3, 4) and PA-6,T (Figure 3.3, 10) will be used to represent the degree of randomness of the PA-12,T block in the following sections. As seen in Table 3.2, an increase in the randomness of PA-12,T MI decreases crystalline melting temperature and enthalpy.

Anionic Polymerization of PA-12,T MI

Without $CaCl_2$ the sequential anionic polymerization of PA-12,T MI forms a gelled product. Therefore, it is the topic of this second section is to examine the effect $CaCl_2$ on the anionic polymerization by varying its concentration from 1-10 mol-% of caprolactam. A five minute polymerization time was arbitrarily chosen and kept constant. PA-12,T MI concentrations were a constant 15 wt-%. This concentration was chosen because it is approximately 5 wt-% less than the solubility limit to ensure complete solubility in caprolactam and large enough to show significant effect that can be seen by high resolution NMR spectroscopy. Sodium hydride concentrations ranged from 1.5-1.6

times the endgroup concentration. The previous section showed that the molecular weight of the MI was not dependent on $CaCl_2$ concentration, therefore endgroup concentrations were calculated from the concentration of DA, assuming that the MI degree of polymerization was 15.

The anionic polymerization of PA-12,T MI is depicted in Figure 3.7. The initiator is formed in-situ when NaH abstracts a hydrogen atom from caprolactam, forming the caprolactam sodium salt and hydrogen gas. The reaction bubbles immediately following NaH addition, affirming formation of initiator. The caprolactam anion then attacks the n-terephthaloyl caprolactam endgroup of the PA-12,T MI (b). This reaction forms a relatively unstable amide anion (c), which abstracts a proton from the surrounding caprolactam medium, reforming the initiating caprolactam anion (d). Propagation occurs through repetition of steps b-d forming PA-12,T- PA-6 block copolymers (e) from the PA-12,T MI (a).

Qualitative observations. The anionic polymerization using 1 and 10 mol-% $CaCl_2$ are qualitatively very different. At 1 mol-% $CaCl_2$ the reaction mixture solidifies in approximately 15 seconds and remains solid throughout the five minute polymerization. Increasing $CaCl_2$ concentrations from 1% decreases the time until solidification of the reaction. At 10 mol-% $CaCl_2$, the reaction mixture is a viscous liquid at the end of 5 minutes. Both PA-12,T and PA-6 homopolymers have melting temperatures above the polymerization temperature, therefore the physical state of the polymerization at a certain reaction time results from the relative concentrations of caprolactam and PA-6. When the conversion of caprolactam to PA-6 is high, little caprolactam is available to fully dissolve the polymer and solidification occurs. When degree of conversion is low, the polymer

can still be dissolved in caprolactam. This qualitative difference hints at the degree of

conversion of the caprolactam with $CaCl_2$ concentrations.
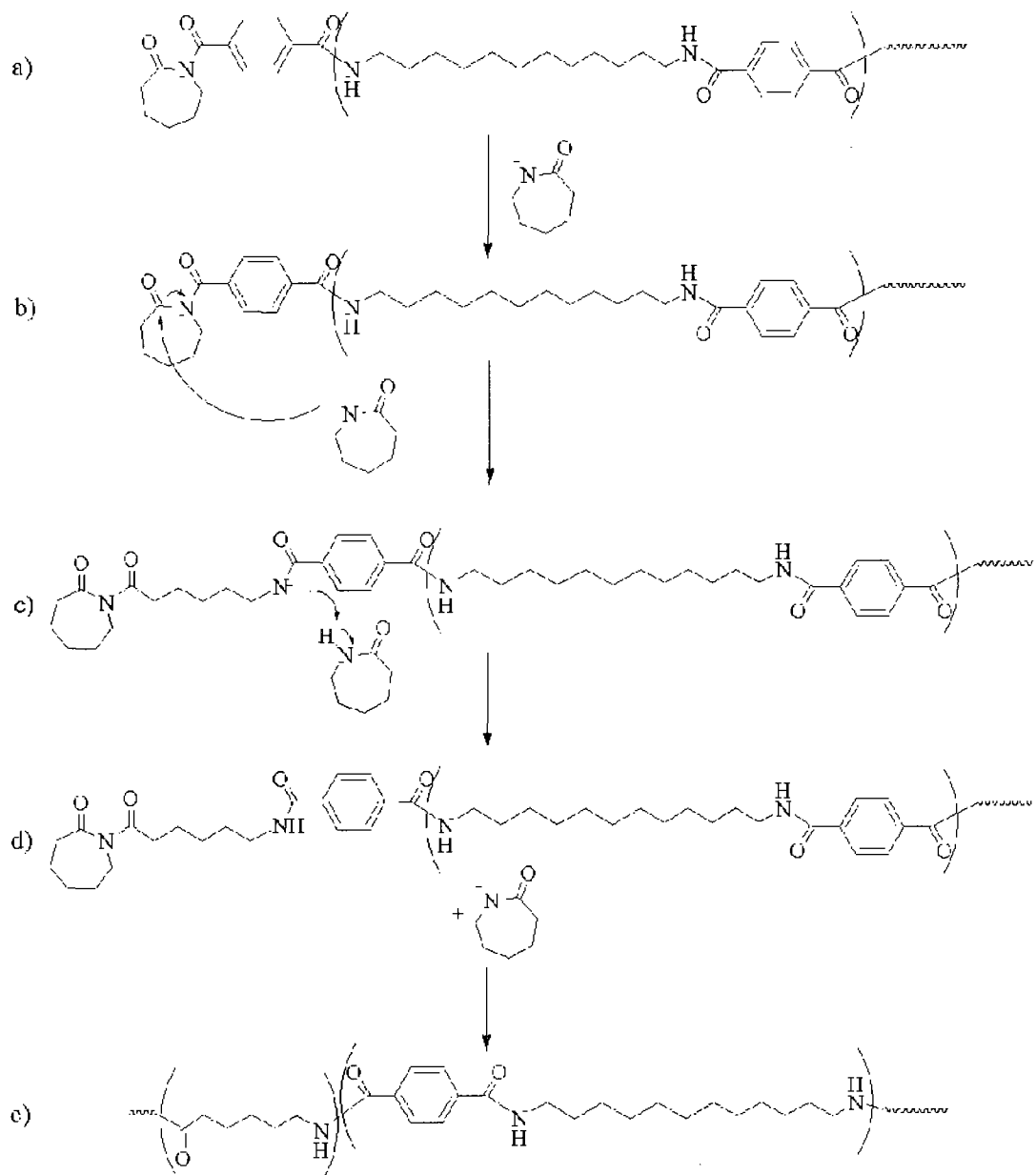
Figure 3.7. Anionic polymerization of (a) PA-12,T MI forming (e) PA-12,T – PA-6

block copolymers

The final solid products also showed considerable variations. At 10% $CaCl_2$, crystallization occurs forming a white product, and the material plug shrinks away from the test tube. At 1% $CaCl_2$, little crystallization occurs and the opaque product adheres to the walls of the test tube.

With the exception of the 1 mol-% $CaCl_2$ sample, all materials were soluble at 1 wt-% in concentrated sulfuric acid. The 1 mol-% $CaCl_2$ sample was partially soluble showing different behavior than a completely gelled sample. For example, completely gelled materials swelled and there was no noticeable difference in viscosity of the sulfuric acid, while the 1 mol-% $CaCl_2$ product exhibited decreased particle size with thickening of the solution. A portion of this sample was recovered by further dilution and the gel particles were removed by filtering.

^{13}C *NMR spectroscopy and IV.* The NMR spectrum of the 8 mol-% $CaCl_2$ sample with that of the PA-12,T MI and PA-6 homopolymers are displayed in Figure 3.8. Figure 3.9 shows the full ^{13}C NMR spectrum of anionic polymerizations of MI with 1, 2, 5, 8, and 10 mol-% $CaCl_2$. Spectra were normalized to the intensity of the PA-6 chemical shift.

Figure 3.8. ^{13}C NMR carbonyl and aliphatic spectra of a) PA-12,T MI, b) PA-12,T - PA-6 block copolymer c) PA-6

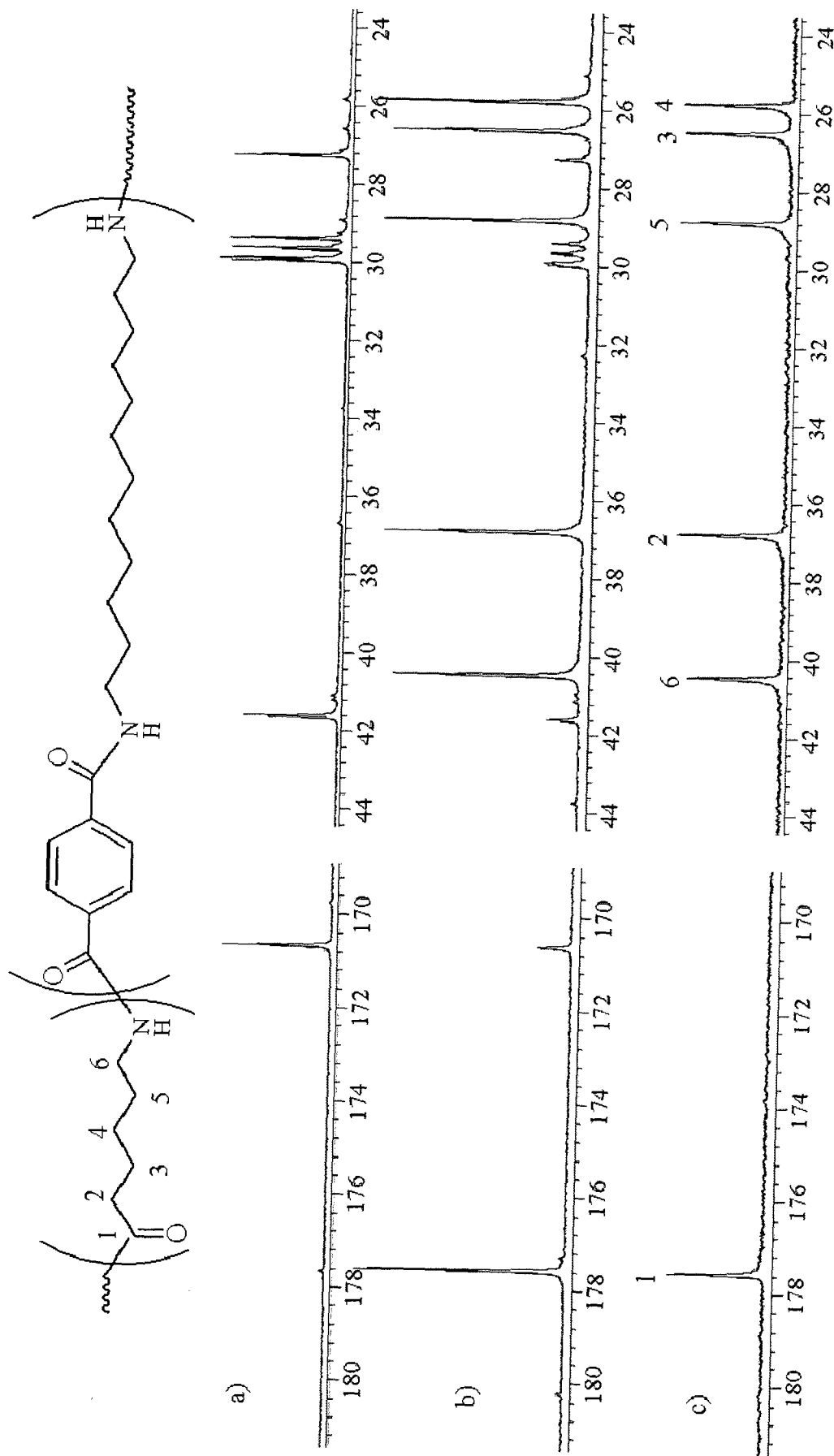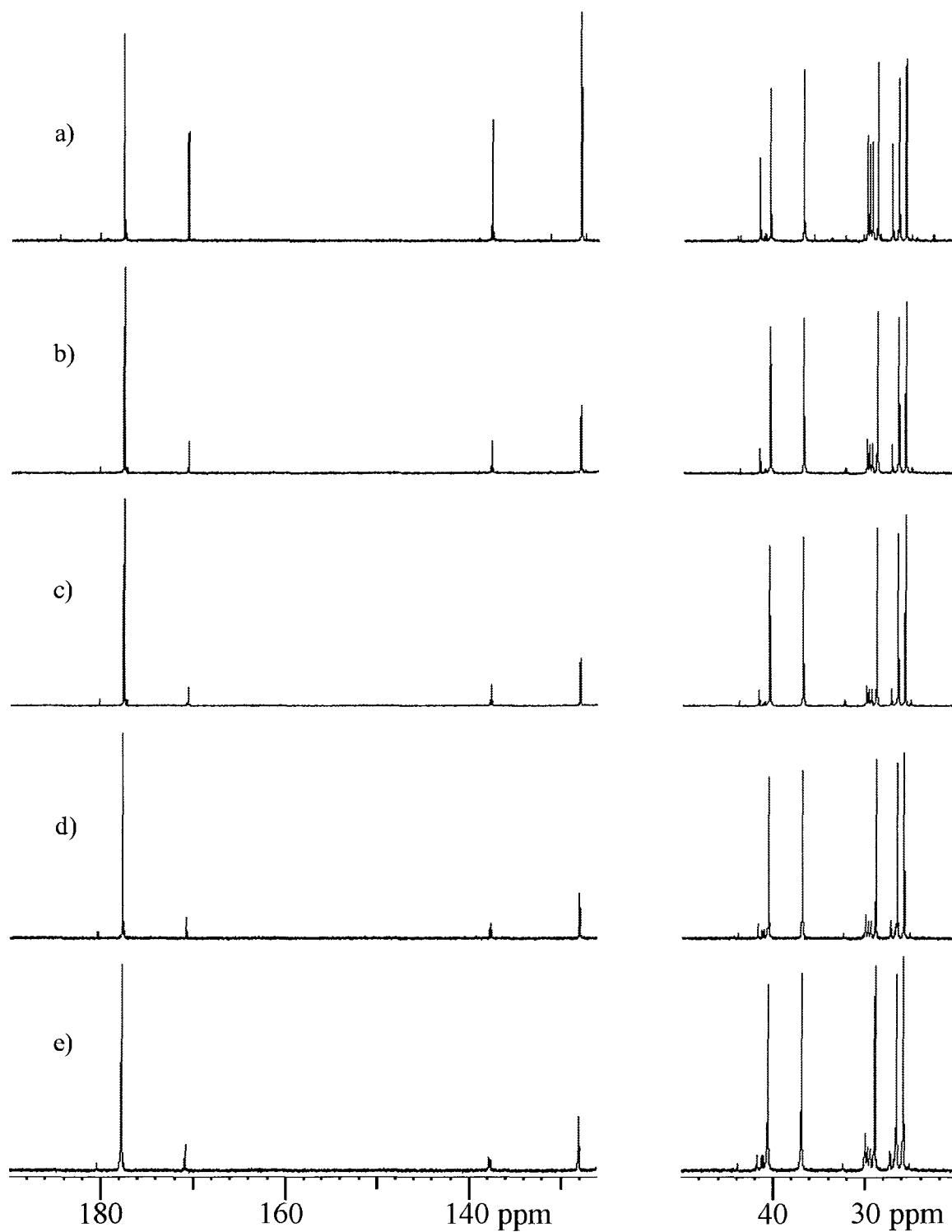**Figure 3.9.** ^{13}C NMR spectra of PA-12,T - PA-6 block copolymers formed in the

presence of a) 10, b) 8, c) 5, d) 2, and e) 1 mol-% CaCl$_2$

PA-6 conversion was determined by dividing the height of the PA-6 carbonyl

peak by the sum of the PA-6 and PA-12,T carbonyl peak heights in the ^{13}C NMR spectra.

The results are plotted in Figure 3.10 as function of CaCl$_2$ concentration. The vertical line

at 89% represents the theoretical incorporation at full conversion based on the initial

reaction mixture. Below 5 mol-% CaCl$_2$, the reaction approaches full conversion of

caprolactam into PA-6 within the five minute reaction time. Reactions above 5 mol-%

CaCl$_2$ do not reach full conversion. For example, at 10 mol-% CaCl$_2$, the PA-6

incorporation is 64%. This is consistent with the retarding effect of CaCl$_2$ on the kinetics

of the anionic polymerization of caprolactam. Note that reaction conversion and CaCl$_2$

concentration do not have a linear relationship. Thus, the five minute reaction time was

long enough to allow full conversion of caprolactam using less than 5 mol-% CaCl$_2$

despite the retarding effects. This is consistent with the observed increase of time until

solidification (approximate full conversion) with increasing CaCl$_2$ concentration.
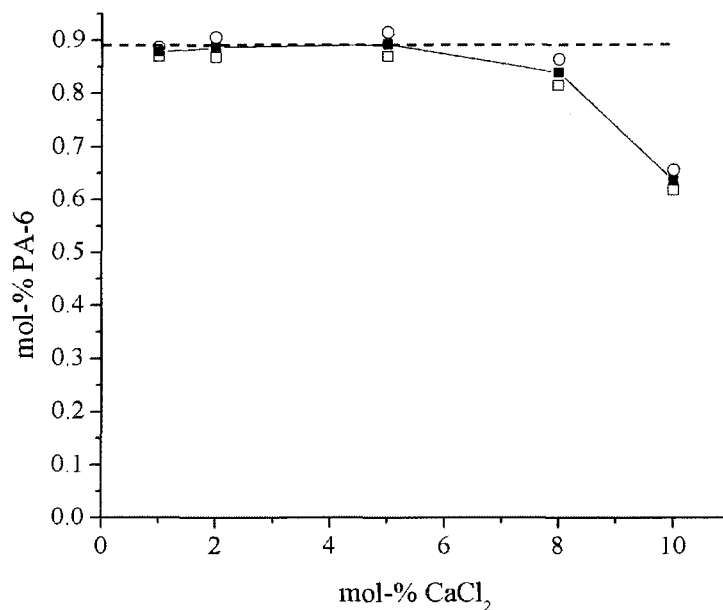
Figure 3.10. PA-6 incorporation based on (○) intensity,(□) integration, and (■) average

of ^{13}C NMR of PA-6 and PA-12,T carbonyl

The intrinsic viscosities of the PA-12,T - PA-6 copolymers and PA-12,T MI as a

function of CaCl$_2$ concentration are shown in Figure 3.11. The data exhibits a linear

increase in molecular weight with decreasing CaCl$_2$ concentration, with the only

deviation occurring for the 1 mol-% CaCl$_2$ sample. As stated earlier, only a portion of the

soluble sample was tested for IV. Removal of the crosslinked or high molecular weight

material causes the apparent decrease in intrinsic viscosity. Also, note that there is no

change in molecular weight of the PA-12,T MI with CaCl$_2$ concentration as discussed

earlier.
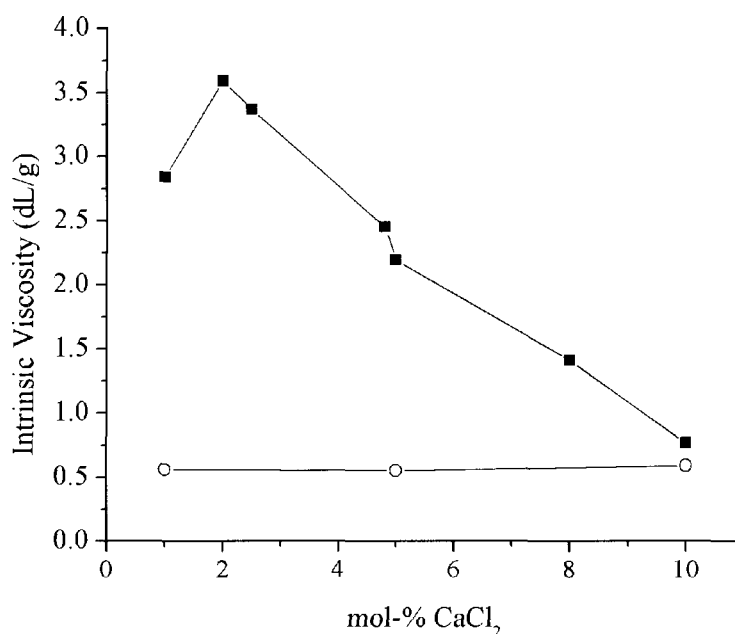
Figure 3.11. Intrinsic viscosities of (■) PA-12,T - PA 6 block copolymers and (○) PA-
12,T MI at 1-10 mol-% CaCl$_2$

If molecular weight is solely dependant on the conversion of caprolactam, then

the intrinsic viscosity should follow a similar trend as Figure 3.10. For example, reactions

containing 5 mol-% or less CaCl$_2$ have reached full conversion and should be similar

molecular weights. As can be seen in Figure 3.11, a maximum IV is not reached

(omitting 1 mol-%). Two possible explanations for this behavior are; 1) a change in coinitiator concentration, or 2) side reactions. It is believed that no drastic changes in coinitiator concentration between samples, because the IV of the PA-12,T MI has been shown to remain constant with $CaCl_2$ concentration. Therefore, this suggests the molecular weight behavior is due to the presence of a side reaction.

Closer inspection of the aliphatic region of the copolymer NMR spectra reveals evidence of a side reaction taking place during the AP of the PA-12,T MI. Figure 3.12 shows the expanded aliphatic region of the ^{13}C NMR spectrum of anionic polymerizations of PA-12,T MI with 1 and 10 mol-% $CaCl_2$. At 1 mol-% $CaCl_2$ the peak height of PA-12,T (42.6 ppm) has dropped to the same level of the two peaks for the 12,6,T unit (41.2 and 41.0 ppm), while at 10 mol-% the amount of PA-12,T prevails. Additionally, all peaks corresponding diamine portion of PA-12,T repeat unit show the same splitting. To further clarify this finding, the peak heights and integrations of the α-amide PA-12,T and PA-6,T were compared. By diving the values of the PA-6,T unit by that of the PA-12,T units, a value of PA-12,T randomness is obtained. For example, with a decrease in the PA-12,T peak or an increase in the PA- 6,T peak, the randomness value corresponding to the destruction of pure PA-12,T segments is given. This data is presented graphically in Figure 3.13 as a function of $CaCl_2$ concentration. Recall that the characterization of the PA-12,T MI showed that 5-15% of step-growth reactions occurred through ring opening of the BCT monomer to form the PA-12,6,T unit. PA-12,T MI randomness values were also calculated and presented in Figure 3.12. With decreasing $CaCl_2$ concentration, PA-12,T randomness is increasing, reducing the amount of purely PA-12,T segments. Transamidation (or interchange reactions) is known to occur in the

anionic polymerization of caprolactam, resulting in branching and crosslinking.[15,16] This

data indicates that transamidation of the PA-12,T segments is competing with the AP of

caprolactam.
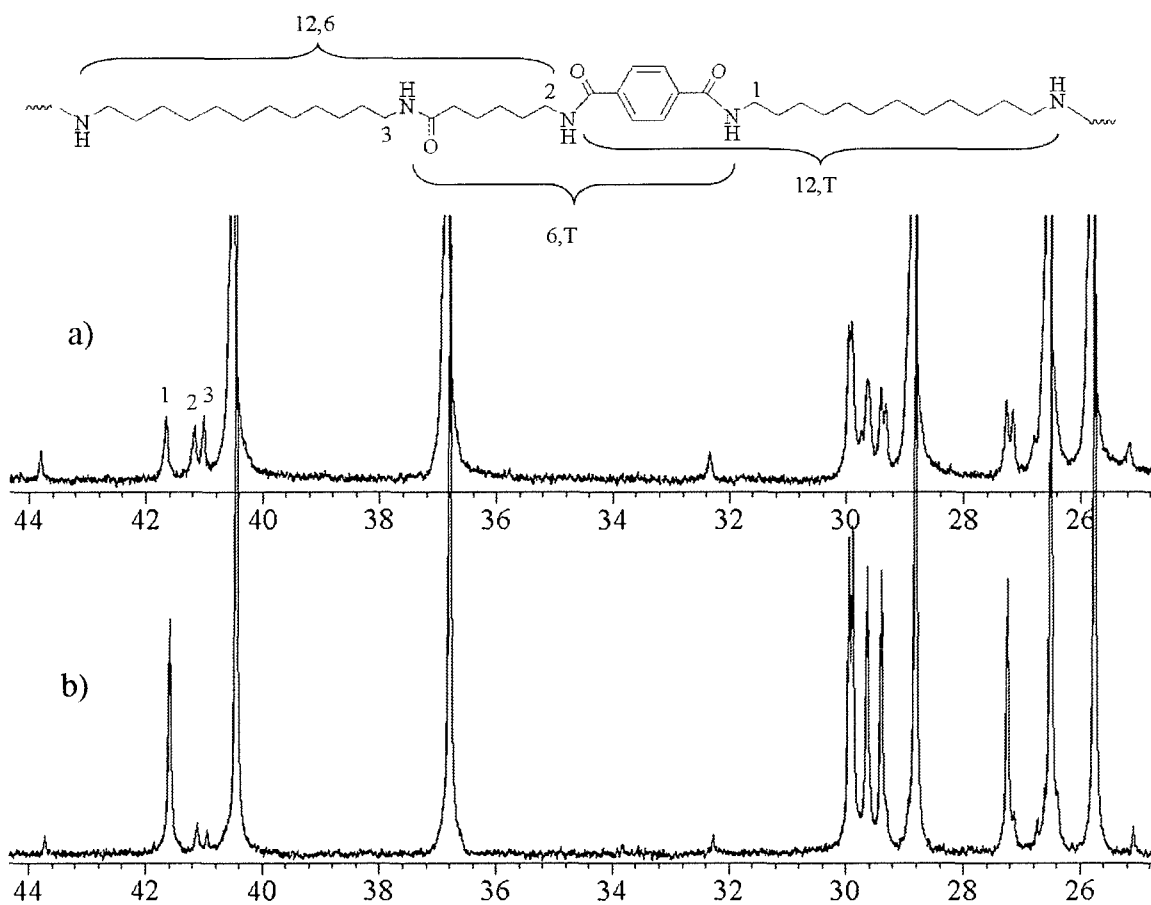
Figure 3.12. ^{13}C NMR aliphatic regions of the AP of PA-12,T MI with a) 1 and b) 10

mol-% $CaCl_2$
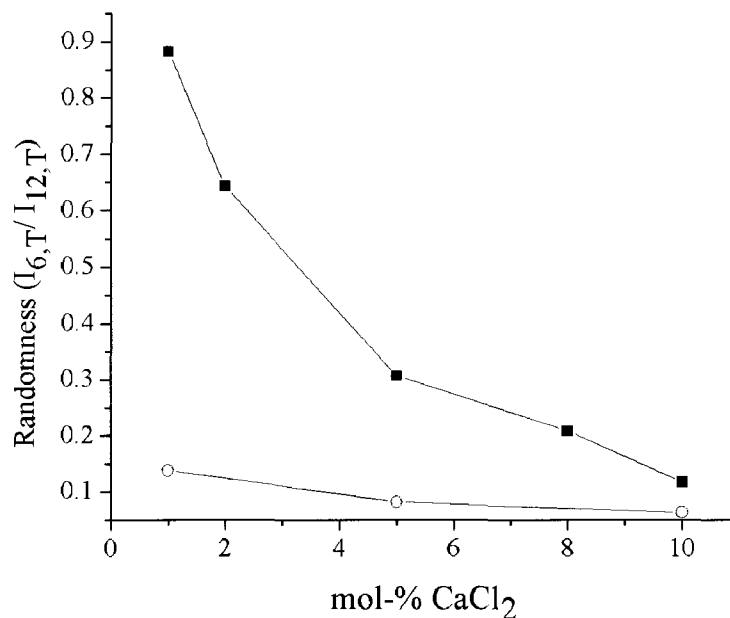
Figure 3.13. Randomness ($I_{6,T}/I_{12,T}$) of PA-12,T – PA-6 copolymers (■) and PA-12,T MI

(○) plotted as a function of $CaCl_2$ concentration.

Two scenarios that have to be considered to fully understand the behavior of the

system studied:

1. Incomplete conversion of caprolactam (>5 mol-% $CaCl_2$)

With greater than 5 mol-% $CaCl_2$, the propagation of the anionic polymerization

and transamidation are in competition. Both processes seem to be deterred by the

presence of $CaCl_2$ (lower conversions and less PA-12,T randomness). Molecular weight

variations are due both reactions, but the extent of each component cannot be properly

elucidated without further experimentation.

2. Full Conversion (<5 mol-% $CaCl_2$)

At full conversion of caprolactam, the copolymer branching and transamidation

reactions have been shown progress due to the rise intrinsic viscosity and consumption of

PA-12,T. It is not clear from this series of experiments if both are caused by the same

reaction, but both transamidation and branching(crosslinking) seem to be uniformly controlled by $CaCl_2$ concentration. These phenomena are responsible for gelling of the anionic polymerization in the absence of $CaCl_2$ and partial gellation of the 1 mol-% $CaCl_2$ sample.

Melting behavior. The melting behavior of the synthesized PA-12,T – PA-6 block copolymers are directly related to the aforementioned change in chemical composition discussed above. Full DSC thermographs are presented in Figure 3.14, and expanded PA-12,T melting temperatures are shown in Figure 3.15. DSC raw data and polymer compositions are given in Table 3.3.

Samples synthesized between 5 and 10 mol-% $CaCl_2$ display a melting peak for PA-6 and PA-12,T segments. In both scans, PA-12,T melting temperatures and enthalpies decrease progressively when samples are polymerized with decreasing $CaCl_2$ concentrations. PA-6 melting peaks show a decrease in melting temperature and increase in melting enthalpy. As discussed in the previous section, there is an increase in reaction conversion of caprolactam and the transamidation reaction of PA-12,T with decreasing $CaCl_2$ concentration. The increase in conversion from 10 to 5 mol-% $CaCl_2$ results in the dilution of PA-12,T segments from 45 to 15 wt-%. As transamidation increases, the length of pure PA-12,T segments decreases. Both dilution and decrease segment length cause the lowering in melting temperature and enthalpy of PA-12,T when $CaCl_2$ concentrations are decreases from 10 to 5 mol-%. Since the AP is complete at lower $CaCl_2$ concentrations, it is the transamidation reaction that negates the formation of PA-12,T crystals.

The increased enthalpy of the PA-6 melting peak from 10-5 mol-% $CaCl_2$ is due

an increase in the overall amount of PA-6 (55-85 wt-%) with increasing reaction

conversion. The lowering of the PA-6 melting temperature with decreasing $CaCl_2$

concentration is a result of the transamidation reaction forming non-crystallizable

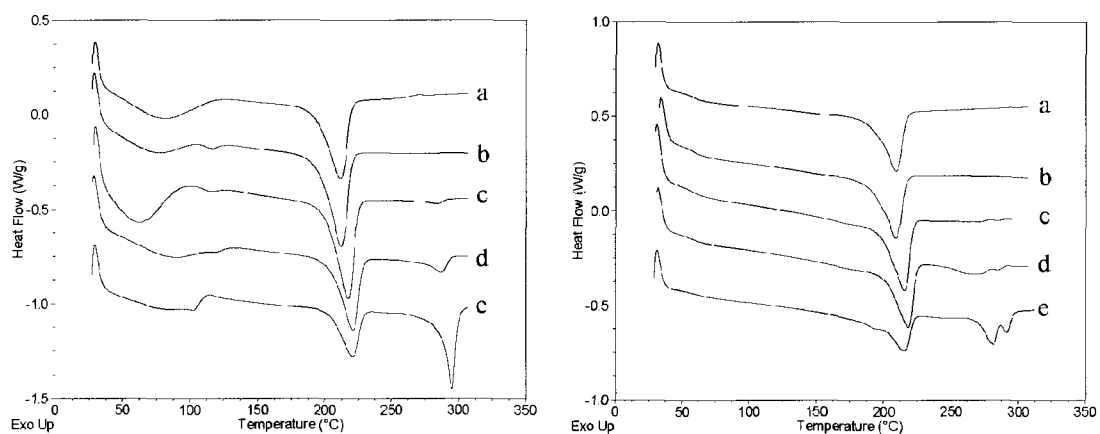segments, which disrupt the size and perfection of PA-6 crystals.

Figure 3.14. First (left) and second (right) heating DSC thermographs of PA-12,T - PA-6

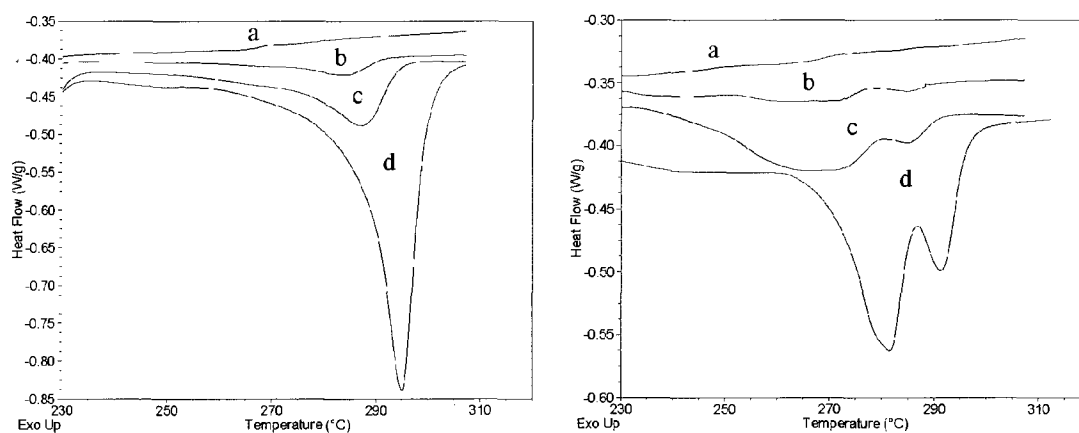copolymers synthesized with a) 1, b) 2.5, c) 5, d) 8, and e) 10 mol-% $CaCl_2$

Figure 3.15. Expanded first (left) and second (right) heating thermographs of PA-12,T -

PA-6 copolymers synthesized with a) 4.5, b) 4, c) 8, d) 10 mol-% $CaCl_2$

Table 3.3. DSC 1st and 2nd heating melting temperatures and enthalpies of PA-12,T - PA-6 copolymers

mol-% CaCl$_2$	Composition (wt-%)		1st Heating				2nd Heating				
			PA -6		PA 12,T		PA -6		PA 12,T		
	PA-6	PA -12,T	T_m	ΔH_{melt}	T_m	ΔH_{melt}	T_m	ΔH_{melt}	$T_m{}^1$	$T_m{}^2$	ΔH_{melt}
1	83%	17%	211.6	44	-	-	208.9	32	-	-	-
2	84%	16%	211.4	49	-	-	206.8	32	-	-	-
2.5	-	-	212.6	49	-	-	209.0	33	-	-	-
4.5	-	-	215.6	44	-	-	211.9	31	-	-	-
5	85%	15%	217.6	49	284.3	2.3	215.5	33	-	-	2.3
8	78%	22%	220.9	37	287.5	8.4	218.0	30	265.61	285.22	9.0
10	55%	45%	220.3	22	295	27	215.1	24	281.77	291.3	15.18

Solubility. Figure 3.16 shows the solubility behavior of the copolymers at 1 wt-% in formic acid (FA). PA-6 is completely soluble in FA while the PA-12,T MI is completely insoluble. Copolymers synthesized with 8 and 10 mol-% CaCl$_2$ form swelled particles in FA. While the PA-6 portions of the block copolymer have the propensity to dissolve, the insolubility of the PA-12,T blocks(crystals) keep PA-6 from fully dissolving. Swelling is noticeably greater with the 8 mol-% sample due to the increased amount of the PA-6. Interestingly, the gels of the 8 mol-% sample are slightly hazy, consistent with the DSC data showing that PA-12,T crystals remain. The 2 and 5 mol-% CaCl$_2$ samples show complete swelling of the FA forming a soft gel. No hazy areas appear because PA-12,T segments are depleted and cannot crystallize as shown by DSC. The high molecular weight and remaining fragments of 12-T blocks and PA-12,6,T units keep the sample from fully dissolving.
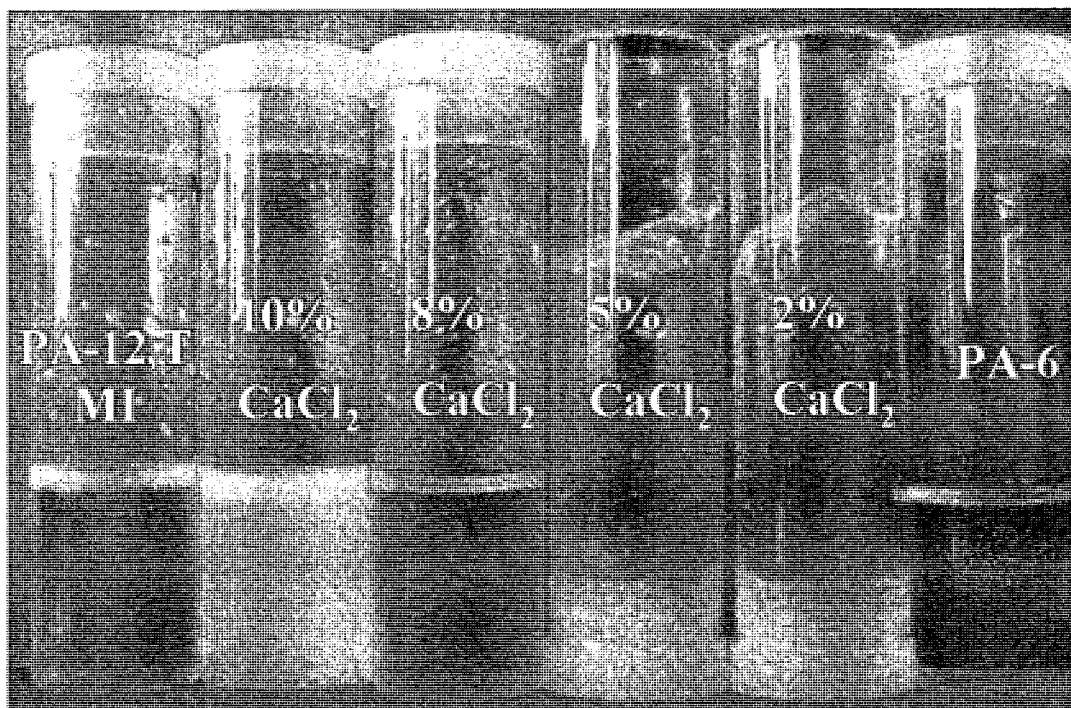
Figure 3.16. Solubility of PA-12,T MI, PA-6, and several copolymers

Conclusions

PA-12,T - PA-6 block copolymers have been synthesized by the one pot reaction involving the anionic polymerization of PA-12,T macroinitiator. By changing $CaCl_2$ concentration, a variety of materials can be obtained using identical reaction conditions. Caprolactam conversion and PA-12,T block transamidation have been proven to be competing reactions which are directly effected by $CaCl_2$ concentration. At $CaCl_2$ concentrations higher than 5 mol-% block copolymers are obtained having distinct PA-6 and PA-12,T melting temperatures and unique swelling in formic acid. At $CaCl_2$ concentrations lower than 5 mol-%, copolymers are less blocky due to transamidation reactions and have much higher molecular weights.

Acknowledgements

References

[1] Aerdts, A. M.; Eersels, K. L. L.; Groeninckx, G. *Macromolecules* **1996**, 29, 3.

[2] Kim, I.; White. J.L. *J. Apl. Poly. Sci.* **2005,** 96, 1875–1887.

[3] Brozek, J.; Budín, J.; Roda, J. *Journal of Thermal Analysis and Calorimetry* **2007**, 89, 211–215.

[4] Ozgun, H. B.; Kubanek, V.; Kralicek, J.; Veruovi, B. *Eur. Polyrn. J.* **1986,** 22, 12, 1009-1014.

[5] Petrov, P.; Gancheva, V.; Phillipova, T.Z.; Velichkova R.; Mateva, R. *J. Poly. Sci: Part A* **2000**, 38, 4154–4164.

[6] Mateva, R.; Filyanova, R.; Dimitrov, R.; Velichkova, R. *J. Apl. Poly. Sci.* **2004**, 91, 3251–3258.

[7] Mateva, R.; Filyanova, R.; Dimitrov, R.; Velichkova, R. Ganchev, V. *J. Poly. Sci: Part A.* **2003**, 41, 487–496.

[8] Youlee, P.; Harris, F.W. *J. Poly. Sci: Part A.* **2000**, 38, 4247–4257.

[9] Mougin, N.; Rempp, P.; Gnanou, Y. *J. Poly. Sci: Part A* **1993**, 31, 1253-1260.

[10] Meng-Song, Y.N.; Chen-Chi, M. *J. Apl. Poly. Sci.* **1994**, 53, 213-224.

[11] Youlee, P. *J. Apl. Poly. Sci.* **2006**, 99, 309–318.

[12] Carlo Alfonso, G.C.; Bonta, G.; Russo, S.; Traverso, A. *Makromol. Chem.* **1981**, 182, 929 – 939.

[13]Carlo Alfonso, G.; Cirillo, G.; Russo, S.; Turturro, A. *Eur. Polvm. J.* **1983**, 19, 10/11, 949-953.

[14]Novitsky, T.; Lange, C; Jarrett, W.; Mathias, L.; Osborn, S.; Ayotte, R.; Manning, S. J. of Apl. Poly. Sci. **2009**. Manuscript In-press. Available upon request.

[15]Petrov, P.; Gancheva, V.; Philipova, T.Z.; Velichkova, R.; and Mateva R.; *J. Poly. Sci. Part A* **2000**, 38, 4154.

[16]Gancheva, V.; Petrov, P.; Vladimirov, N.; Velichkova, R.; Mateva, R. *Poly. Int.* **2008**, 57, 1075–1078.

CONCLUSIONS

In the final section, the extension of this work is briefly discussed. In Chapter II, we have found that crystalline melting temperature and enthalpy is affected by the addition of the PA-6,T monomer. Copolymers were found to be crystalline at all compositions, and no totally amorphous materials were formed despite the lowering of the melting temperature and enthalpy. Therefore, it would be interesting the further characterize these materials to understand:

- Crystal type- alpha, gamma, or pseudo-hexagonal phase

- Crystal composition – Do PA-12,T – 6,T alternating segments crystallize? (solid state ^{13}C NMR)

- Crystal size – How big are the crystals versus wt-% PA-6,T comonomer? (AFM)

- Mechanical Properties – How do crystalline changes affect strength and toughness?

- Annealing properties

Also, the crystallization rates of these materials are very different. At the Washington D.C., ACS meeting in 2009, Dr. Harry Allcock posed an interesting question, "Using this idea, can you make a material that turns consistently opaque with a corresponding increase in temperature?" This research has left questions like this unknown, but provides a synthesis that can be scaled-up for both mechanical and annealing properties.

A variety of questions are unveiled by the findings in Chapter III. While the data shows that $CaCl_2$ has a large effect on the conversion and transamidation of the anionic

polymerization of PA-12,T macroinitiators, the actual mechanism is unknown. Gaining this knowledge would enable better control of the final polymer structure. The following variables of the anionic polymerization left constant in this study still need to be examined:

- Temperature – held at a constant 200 °C, but raising and lowering would affect the rate and crystallization of the reaction.

- Macroinitiator concentration – held to a constant 15 wt-%, but if increased closer to the solubility limit (22 wt-%), could the PA-12,T crystallize out before transamidation preventing randomization?

- Macroinitiator molecular weight – held at constant DP of 15, but by adjusting the stoichiometry of the step growth reaction to obtain a higher DP, could the randomization of PA-12,T block be mitigated?

- Inorganic salt – LiCl has been also shown to have different effects on AP than $CaCl_2$ by increasing the initial rate of the reaction at low concentrations (<5 mol-%).

GPC using HFIP was not available to characterize the molecular weight and molecular weight distribution of the samples. This would analysis would provide an interesting piece of information that would help examine the molecular weight build up of the reaction as a function of $CaCl_2$ concentration, conversion, and transamidation.

An attractive feature of the studied block copolymer synthesis is the variety of block copolymers that could be made by simply changing the monomers. PA-12,T and PA-6 blocks are both crystalline. Using different monomers, block copolymers with a

crystallizable MI and amorphous AP reaction mixture (and vice versa) can be studied. The following briefly discusses the variation of monomers that could be investigated.

- Biscaprolactam species – It would be interesting to compare the terephthalamide to the isophthalamide biscaprolactam monomer. Since polyisophthalamides are not crystalline, the effect of crystallinity on the AP of MI can be elucidated. Also, linear biscaprolactam monomers could be used for further comparison. Since linear polyamides are expected to be more soluble in lactams than polyphthalamides, higher concentrations and/or molecular weights could be used.

- Diamine – Different lengths of diamines can be used to change amide density of the middle block which will affect solubility and final properties. Also, aromatic diamines could be studied to include fully aromatic polyamide blocks.

- Solvent/AP monomer – along with caprolactam, laurolactam is commercially available. Both homopolymers are crystalline, but amorphous blocks can be attained by using caprolactam/laurylactam mixtures.

Since reactions produce a solid polymer with near full conversion of monomer very quickly, the applicability of this synthesis to reaction injection molding needs to be accessed. This would involve adding the anionic initaitor as a specific point in the barrel of a twin screw extruder to afford bulk materials into a mold. By simply using differents amounts of $CaCl_2$, crosslinking, molecular weight, and transamidation can be controlled, and a variety of materials can be synthezied with one process.

Finally, mechanical and thermomechanical properties of the block copolymers needs to be examined. Their DSC and solubility behavior have been shown to be quite different, therefore it is expected that mechanical properties and the glass transition temperatures will follow. Using this data, application of the materials can then be properly asscessed.